MZ-TH/12-01

Quantum Einstein Gravity*

Martin Reuter and Frank Saueressig

Institute of Physics, University of Mainz
Staudingerweg 7, D-55099 Mainz, Germany

reuter@thep.physik.uni-mainz.de
saueressig@thep.physik.uni-mainz.de

Abstract

We give a pedagogical introduction to the basic ideas and concepts of the Asymptotic Safety program in Quantum Einstein Gravity. Using the continuum approach based upon the effective average action, we summarize the state of the art of the field with a particular focus on the evidence supporting the existence of the non-trivial renormalization group fixed point at the heart of the construction. As an application, the multifractal structure of the emerging space-times is discussed in detail. In particular, we compare the continuum prediction for their spectral dimension with Monte Carlo data from the Causal Dynamical Triangulation approach.

*To appear in the *New Journal of Physics* special issue on Quantum Einstein Gravity.

1 Introduction

Finding a consistent and fundamental quantum theory for gravity is still one of the most challenging open problems in theoretical high energy physics to date [1]. As is well known, the perturbative quantization of the classical description for gravity, General Relativity, results in a non-renormalizable quantum theory [2–4]. One possible lesson drawn from this result may assert that gravity constitutes an effective field theory valid at low energies, whose UV completion requires the introduction of new degrees of freedom and symmetries. This is the path followed, e.g., by string theory. In a less radical approach, one retains the fields and symmetries known from General Relativity and conjectures that gravity constitutes a fundamental theory at the non-perturbative level. One proposal along this line is the Asymptotic Safety scenario [5,6] which, motivated by gravity in $2+\epsilon$ dimensions [7,8], was initially put forward by Weinberg [9,10]. The key ingredient in this construction is a non-Gaussian fixed point (NGFP) of the gravitational renormalization group (RG) flow, which controls the behavior of the theory at high energies and renders physical quantities safe from unphysical divergences.

The primary tool for investigating this scenario is the functional renormalization group equation (FRGE) for gravity [11], which constitutes the spring-board for the detailed analysis of the gravitational RG flow at the non-perturbative level [11–36].[1] The FRGE defines a Wilsonian RG flow on a theory space which consists of all diffeomorphism invariant functionals of the metric $g_{\mu\nu}$ and yielded substantial evidence for the existence and predictivity of the NGFP underlying the Asymptotic Safety conjecture. The theory emerging from this construction, Quantum Einstein Gravity (henceforth denoted "QEG"), defines a consistent and predictive quantum theory for gravity within the framework of quantum field theory. We stress that QEG is not a quantization of classical General Relativity: its bare action corresponds to a non-trivial fixed point of the RG flow and is a *prediction* therefore.

The approach of [11] employs the effective average action Γ_k [38–41] which has crucial

[1] Independent support for the Asymptotic Safety conjecture comes from a 2-dimensional symmetry reduction of the gravitational path-integral [37].

advantages as compared to other continuum implementations of the Wilsonian RG flow [42]. In particular, the RG scale dependence of Γ_k is governed by the FRGE [38]

$$k\partial_k\Gamma_k[\Phi,\bar{\Phi}] = \frac{1}{2}\mathrm{Str}\left[\left(\frac{\delta^2\Gamma_k}{\delta\Phi^A\delta\Phi^B}+\mathcal{R}_k\right)^{-1}k\partial_k\mathcal{R}_k\right]. \tag{1.1}$$

Here Φ^A is the collection of all dynamical fields considered and $\bar{\Phi}^A$ denotes their background counterparts. Moreover $\mathcal{R}_k$ is a matrix-valued infrared cutoff, which provides a k-dependent mass-term for fluctuations with momenta $p^2 \ll k^2$, while vanishing for $p^2 \gg k^2$. Solutions of the flow equation give rise to families of effective field theories $\{\Gamma_k[g_{\mu\nu}], 0 \leq k < \infty\}$ labeled by the coarse graining scale k. The latter property opens the door to a rather direct extraction of physical information from the RG flow, at least in single-scale cases: If the physical process under consideration involves a single typical momentum scale p_0 only, it can be described by a tree-level evaluation of $\Gamma_k[g_{\mu\nu}]$, with $k = p_0$.[2]

A striking consequence of the scale-dependence in Γ_k is the observation that the effective QEG space-time should have certain features in common with a fractal [13, 15]. The property underlying this assertion is that the effective field equations derived from the gravitational average action equip every given smooth space-time manifold with, in principle, infinitely many different (pseudo) Riemannian structures, one for each coarse graining scale [43,44]. Thus, very much like in the famous example of the coast line of England [45], the proper length on a QEG space-time depends on the "length of the yardstick" used to measure it. Earlier on similar fractal properties had already been found in other quantum gravity theories, in particular near dimension 2 [46], in a non-asymptotically safe model [47], and by analyzing the conformal anomaly [48].

In ref. [13] the consequences of this scale-dependence for the 4-dimensional graviton propagator has been studied in the regime of asymptotically large momenta and it has been found that near the Planck scale a kind of dynamical dimensional reduction oc-

[2]The precision which can be achieved by this effective field theory description depends on the size of the fluctuations relative to mean values. If they turn out large, or if more than one scale is involved, it might be necessary to go beyond the tree-level analysis.

curs. As a consequence of the NGFP controlling the UV behavior of the theory, the 4-dimensional graviton propagator essentially behaves 2-dimensional on microscopic scales. Subsequently, the "finger prints" of the NGFP on the fabric of the effective QEG space-times have been discussed in [15], where it was shown that Asymptotic Safety induces a characteristic self-similarity of space-time on length-scales below the Planck length $\ell_{\rm PL}$. In particular the spectral dimension of the effective QEG space-times in the asymptotic scaling regime implied by the NGFP becomes $d_s = d/2$ with d the classical space-time dimension [13,15,49]. Based on this observation it was argued in a cosmological context that the geometry fluctuations originating from the scaling regime can give rise to a scale free spectrum of primordial density perturbations responsible for structure formation [50, 51].

Along a different line of investigations, the Causal Dynamical Triangulation (CDT) approach has been developed and first Monte Carlo simulations were performed [52–57], see [58] for a recent review. In this framework one attempts to compute quantum gravity partition functions by numerically constructing the continuum limit of an appropriate statistical mechanics system. From the perspective of the latter, this limit amounts to a second order phase transition. If CDT and its counterpart QEG, formulated in the continuum by means of the average action, belong to the same universality class[3] one may expect that the phase transition of the former is described by the non-trivial fixed point underlying the Asymptotic Safety of the latter.

Remarkably, ref. [54] reported results which indicated that the 4-dimensional CDT space-times, too, undergo a dimensional reduction from four to two dimensions as one "zooms" in on short distances. In particular it had been demonstrated that the spectral dimension d_s measured in the CDT simulations has the very same limiting behaviors, $4 \to 2$, as in QEG. Therefore it was plausible to assume that both approaches indeed "see" the same continuum physics.

This interpretation became problematic, however, when it turned out that the Monte Carlo data corresponds to a regime where the cutoff length inherent in the triangulations is

[3]For the time being this is merely a conjecture, of course, albeit a very natural one.

still significantly larger than the Planck length. The situation became even more puzzling when ref. [56] carried out CDT simulations for $d = 3$ macroscopic dimensions, which favor a value near $d_s = 2$ on the shortest length-scale probed. Furthermore, the authors of ref. [59] reported simulations within the *euclidean* dynamical triangulation (EDT) approach in $d = 4$, where the spectral dimension dropped from 4 to about 1.5. Obviously, both of these observations conflict the QEG expectations if one interprets the latter dimension as the value in the continuum limit.

In order to resolve this puzzle, [60] computed several types of scale dependent effective dimensions, specifically the spectral dimension d_s and the walk dimension d_w for the effective QEG space-times. Surprisingly, the analysis revealed a further regime which exhibits the phenomenon of dynamical dimensional reduction on length scales slightly *larger* than $\ell_{\rm PL}$. There the spectral dimension is even smaller than near the fixed point, namely $d_s = 4/3$ in the case of 4 dimensions classically. Moreover it was found that the (3-dimensional) results reported in [56] are in good agreement with QEG. This analysis also confirmed the supposition [56] that the shortest possible length scale achieved in the simulations is not yet close to the Planck length. Rather the Monte Carlo data probes the transition between the classical and the newly discovered "semi-classical" regime.

It is intriguing that Loop Quantum Gravity and spin foam models also show indications for a similar dimensional reduction [61–63], with some hints for an intermittent regime where the spectral dimension is smaller than in the deep ultraviolet. In ref. [64] an argument based upon the strong coupling limit of the Wheeler-DeWitt equation was put forward as a possible explanation of this dimensional reduction. Within non-commutative geometry Connes et al. [65] interpreted the dynamical dimensional reduction to $d_s = 2$, which was observed in QEG, in the context of the derivation of the Standard Model from a spectral triple. In fact, from the data encoded in a spectral triple, its Dirac operator in particular, one can compute a type of spectral dimension of the resulting non-commutative space which is closely related to the one considered here. Also for standard fractals such as Cantor sets, it has been possible to find spectral triples representing them and to compute the corresponding dimensions [66].

Furthermore, a number of model systems (quantum sphere, κ-Minkowski space, etc.) give rise to a similar reduction as fully fledged quantum gravity [67]. Among other developments, these findings also motivated the investigation of physics on *prescribed* fractal space-times. In refs. [68, 69] a fractional differential calculus [70] was employed in order to incorporate fractal features, and in [71] recent exact results on spectral zeta-functions on certain fractals [72] were used to study the thermodynamics of photons on fractals. In ref. [73] matter quantum field theories were constructed and renormalized on a fractal background. The almost universal appearance of fractional properties of space-time and its accessibility in various, a priori different, approaches to quantum gravity make the generalized notions of dimensionality which we are going to review here a valuable tool in comparing the physics content of these different formulations.

The present article is intended to provide the necessary background for understanding the frontier developments in Asymptotic Safety. In the next section we follow [5] and introduce the general concepts related to the Wilsonian picture of renormalization: theory space, renormalization group flows, non-perturbative renormalizability, and the non-perturbative approximation scheme of truncating theory space. The construction of the effective average action and its FRGE for gravity [11] is reviewed in section 3. In section 4 we illustrate the most commonly used approximation scheme of "truncating theory space" by means of a simple example, the so-called Einstein-Hilbert truncation. Section 5 contains a state of the art summary of the results obtained using truncated flow equations, with an emphasis on the question as to whether there exists a non-trivial fixed point for the average action's RG flow. If so, QEG could be established as a fundamental theory of quantum gravity which is non-perturbatively renormalizable and "asymptotically safe" from unphysical divergences. The remainder of the review is dedicated to the discussion of the multifractal space-times emerging from QEG: section 6 reviews the structures underlying these fractal properties, the scale-dependent space-time metrics. Subsequently, the spectral, walk, and Hausdorff dimensions introduced in appendix A are computed in the framework of QEG in sections 7 and 8. In particular subsection 8.3 compares the QEG results for the spectral dimension with the one found in the CDT program. We close with

a short summary and some concluding remarks in section 9.

2 RG flows, theory space, and Asymptotic Safety

The key idea of the Wilsonian renormalization group is the description of a physical system in terms of a one-parameter family of effective actions, each valid at a certain energy scale k. The RG flow of the theory thereby connects the effective descriptions at different scales. The arena in which this dynamics takes place is the "theory space" sketched in fig. 1. In order to describe it, we first specify our "theory" by fixing its field content $\Phi(x)$ and, possibly, imposing certain symmetry requirements (a $\mathbb{Z}_2$-symmetry for a single scalar, or diffeomorphism invariance if Φ denotes the space-time metric, for instance). The theory space corresponding to this theory consists of all (action) functionals $A : \Phi \mapsto A[\Phi]$ depending on this set of fields and compatible with the symmetry requirements. Thus the theory space $\{A[\,\cdot\,]\}$ is fixed once the field content and the symmetries are given.

Let us assume we can find a set of "basis functionals" $\{P_\alpha[\,\cdot\,]\}$ so that every point of theory space has an expansion of the form

$$A[\Phi, \bar{\Phi}] = \sum_{\alpha=1}^{\infty} \bar{u}_\alpha \, P_\alpha[\Phi, \bar{\Phi}] \,. \tag{2.1}$$

The basis $\{P_\alpha[\,\cdot\,]\}$ will include both local field monomials and non-local invariants and we may use the "generalized couplings" $\{\bar{u}_\alpha, \alpha = 1, 2, \cdots\}$ as local coordinates. More precisely, the theory space is coordinatized by the subset of "essential couplings", i.e., those coordinates which cannot be absorbed by a field reparameterization.

Geometrically speaking the FRGE for the effective average action, eq. (1.1), defines a vector field $\vec{\beta}$ on theory space. The integral curves along this vector field are the "RG trajectories" $k \mapsto \Gamma_k$ parameterized by the scale k. They start, for $k \to \infty$, at the microscopic action S and terminate at the ordinary effective action at $k = 0$. The natural orientation of the trajectories is from higher to lower scales k, the direction of increasing

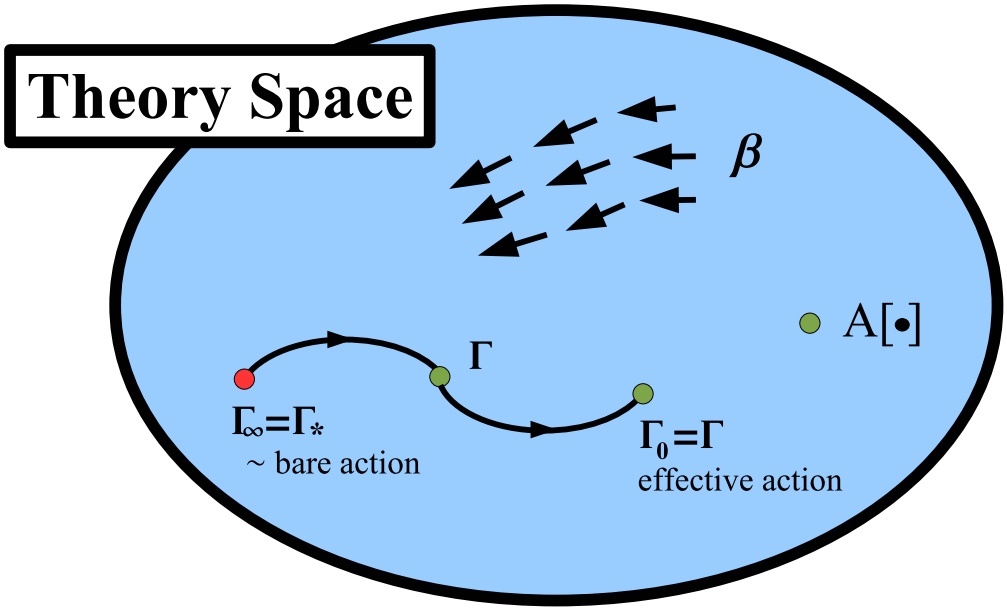

Figure 1: The points of theory space are action functionals $A[\,\cdot\,]$. The RG equation defines a vector field $\vec{\beta}$ on this space; its integral curves are the RG trajectories $k \mapsto \Gamma_k$. They emanate from the fixed point action Γ_* and end at the standard effective action Γ.

"coarse graining". Expanding Γ_k as in (2.1),

$$\Gamma_k[\Phi, \bar{\Phi}] = \sum_{\alpha=1}^{\infty} \bar{u}_\alpha(k)\, P_\alpha[\Phi, \bar{\Phi}]\,, \tag{2.2}$$

the trajectory is described by infinitely many "running couplings" $\bar{u}_\alpha(k)$. Inserting (2.2) into the FRGE we obtain a system of infinitely many coupled differential equations for the $\bar{u}_\alpha$'s:

$$k\partial_k\, \bar{u}_\alpha(k) = \overline{\beta}_\alpha(\bar{u}_1, \bar{u}_2, \cdots; k)\,, \quad \alpha = 1, 2, \cdots\,. \tag{2.3}$$

Here the "beta functions" $\overline{\beta}_\alpha$ arise by expanding the trace on the RHS of the FRGE in terms of $\{P_\alpha[\,\cdot\,]\}$, i.e., $\frac{1}{2}\mathrm{Tr}\,[\cdots] = \sum_{\alpha=1}^{\infty} \overline{\beta}_\alpha(\bar{u}_1, \bar{u}_2, \cdots; k) P_\alpha[\Phi, \bar{\Phi}]$. The expansion coefficients $\overline{\beta}_\alpha$ have the interpretation of beta functions similar to those of perturbation theory, but not restricted to relevant couplings. In standard field theory jargon one would refer to $\bar{u}_\alpha(k = \infty)$ as the "bare" parameters and to $\bar{u}_\alpha(k = 0)$ as the "renormalized" or "dressed" parameters.

The notation with the bar on $\bar{u}_\alpha$ and $\overline{\beta}_\alpha$ is to indicate that we are still dealing with dimensionful couplings. Usually the flow equation is reexpressed in terms of the dimensionless couplings

$$u_\alpha \equiv k^{-d_\alpha}\, \bar{u}_\alpha \,, \tag{2.4}$$

where d_α is the canonical mass dimension of $\bar{u}_\alpha$. Correspondingly the essential u_α's are used as coordinates of theory space. The resulting RG equations

$$k\partial_k u_\alpha(k) = \beta_\alpha(u_1, u_2, \cdots) \tag{2.5}$$

are a coupled system of autonomous differential equations. The β_α's have no explicit k-dependence and define a "time independent" vector field on theory space. The RG trajectories arise as solutions or, equivalently, integral curves of (2.5).

Based on these structures, the concept of renormalization can be understood as follows. The boundary of theory space depicted in fig. 1 is meant to separate points with coordinates $\{u_\alpha, \alpha = 1, 2, \cdots\}$ with all the essential couplings u_α well defined, from points with undefined, divergent couplings. The basic task of renormalization theory consists in constructing an "infinitely long" RG trajectory which lies entirely within this theory space, i.e., a trajectory which neither leaves theory space (that is, develops divergences) in the UV limit $k \to \infty$ nor in the IR limit $k \to 0$. Every such trajectory defines one possible quantum theory.

The key idea of Asymptotic Safety is to perform the UV limit $k \to \infty$ at a fixed point $\{u^*_\alpha, \alpha = 1, 2, \cdots\} \equiv u^*$ of the RG flow. The fixed point is a zero of the vector field $\vec{\beta} \equiv (\beta_\alpha)$, i.e., $\beta_\alpha(u^*) = 0$ for all $\alpha = 1, 2, \cdots$. The RG trajectories have a low "velocity" near a fixed point because the β_α's are small there and directly at the fixed point the running stops completely. As a result, one can "use up" an infinite amount of RG time near/at the fixed point if one bases the quantum theory on a trajectory which runs into a fixed point for $k \to \infty$. The fact, that, in the UV limit the trajectory ends at a fixed point, an "inner point" of theory space giving rise to a well behaved action functional, ensures that the trajectory does not escape from theory space, i.e., does not

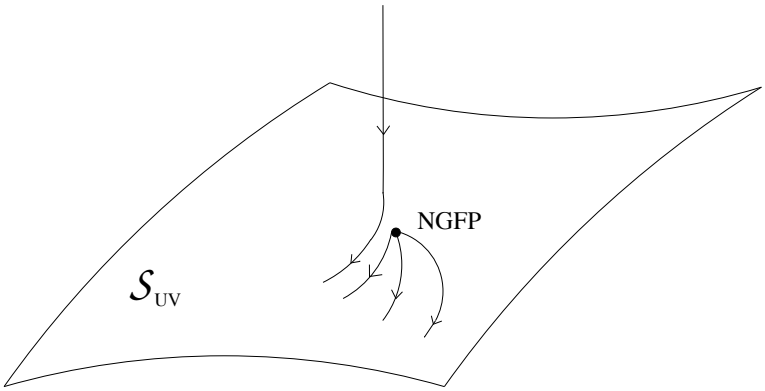

Figure 2: Schematic picture of the UV critical hypersurface $\mathcal{S}_{\rm UV}$ of the NGFP. It is spanned by RG trajectories emanating from the NGFP as the RG scale k is lowered. Trajectories not in the surface are attracted towards $\mathcal{S}_{\rm UV}$ as k decreases. (The arrows point in the direction of decreasing k, from the "UV" to the "IR".)

develop pathological properties such as divergent couplings. For $k \to \infty$ the resulting quantum theory is "asymptotically safe" from unphysical divergences.

In a sense, standard perturbation theory takes the $k \to \infty$-limit at the Gaussian fixed point (GFP), i.e., a fixed point where $u^*_\alpha = 0, \forall \alpha = 1, 2, \ldots$. This construction is the one underlying asymptotic freedom. More general, however, one can also use a non-Gaussian fixed point (NGFP) for letting $k \to \infty$, where, by definition, not all of the coordinates u^*_α vanish. In the context of gravity, Weinberg [9] proposed that the UV completion of the theory is precisely given by such a NGFP, which therefore constitutes the essential ingredient in the Asymptotic Safety program.

Given a NGFP, an important concept is its *UV critical hypersurface* $\mathcal{S}_{\rm UV}$, or synonymously, its *unstable manifold*. By definition, it consists of all points of theory space which are pulled into the NGFP by the inverse RG flow, i.e., for *in*creasing k. Its dimensionality $\dim(\mathcal{S}_{\rm UV}) \equiv \Delta_{\rm UV}$ is given by the number of attractive (for *in*creasing cutoff k) directions in the space of couplings.

For the RG equations (2.5), the linearized flow near the fixed point is governed by the

Jacobi matrix $\mathbf{B} = (B_{\alpha\gamma})$, $B_{\alpha\gamma} \equiv \partial_\gamma \beta_\alpha(u^*)$:

$$k\,\partial_k\, u_\alpha(k) = \sum_\gamma B_{\alpha\gamma}\,\left(u_\gamma(k) - u^*_\gamma\right)\ . \tag{2.6}$$

The general solution to this equation reads

$$u_\alpha(k) = u^*_\alpha + \sum_I C_I\, V^I_\alpha\,\left(\frac{k_0}{k}\right)^{\theta_I} \tag{2.7}$$

where the V^I's are the right-eigenvectors of $\mathbf{B}$ with eigenvalues $-\theta_I$, i.e., $\sum_\gamma B_{\alpha\gamma}\, V^I_\gamma = -\theta_I\, V^I_\alpha$. Since $\mathbf{B}$ is not symmetric in general the θ_I's are not guaranteed to be real. We assume that the eigenvectors form a complete system though. Furthermore, k_0 is a fixed reference scale, and the C_I's are constants of integration. The quantities θ_I are referred to as *critical exponents* since when the renormalization group is applied to critical phenomena (second order phase transitions) the traditionally defined critical exponents are related to the θ_I's in a simple way [40].

If $u_\alpha(k)$ is to describe a trajectory in $\mathcal{S}_{\rm UV}$, $u_\alpha(k)$ must approach u^*_α in the limit $k \to \infty$ and therefore we must set $C_I = 0$ for all I with $\mathrm{Re}\,\theta_I < 0$. Hence the dimensionality $\Delta_{\rm UV}$ equals the number of $\mathbf{B}$-eigenvalues with a negative real part, i.e., the number of θ_I's with $\mathrm{Re}\,\theta_I > 0$. The corresponding eigenvectors span the tangent space to $\mathcal{S}_{\rm UV}$ at the NGFP. If we *lower* the cutoff for a generic trajectory with all C_I nonzero, only $\Delta_{\rm UV}$ "relevant" parameters corresponding to the eigendirections tangent to $\mathcal{S}_{\rm UV}$ grow ($\mathrm{Re}\,\theta_I > 0$), while the remaining "irrelevant" couplings pertaining to the eigendirections normal to $\mathcal{S}_{\rm UV}$ decrease ($\mathrm{Re}\,\theta_I < 0$). Thus near the NGFP a generic trajectory is attracted towards $\mathcal{S}_{\rm UV}$, see fig. 2.

Coming back to the Asymptotic Safety construction, let us now use this fixed point in order to take the limit $k \to \infty$. The trajectories which define an infinite cutoff limit are special in the sense that all irrelevant couplings are set to zero: $C_I = 0$ if $\mathrm{Re}\,\theta_I < 0$. These conditions place the trajectory exactly on $\mathcal{S}_{\rm UV}$. There is a $\Delta_{\rm UV}$-parameter family of such trajectories, and the experiment must decide which one is realized in Nature. Therefore

the predictive power of the theory increases with decreasing dimensionality of $\mathcal{S}_{\rm UV}$, i.e., number of UV attractive eigendirections of the NGFP. If $\Delta_{\rm UV} < \infty$, the quantum field theory thus constructed is comparable to and as predictive as a perturbatively renormalizable model with $\Delta_{\rm UV}$ "renormalizable couplings", i.e., couplings relevant at the GFP, see [5] for a more detailed discussion.

Up to this point our discussion did not involve any approximation. In practice, however, it is usually impossible to find exact solutions to the flow equation. As a way out, one could evaluate the trace on the RHS of the FRGE by expanding it with respect to some small coupling constant, for instance, thus recovering the familiar perturbative beta functions. A more interesting option which gives rise to non-perturbative approximate solutions is to truncate the theory space $\{A[\,\cdot\,]\}$. The basic idea is to project the RG flow onto a finite dimensional subspace of theory space. The subspace should be chosen in such a way that the projected flow encapsulates the essential physical features of the exact flow on the full space.

Concretely the projection onto a truncation subspace is performed as follows. One makes an ansatz of the form $\Gamma_k[\Phi,\bar\Phi] = \sum_{i=1}^N \bar u_i(k) P_i[\Phi,\bar\Phi]$, where the k-independent functionals $\{P_i[\,\cdot\,], i = 1,\cdots,N\}$ form a 'basis' on the subspace selected. For a scalar field ϕ, say, examples include pure potential terms $\int d^dx \phi^m(x)$, $\int d^dx \phi^n(x) \ln \phi^2(x)$, $\cdots$, a standard kinetic term $\int d^dx (\partial\phi)^2$, higher order derivative terms $\int d^dx\, \phi \left(\partial^2\right)^n \phi$, $\cdots$, and non-local terms like $\int d^dx\, \phi \ln(-\partial^2)\phi$, $\cdots$. Even if $S = \Gamma_\infty$ is simple, a standard ϕ^4 action, say, the evolution from $k = \infty$ downwards will generate such terms, a priori only constrained by symmetry requirements. The difficult task in practical RG applications consists in selecting a set of P_i's which, on the one hand, is generic enough to allow for a sufficiently precise description of the physics one is interested in, and which, on the other hand, is small enough to be computationally manageable.

The projected RG flow is described by a set of ordinary (if $N < \infty$) differential equations for the couplings $\bar u_i(k)$. They arise as follows. Let us assume we expand the Φ-dependence of $\frac{1}{2}{\rm Tr}[\cdots]$ (with the ansatz for $\Gamma_k[\Phi,\bar\Phi]$ inserted) in a basis $\{P_\alpha[\,\cdot\,]\}$ of the

full theory space which contains the P_i's spanning the truncated space as a subset:

$$\frac{1}{2}\mathrm{Tr}[\cdots] = \sum_{\alpha=1}^{\infty} \overline{\beta}_\alpha(\bar{u}_1, \cdots, \bar{u}_N; k)\, P_\alpha[\Phi, \bar{\Phi}] = \sum_{i=1}^{N} \overline{\beta}_i(\bar{u}_1, \cdots, \bar{u}_N; k)\, P_i[\Phi, \bar{\Phi}] + \mathrm{rest}\,. \quad (2.8)$$

Here the "rest" contains all terms outside the truncated theory space; the approximation consists in neglecting precisely those terms. Thus, equating (2.8) to the LHS of the flow equation, $\partial_t \Gamma_k = \sum_{i=1}^{N} \partial_t \bar{u}_i(k) P_i$, the linear independence of the P_i's implies the coupled system of ordinary differential equations

$$\partial_t \bar{u}_i(k) = \overline{\beta}_i(\bar{u}_1, \cdots, \bar{u}_N; k)\,, \quad i = 1, \cdots, N\,. \quad (2.9)$$

Solving (2.9) one obtains an *approximation* to the exact RG trajectory projected onto the chosen subspace. Note that this approximate trajectory does, in general, not coincide with the projection of the exact trajectory, but if the subspace is well chosen, it will not be very different from it. In fact, the most non-trivial problem in using truncated flow equations is to find and justify a truncation subspace which should be as low dimensional as possible to make the calculations feasible, but at the same time large enough to describe at least qualitatively the essential physics. We shall return to the issue of testing the quality of a given truncation later on.

3 The effective average action for gravity

In the case of QEG, ideally, we would like theory space to consist of functionals $A[g_{\mu\nu}]$ depending on a symmetric tensor field, the metric, in a diffeomorphism invariant way. Given a theory space, the form of the FRGE and, as a result, the vector field $\vec{\beta}$ are completely fixed. However, in the case of gravity it is much harder to make this idea work in a concrete way as compared to a simple matter field theory on a non-dynamical space-time, for instance. The reasons are of both conceptual and technical nature:

(1) The theory of quantum gravity we are aiming at should be formulated in a background

independent way. It should *explain* rather than presuppose the existence and the properties of space-time. Hence no special space-time manifold, in particular no special causal, let alone Riemannian, structure should play a distinguished role at the fundamental level of the theory. In particular it should also cover "exotic" phases in which the metric is degenerate or has no expectation value at all. Since almost our entire repertoire of quantum field theory methods applies only to the case of an externally given space-time manifold, usually Minkowski space, this is a severe conceptual problem. In fact, it is *the* central challenge for basically all approaches to quantum gravity, in one guise or another [1].

(2) The second difficulty, while less deep, is important for the practical applicability of the RG methods to be developed. It occurs already in the standard functional integral quantization of gauge or gravity theories, and is familiar from Yang-Mills theories. If one gauge-fixes the functional integral with an ordinary (covariant) gauge fixing condition like $\partial^\mu A^a_\mu = 0$, couples the (non-abelian) gauge field A^a_μ to a source, and constructs the ordinary effective action, the resulting functional $\Gamma[A^a_\mu]$ is *not* invariant under the gauge transformations of A^a_μ, $A^a_\mu \mapsto A^a_\mu + D^{ab}_\mu(A)\,\omega^b$. Only at the level of physical quantities constructed from $\Gamma[A^a_\mu]$, S-matrix elements for instance, gauge invariance is recovered.

(3) A more profound problem is related to the fact that in a gauge theory a "coarse graining" based on a naive Fourier decomposition of $A^a_\mu(x)$ is not gauge covariant and hence not physical. In fact, if one were to gauge transform a slowly varying $A^a_\mu(x)$ using a parameter function $\omega^a(x)$ with a fast x-variation, a gauge field with a fast x-variation would arise which, however, still describes the same physics. In a non-gauge theory the coarse graining is performed by expanding the field in terms of eigenfunctions of the (positive) operator $-\partial^2$ and declaring its eigenmodes 'long' or 'short' wavelength depending on whether the corresponding eigenvalue p^2 is smaller or larger than a given k^2. In a gauge theory the best one can do in installing this procedure is to expand with respect to the *covariant* Laplacian or a similar operator, and then organize the modes according to the size of their eigenvalues. While gauge covariant, this approach sacrifices to some extent the intuition of a Fourier coarse graining in terms of slow and fast modes. Analogous remarks apply to theories of gravity covariant under general coordinate transformations.

The key idea which led to a solution of all three problems was the use of the background field method [74]. At first sight it seems to be a contradiction in terms to use background fields in order to achieve "background independence". However, actually it is not, since the background metric introduced, $\bar{g}_{\mu\nu}$, is kept *completely arbitrary*, and no physics ever may depend on it. In fact, it becomes a second argument of $\Gamma_k[g_{\mu\nu}, \bar{g}_{\mu\nu}]$ and may be freely chosen from the same function space the dynamical metric "lives" in. The use of a background field also opens the door for complying with the requirement of a gauge invariant effective action. It is well known [75, 76] that there exist special gauge choices, the so-called background gauge fixing conditions, that make the (ordinary) effective action a gauge or diffeomorphism invariant functional of its arguments (including the background fields!). As it turned out [11,39] this technique also lends itself for implementing a covariant IR cutoff, and it is at the core of the effective average action for Yang-Mills theories [39,41] and for gravity [11]. In the following we briefly review the effective average action for gravity which has been introduced in ref. [11].

The ultimate goal is to give meaning to an integral over 'all' metrics $\gamma_{\mu\nu}$ of the form $\int \mathcal{D}\gamma_{\mu\nu}\, \exp\{-S[\gamma_{\mu\nu}] + \text{source terms}\}$ whose bare action $S[\gamma_{\mu\nu}]$ is invariant under general coordinate transformations,

$$\delta\gamma_{\mu\nu} = \mathcal{L}_v \gamma_{\mu\nu} \equiv v^\rho \partial_\rho \gamma_{\mu\nu} + \partial_\mu v^\rho \gamma_{\rho\nu} + \partial_\nu v^\rho \gamma_{\rho\mu}\,, \tag{3.1}$$

where $\mathcal{L}_v$ is the Lie derivative with respect to the vector field $v^\mu \partial_\mu$. To start with we consider $\gamma_{\mu\nu}$ to be a Riemannian metric and assume that $S[\gamma_{\mu\nu}]$ is positive definite. Heading towards the background field formalism, the first step consists in decomposing the variable of integration according to $\gamma_{\mu\nu} = \bar{g}_{\mu\nu} + h_{\mu\nu}$, where $\bar{g}_{\mu\nu}$ is a fixed background metric. Note that we are not implying a perturbative expansion here, $h_{\mu\nu}$ is not supposed to be small in any sense. After the background split the measure $\mathcal{D}\gamma_{\mu\nu}$ becomes $\mathcal{D}h_{\mu\nu}$ and the gauge transformations which we have to gauge-fix read

$$\delta h_{\mu\nu} = \mathcal{L}_v \gamma_{\mu\nu} = \mathcal{L}_v(\bar{g}_{\mu\nu} + h_{\mu\nu})\,, \quad \delta\bar{g}_{\mu\nu} = 0\,. \tag{3.2}$$

Picking an a priori arbitrary gauge fixing condition $F_\mu(h;\bar{g}) = 0$ the Faddeev-Popov trick can be applied straightforwardly [75]. Upon including an IR cutoff $\Delta_k S[h, C, \bar{C}; \bar{g}]$ (cfg. eq. (3.13) below) we are led to the following k-dependent generating functional W_k for the connected Green functions:

$$\exp\{W_k[t^{\mu\nu}, \sigma^\mu, \bar{\sigma}_\mu; \bar{g}_{\mu\nu}]\} = \int \mathcal{D}h_{\mu\nu}\mathcal{D}C^\mu\mathcal{D}\bar{C}_\mu \, \exp\Big\{ - S[\bar{g}+h] - S_{\rm gf}[h;\bar{g}] \\ - S_{\rm gh}[h, C, \bar{C}; \bar{g}] - \Delta_k S[h, C, \bar{C}; \bar{g}] - S_{\rm source}\Big\} . \tag{3.3}$$

Here $S_{\rm gf}$ denotes the gauge fixing term

$$S_{\rm gf}[h;\bar{g}] = \frac{1}{2\alpha}\int d^dx \sqrt{\bar{g}}\, \bar{g}^{\mu\nu} F_\mu F_\nu \,, \tag{3.4}$$

and $S_{\rm gh}$ is the action for the corresponding Faddeev–Popov ghosts C^μ and $\bar{C}_\mu$:

$$S_{\rm gh}[h, C, \bar{C}; \bar{g}] = -\kappa^{-1}\int d^dx \sqrt{\bar{g}}\, \bar{C}_\mu\, \bar{g}^{\mu\nu}\, \frac{\partial F_\nu}{\partial h_{\alpha\beta}}\, \mathcal{L}_C\left(\bar{g}_{\alpha\beta} + h_{\alpha\beta}\right) . \tag{3.5}$$

The Faddeev–Popov action $S_{\rm gh}$ is obtained along the same lines as in Yang–Mills theory: one applies a gauge transformation (3.2) to F_μ and replaces the parameters v^μ by the ghost field C^μ. The integral over C^μ and $\bar{C}_\mu$ exponentiates the Faddeev-Popov determinant $\det[\delta F_\mu/\delta v^\nu]$. In (3.3) we coupled $h_{\mu\nu}$, C^μ and $\bar{C}_\mu$ to sources $t^{\mu\nu}$, $\bar{\sigma}_\mu$ and σ^μ, respectively: $S_{\rm source} = -\int d^dx\, \sqrt{\bar{g}}\Big\{t^{\mu\nu}h_{\mu\nu} + \bar{\sigma}_\mu C^\mu + \sigma^\mu \bar{C}_\mu\Big\}$. The k- and source-dependent expectation values of $h_{\mu\nu}$, C^μ and $\bar{C}_\mu$ are then given by

$$\bar{h}_{\mu\nu} = \frac{1}{\sqrt{\bar{g}}}\frac{\delta W_k}{\delta t^{\mu\nu}} \qquad , \qquad \xi^\mu = \frac{1}{\sqrt{\bar{g}}}\frac{\delta W_k}{\delta \bar{\sigma}_\mu} \qquad , \qquad \bar{\xi}_\mu = \frac{1}{\sqrt{\bar{g}}}\frac{\delta W_k}{\delta \sigma^\mu} . \tag{3.6}$$

As usual we assume that one can invert the relations (3.6) and solve for the sources $(t^{\mu\nu}\,,\,\sigma^\mu\,,\,\bar{\sigma}_\mu)$ as functionals of $(\bar{h}_{\mu\nu}\,,\,\xi^\mu\,,\,\bar{\xi}_\mu)$ and, parametrically, of $\bar{g}_{\mu\nu}$. The Legendre transform $\widetilde{\Gamma}_k$ of W_k reads

$$\widetilde{\Gamma}_k[\bar{h}, \xi, \bar{\xi}; \bar{g}] = \int d^dx\, \sqrt{\bar{g}}\left\{t^{\mu\nu}\bar{h}_{\mu\nu} + \bar{\sigma}_\mu\xi^\mu + \sigma^\mu\bar{\xi}_\mu\right\} - W_k[t, \sigma, \bar{\sigma}; \bar{g}] . \tag{3.7}$$

This functional inherits a parametric $\bar{g}_{\mu\nu}$-dependence from W_k.

As mentioned earlier for a generic gauge fixing condition the Legendre transform (3.7) is not a diffeomorphism invariant functional of its arguments since the gauge breaking under the functional integral is communicated to $\widetilde{\Gamma}_k$ via the sources. While $\widetilde{\Gamma}_k$ does indeed describe the correct 'on-shell' physics satisfying all constraints coming from BRST invariance, it is not invariant off-shell [75, 76]. The situation is different for the class of gauge fixing conditions of the background type. While – as any gauge fixing condition must – they break the invariance under (3.2) they are chosen to be invariant under the so-called background gauge transformations

$$\delta h_{\mu\nu} = \mathcal{L}_v h_{\mu\nu} \,, \qquad \delta \bar{g}_{\mu\nu} = \mathcal{L}_v \bar{g}_{\mu\nu} \,. \tag{3.8}$$

The complete metric $\gamma_{\mu\nu} = g_{\mu\nu} + h_{\mu\nu}$ transforms as $\delta\gamma_{\mu\nu} = \mathcal{L}_v \gamma_{\mu\nu}$ both under (3.8) and under (3.2). The crucial difference is that the ('quantum') gauge transformations (3.2) keep $\bar{g}_{\mu\nu}$ unchanged so that the entire change of $\gamma_{\mu\nu}$ is ascribed to $h_{\mu\nu}$. This is the point of view one adopts in a standard perturbative calculation around flat space where one fixes $\bar{g}_{\mu\nu} = \eta_{\mu\nu}$ and allows for no variation of the background. In the present construction, instead, we leave $\bar{g}_{\mu\nu}$ unspecified but insist on covariance under (3.8). This will lead to a completely background covariant formulation.

Clearly there exist many possible gauge fixing terms $S_{\rm gf}[h;\bar{g}]$ of the form (3.4) which break (3.2) and are invariant under (3.8). A convenient choice which has been employed in practical calculations is the one-parameter family of gauge conditions

$$F_\mu[h;\bar{g}] = \sqrt{2}\,\kappa \left(\bar{D}^\nu \, h_{\mu\nu} - \varpi \, \bar{D}_\mu \, h^\nu{}_\nu \right) , \tag{3.9}$$

parameterized by ϖ. The covariant derivative $\bar{D}_\mu$ involves the Christoffel symbols $\bar{\Gamma}^\rho_{\mu\nu}$ of the background metric. Note that (3.9) is linear in the quantum field $h_{\alpha\beta}$. For $\varpi = \frac{1}{2}$, (3.9) reduces to the background version of the harmonic coordinate condition [75]: on a flat background with $\bar{g}_{\mu\nu} = \eta_{\mu\nu}$ the condition $F_\mu = 0$ becomes the familiar harmonic

coordinate condition, $\partial^\mu h_{\mu\nu} = \frac{1}{2}\partial_\nu h_\mu{}^\mu$. In eqs. (3.9) and (3.5) κ is an arbitrary constant with the dimension of a mass. We shall set $\kappa \equiv (32\pi\bar{G})^{-1/2}$ with $\bar{G}$ a constant reference value of Newton's constant. The ghost action for the gauge condition (3.9) reads

$$S_{\rm gh}[h, C, \bar{C}; \bar{g}] = -\sqrt{2}\int d^d x\, \sqrt{\bar{g}}\, \bar{C}_\mu \mathcal{M}[g, \bar{g}]^\mu{}_\nu C^\nu \tag{3.10}$$

with the Faddeev–Popov operator

$$\mathcal{M}[g, \bar{g}]^\mu{}_\nu = \bar{D}^\rho\, g^\mu{}_\nu\, D_\rho + \bar{D}^\rho\, g_{\rho\nu} D^\mu - 2\,\varpi\, \bar{D}^\mu\, \bar{g}^{\rho\sigma}\, g_{\rho\nu} D_\sigma\,. \tag{3.11}$$

It will prove crucial that for every background-type choice of F_μ, $S_{\rm gh}$ is invariant under (3.8) together with

$$\delta C^\mu = \mathcal{L}_v C^\mu\,, \qquad \delta \bar{C}_\mu = \mathcal{L}_v \bar{C}_\mu\,. \tag{3.12}$$

The essential piece in eq. (3.3) is the IR cutoff for the gravitational field $h_{\mu\nu}$ and for the ghosts. It is taken to be of the form

$$\Delta_k S = \frac{\kappa^2}{2}\int d^d x\, \sqrt{\bar{g}}\, h_{\mu\nu} \mathcal{R}_k^{\rm grav}[\bar{g}]^{\mu\nu\rho\sigma} h_{\rho\sigma} + \sqrt{2}\int d^d x\, \sqrt{\bar{g}}\, \bar{C}_\mu \mathcal{R}_k^{\rm gh}[\bar{g}] C^\mu\,. \tag{3.13}$$

The cutoff operators $\mathcal{R}_k^{\rm grav}$ and $\mathcal{R}_k^{\rm gh}$ serve the purpose of discriminating between high–momentum and low–momentum modes. Eigenmodes of $-\bar{D}^2$ with eigenvalues $p^2 \gg k^2$ are integrated out without any suppression whereas modes with small eigenvalues $p^2 \ll k^2$ are suppressed. The operators $\mathcal{R}_k^{\rm grav}$ and $\mathcal{R}_k^{\rm gh}$ have the structure $\mathcal{R}_k[\bar{g}] = \mathcal{Z}_k k^2 R^{(0)}(-\bar{D}^2/k^2)$, where the dimensionless function $R^{(0)}$ interpolates between $R^{(0)}(0) = 1$ and $R^{(0)}(\infty) = 0$. A convenient choice is, e.g., the exponential cutoff $R^{(0)}(w) = w[\exp(w) - 1]^{-1}$ or the optimized cutoff $R^{(0)}(w) = (1 - w)\theta(1 - w)$, where $w = p^2/k^2$. The factors $\mathcal{Z}_k$ are different for the graviton and the ghost cutoff. They are determined by the condition that all fluctuation spectra are cut off at precisely the same k^2, such that $\mathcal{R}_k$ combines with $\Gamma_k^{(2)}$ to the inverse propagator $\Gamma_k^{(2)} + \mathcal{R}_k = \mathcal{Z}_k(p^2 + k^2) + \cdots$, as it is necessary if the IR cutoff is to give rise to a (mass)^2 of size k^2 rather than $(\mathcal{Z}_k)^{-1}k^2$. Following this condition the ghost $\mathcal{Z}_k \equiv Z_k^{\rm gh}$ is a pure number, whereas for the metric fluctuation $\mathcal{Z}_k \equiv \mathcal{Z}_k^{\rm grav}$ is a

tensor, constructed only from the background metric $\bar{g}_{\mu\nu}$.

A feature of $\Delta_k S$ which is essential from a practical point of view is that the modes of $h_{\mu\nu}$ and the ghosts are organized according to their eigenvalues with respect to the *background* Laplace operator $\bar{D}^2 = \bar{g}^{\mu\nu}\bar{D}_\mu\bar{D}_\nu$ rather than $D^2 = g^{\mu\nu}D_\mu D_\nu$, which would pertain to the full quantum metric $\bar{g}_{\mu\nu} + h_{\mu\nu}$. Using $\bar{D}^2$, the functional $\Delta_k S$ is quadratic in the quantum field $h_{\mu\nu}$, while it becomes extremely complicated if D^2 is used instead. The virtue of a quadratic $\Delta_k S$ is that it gives rise to a flow equation which contains only *second* functional derivatives of Γ_k but no higher ones. The flow equations resulting from the cutoff operator D^2 are prohibitively complicated and can hardly be used for practical computations. A second property of $\Delta_k S$ which is crucial for our purposes is that it is invariant under the background gauge transformations (3.8) with (3.13).

Having specified all the ingredients which enter the functional integral (3.3) for the generating functional W_k we can write down the final definition of the effective average action Γ_k. It is obtained from the Legendre transform $\widetilde{\Gamma}_k$ by subtracting the cutoff action $\Delta_k S$ with the classical fields inserted:

$$\Gamma_k[\bar{h}, \xi, \bar{\xi}; \bar{g}] = \widetilde{\Gamma}_k[\bar{h}, \xi, \bar{\xi}; \bar{g}] - \Delta_k S[\bar{h}, \xi, \bar{\xi}; \bar{g}]\,. \tag{3.14}$$

It is convenient to define the expectation value of the quantum metric $\gamma_{\mu\nu}$,

$$g_{\mu\nu}(x) \equiv \bar{g}_{\mu\nu}(x) + \bar{h}_{\mu\nu}(x)\,, \tag{3.15}$$

and consider Γ_k as a functional of $g_{\mu\nu}$ rather than $\bar{h}_{\mu\nu}$:

$$\Gamma_k[g_{\mu\nu}, \bar{g}_{\mu\nu}, \xi^\mu, \bar{\xi}_\mu] \equiv \Gamma_k[g_{\mu\nu} - \bar{g}_{\mu\nu}, \xi^\mu, \bar{\xi}_\mu; \bar{g}_{\mu\nu}]\,. \tag{3.16}$$

So, what did we gain going through this seemingly complicated background field construction, eventually ending up with an action functional which depends on *two* metrics even? The main advantage of this setting is that the corresponding functionals $\widetilde{\Gamma}_k$, and as a result Γ_k, are invariant under general coordinate transformations where all its arguments

transform as tensors of the corresponding rank:

$$\Gamma_k[\Phi + \mathcal{L}_v\Phi] = \Gamma_k[\Phi]\,, \qquad\qquad \Phi \equiv \left\{g_{\mu\nu}, \bar{g}_{\mu\nu}, \xi^\mu, \bar{\xi}_\mu\right\}\,. \tag{3.17}$$

Note that in (3.17), contrary to the "quantum gauge transformation" (3.2), also the background metric transforms as an ordinary tensor field: $\delta\bar{g}_{\mu\nu} = \mathcal{L}_v\bar{g}_{\mu\nu}$. Eq. (3.17) is a consequence of

$$W_k\left[\mathcal{J} + \mathcal{L}_v\mathcal{J}\right] = W_k\left[\mathcal{J}\right]\,, \qquad \mathcal{J} \equiv \{t^{\mu\nu}, \sigma^\mu, \bar{\sigma}_\mu;\, \bar{g}_{\mu\nu}\}\,. \tag{3.18}$$

This invariance property follows from (3.3) if one performs a compensating transformation (3.8), (3.13) on the integration variables $h_{\mu\nu}$, C^μ and $\bar{C}_\mu$ and uses the invariance of $S[\bar{g}+h]$, $S_{\rm gf}$, $S_{\rm gh}$ and $\Delta_k S$. At this point we assume that the functional measure in (3.3) is diffeomorphism invariant.

Since the $\mathcal{R}_k$'s vanish for $k = 0$, the limit $k \to 0$ of $\Gamma_k[g_{\mu\nu}, \bar{g}_{\mu\nu}, \xi^\mu, \bar{\xi}_\mu]$ brings us back to the standard effective action functional which still depends on two metrics, though. The "ordinary" effective action $\Gamma[g_{\mu\nu}]$ with one metric argument is obtained from this functional by setting $\bar{g}_{\mu\nu} = g_{\mu\nu}$, or equivalently $\bar{h}_{\mu\nu} = 0$ [75, 76]:

$$\Gamma[g] \equiv \lim_{k\to 0}\Gamma_k[g, \bar{g} = g, \xi = 0, \bar{\xi} = 0] = \lim_{k\to 0}\Gamma_k[\bar{h} = 0, \xi = 0, \bar{\xi} = 0; g = \bar{g}]\,. \tag{3.19}$$

This equation brings about the "magic property" of the background field formalism: a priori the 1PI n-point functions of the metric are obtained by an n-fold functional differentiation of $\Gamma_0[\bar{h}, 0, 0; \bar{g}_{\mu\nu}]$ with respect to $\bar{h}_{\mu\nu}$. Hereby $\bar{g}_{\mu\nu}$ is kept fixed; it acts simply as an externally prescribed function which specifies the form of the gauge fixing condition. Hence the functional Γ_0 and the resulting *off-shell* Green functions do depend on $\bar{g}_{\mu\nu}$, but the *on-shell* Green functions, related to observable scattering amplitudes, do not depend on $\bar{g}_{\mu\nu}$. In this respect $\bar{g}_{\mu\nu}$ plays a role similar to the gauge parameter α in the standard approach. Remarkably, the same on-shell Green functions can be obtained by differentiating the functional $\Gamma[g_{\mu\nu}]$ of (3.19) with respect to $g_{\mu\nu}$, or equivalently

$\Gamma_0[\bar{h}=0,\xi=0,\bar{\xi}=0;\bar{g}=g]$, with respect to its $\bar{g}$ argument. In this context, 'on-shell' means that the metric satisfies the effective field equation $\delta\Gamma_0[g]/\delta g_{\mu\nu}=0$.

With (3.19) and its k-dependent counterpart

$$\bar{\Gamma}_k[g_{\mu\nu}] \equiv \Gamma_k[g_{\mu\nu}, g_{\mu\nu}, 0, 0] \tag{3.20}$$

we succeeded in constructing a diffeomorphism invariant generating functional for gravity: thanks to (3.17) $\Gamma[g_{\mu\nu}]$ and $\bar{\Gamma}_k[g_{\mu\nu}]$ are invariant under general coordinate transformations $\delta g_{\mu\nu}=\mathcal{L}_v g_{\mu\nu}$. However, there is a price to be paid for their invariance: the simplified functional $\bar{\Gamma}_k[g_{\mu\nu}]$ does not satisfy an exact RG equation, basically because it contains insufficient information. The actual RG evolution has to be performed at the level of the functional $\Gamma_k[g,\bar{g},\xi,\bar{\xi}\,]$. Only *after* the evolution one may set $\bar{g}=g$, $\xi=0,\bar{\xi}=0$. As a result, the actual theory space of QEG, $\{A[g,\bar{g},\xi,\bar{\xi}\,]\}$, consists of functionals of all four variables, $g_{\mu\nu},\bar{g}_{\mu\nu},\xi^\mu,\bar{\xi}_\mu$, subject to the invariance condition (3.17).

Taking a scale derivative of the regularized functional integral (3.3) and reexpressing the result in terms of Γ_k one finds the following FRGE [11]:

$$\begin{aligned}\partial_t\Gamma_k[\bar{h},\xi,\bar{\xi};\bar{g}] =& \frac{1}{2}\mathrm{Tr}\left[\left(\Gamma_k^{(2)}+\widehat{\mathcal{R}}_k\right)^{-1}_{\bar{h}\bar{h}}\left(\partial_t\widehat{\mathcal{R}}_k\right)_{\bar{h}\bar{h}}\right] \\ &-\frac{1}{2}\mathrm{Tr}\left[\left\{\left(\Gamma_k^{(2)}+\widehat{\mathcal{R}}_k\right)^{-1}_{\bar{\xi}\xi}-\left(\Gamma_k^{(2)}+\widehat{\mathcal{R}}_k\right)^{-1}_{\xi\bar{\xi}}\right\}\left(\partial_t\widehat{\mathcal{R}}_k\right)_{\bar{\xi}\xi}\right].\end{aligned} \tag{3.21}$$

Here $\Gamma_k^{(2)}$ denotes the Hessian of Γ_k with respect to the dynamical fields $\bar{h}$, ξ, $\bar{\xi}$ at fixed $\bar{g}$. It is a block matrix labeled by the fields $\varphi_i\equiv\{\bar{h}_{\mu\nu},\,\xi^\mu,\bar{\xi}_\mu\}$:

$$\Gamma_k^{(2)\,ij}(x,y) \equiv \frac{1}{\sqrt{\bar{g}(x)\bar{g}(y)}}\,\frac{\delta^2\Gamma_k}{\delta\varphi_i(x)\delta\varphi_j(y)}\,. \tag{3.22}$$

(In the ghost sector the derivatives are understood as left derivatives.) Likewise, $\widehat{\mathcal{R}}_k$ is a block diagonal matrix with entries $(\widehat{\mathcal{R}}_k)^{\mu\nu\rho\sigma}_{\bar{h}\bar{h}}\equiv\kappa^2(\mathcal{R}_k^{\mathrm{grav}}[\bar{g}])^{\mu\nu\rho\sigma}$ and $\widehat{\mathcal{R}}_{\bar{\xi}\xi}=\sqrt{2}\mathcal{R}_k^{\mathrm{gh}}[\bar{g}]$. Performing the trace in the position representation it includes an integration $\int d^dx\sqrt{\bar{g}(x)}$ involving the background volume element. For any cutoff which is qualitatively similar to

the exponential cutoff the traces on the RHS of eq. (3.21) are well convergent, both in the IR and the UV. The interplay between the $\widehat{\mathcal{R}}_k$ in the denominator and the factor $\partial_t \widehat{\mathcal{R}}_k$ in the numerator thereby ensures that the dominant contributions come from a narrow band of generalized momenta centered around k. Large momenta are exponentially suppressed.

Besides the FRGE the effective average action also satisfies an exact integro-differential equation, which can be used to find the $k \to \infty$ limit of the average action:

$$\Gamma_{k\to\infty}[\bar{h}, \xi, \bar{\xi}; \bar{g}] = S[\bar{g} + \bar{h}] + S_{\rm gf}[\bar{h}; \bar{g}] + S_{\rm gh}[\bar{h}, \xi, \bar{\xi}; \bar{g}]\,. \tag{3.23}$$

Intuitively, this limit can be understood from the observation that for $k \to \infty$ all quantum fluctuation in the path integral are suppressed by an infinity mass-term. Thus, in this limit no fluctuations are integrated out and $\Gamma_{k\to\infty}$ agrees with the microscopic action S supplemented by the gauge fixing and ghost actions. At the level of the functional $\bar{\Gamma}_k[g]$, eq. (3.23) boils down to $\bar{\Gamma}_{k\to\infty}[g] = S[g]$. However, as $\Gamma_k^{(2)}$ involves derivatives with respect to $\bar{h}_{\mu\nu}$ (or equivalently $g_{\mu\nu}$) at fixed $\bar{g}_{\mu\nu}$ it is clear that the evolution cannot be formulated entirely in terms of $\bar{\Gamma}_k$ alone.

The background gauge invariance of Γ_k, expressed in eq. (3.17), is of enormous practical importance. It implies that if the initial functional does not contain non-invariant terms, the flow will not generate such terms. Very often this reduces the number of terms to be retained in a reliable truncation ansatz quite considerably. Nevertheless, even if the initial action is simple, the RG flow will generate all sorts of local and non-local terms in Γ_k which are consistent with the symmetries.

4 Truncated flow equations

Solving the FRGE (3.21) subject to the initial condition (3.23) is equivalent to (and in practice as difficult as) calculating the original functional integral over $\gamma_{\mu\nu}$. It is therefore important to devise efficient approximation methods. The truncation of theory space is the one which makes maximum use of the FRGE reformulation of the quantum field theory

problem at hand.

As for the flow on the theory space $\{A[g,\bar{g},\xi,\bar{\xi}]\}$, a still very general truncation consists of neglecting the evolution of the ghost action by making the ansatz

$$\Gamma_k[g,\bar{g},\xi,\bar{\xi}] = \bar{\Gamma}_k[g] + \widehat{\Gamma}_k[g,\bar{g}] + S_{\rm gf}[g-\bar{g};\bar{g}] + S_{\rm gh}[g-\bar{g},\xi,\bar{\xi};\bar{g}]\,, \tag{4.1}$$

where we extracted the classical $S_{\rm gf}$ and $S_{\rm gh}$ from Γ_k. The remaining functional depends on both $g_{\mu\nu}$ and $\bar{g}_{\mu\nu}$. It is further decomposed as $\bar{\Gamma}_k + \widehat{\Gamma}_k$ where $\bar{\Gamma}_k$ is defined as in (3.20) and $\widehat{\Gamma}_k$ contains the deviations for $\bar{g} \neq g$. Hence, by definition, $\widehat{\Gamma}_k[g,g] = 0$, and $\widehat{\Gamma}_k$ contains, in particular, quantum corrections to the gauge fixing term which vanishes for $\bar{g} = g$, too. This ansatz satisfies the initial condition (3.23) if[4]

$$\bar{\Gamma}_{k\to\infty} = S \qquad \text{and} \qquad \widehat{\Gamma}_{k\to\infty} = 0\,. \tag{4.2}$$

Inserting (4.1) into the exact FRGE (3.21) one obtains an evolution equation on the truncated space $\{A[g,\bar{g}]\}$:

$$\begin{aligned}\partial_t\Gamma_k[g,\bar{g}] \;&=\; \frac{1}{2}{\rm Tr}\left[\left(\kappa^{-2}\Gamma_k^{(2)}[g,\bar{g}] + \mathcal{R}_k^{\rm grav}[\bar{g}]\right)^{-1}\partial_t\mathcal{R}_k^{\rm grav}[\bar{g}]\right] \\ &\quad -{\rm Tr}\left[\left(-\mathcal{M}[g,\bar{g}] + \mathcal{R}_k^{\rm gh}[\bar{g}]\right)^{-1}\partial_t\mathcal{R}_k^{\rm gh}[\bar{g}]\right]\,.\end{aligned} \tag{4.3}$$

This equation evolves the functional

$$\Gamma_k[g,\bar{g}] \equiv \bar{\Gamma}_k[g] + S_{\rm gf}[g-\bar{g};\bar{g}] + \widehat{\Gamma}_k[g,\bar{g}]\,. \tag{4.4}$$

Here $\Gamma_k^{(2)}$ denotes the Hessian of $\Gamma_k[g,\bar{g}]$ with respect to $g_{\mu\nu}$ at fixed $\bar{g}_{\mu\nu}$ and $\mathcal{M}$ is given in eq. (3.11).

The truncation ansatz (4.1) is still too general for practical calculations to be easily possible. The first truncation for which the RG flow has been found [11] is the "Einstein-Hilbert truncation" which retains in $\bar{\Gamma}_k[g]$ only the terms $\int d^dx\,\sqrt{g}$ and $\int d^dx\,\sqrt{g}R$, already

[4] See [77] for a detailed discussion of the relation between S and $S_{\rm bare}$.

present in the in the classical action, with k-dependent coupling constants, and includes only the wave function renormalization in $\widehat{\Gamma}_k$:

$$\Gamma_k[g,\bar{g}] = 2\kappa^2 Z_{Nk}\int d^dx\,\sqrt{g}\left\{-R+2\bar{\lambda}_k\right\} + \frac{Z_{Nk}}{2\alpha}\int d^dx\,\sqrt{\bar{g}}\,\bar{g}^{\mu\nu}F_\mu F_\nu\,. \tag{4.5}$$

In this case the truncation subspace is 2-dimensional. The ansatz (4.5) contains two free functions of the scale, the running cosmological constant $\bar{\lambda}_k$ and Z_{Nk} or, equivalently, the running Newton constant $G_k \equiv \bar{G}/Z_{Nk}$. Here $\bar{G}$ is a fixed constant, and $\kappa \equiv (32\pi\bar{G})^{-1/2}$. As for the gauge fixing term, F_μ is given by eq. (3.9) with $\bar{h}_{\mu\nu} \equiv g_{\mu\nu} - \bar{g}_{\mu\nu}$ replacing $h_{\mu\nu}$; it vanishes for $g = \bar{g}$. The ansatz (4.5) has the general structure of (4.1) with

$$\widehat{\Gamma}_k = (Z_{Nk}-1)S_{\rm gf}\,. \tag{4.6}$$

Within the Einstein-Hilbert approximation the gauge fixing parameter α is kept constant. Here we shall set $\alpha = 1$ and comment on generalizations later on.

Upon inserting the ansatz (4.5) into the flow equation (4.3) it boils down to a system of two ordinary differential equations for Z_{Nk} and $\bar{\lambda}_k$. Their derivation is rather technical, so we shall focus on the conceptual aspects here. In order to find $\partial_t Z_{Nk}$ and $\partial_t\bar{\lambda}_k$ it is sufficient to consider (4.3) for $g_{\mu\nu} = \bar{g}_{\mu\nu}$. In this case the LHS of the flow equation becomes $2\kappa^2\int d^dx\sqrt{\bar{g}}[-R\partial_t Z_{Nk} + 2\partial_t(Z_{Nk}\bar{\lambda}_k)]$. The RHS is assumed to admit an expansion in terms of invariants $P_i[g_{\mu\nu}]$. In the Einstein-Hilbert truncation only two of them, $\int d^dx\,\sqrt{\bar{g}}$ and $\int d^dx\,\sqrt{\bar{g}}R$, need to be retained. They can be extracted from the traces in (4.3) by standard derivative expansion techniques. Equating the result to the LHS and comparing the coefficients of $\int d^dx\sqrt{\bar{g}}$ and $\int d^dx\sqrt{\bar{g}}R$, a pair of coupled differential equations for Z_{Nk} and $\bar{\lambda}_k$ arises. It is important to note that, on the RHS, we may set $g_{\mu\nu} = \bar{g}_{\mu\nu}$ only *after* the functional derivatives of $\Gamma_k^{(2)}$ have been obtained since they must be taken at fixed $\bar{g}_{\mu\nu}$.

As demonstrated explicitly in [27, 36], this calculation can be performed without ever considering any specific metric $g_{\mu\nu} = \bar{g}_{\mu\nu}$. This reflects the fact that the approach is

background covariant. The RG flow is universal in the sense that it does not depend on any specific metric. In this respect gravity is not different from the more traditional applications of the renormalization group: the RG flow in the Ising universality class, say, has nothing to do with any specific spin configuration, it rather reflects the statistical properties of very many such configurations.

While there is no conceptual necessity to fix the background metric, it nevertheless is sometimes advantageous from a computational point of view to pick a specific class of backgrounds. Leaving $\bar{g}_{\mu\nu}$ completely general, the calculation of the functional traces is very hard work usually. In principle there exist well known derivative expansion and heat kernel techniques which could be used for this purpose, but their application is an extremely lengthy and tedious task usually. Moreover, typically the operators $\Gamma_k^{(2)}$ and $\mathcal{R}_k$ are of a complicated non-standard type so that no efficient use of the tabulated Seeley coefficients can be made. However, often calculations of this type simplify if one can assume that $g_{\mu\nu} = \bar{g}_{\mu\nu}$ has specific properties. Since the beta functions are background independent we may therefore restrict $\bar{g}_{\mu\nu}$ to lie in a conveniently chosen class of geometries which is still general enough to disentangle the invariants retained and at the same time simplifies the calculation.

For the Einstein-Hilbert truncation the most efficient choice is a family of d-spheres $S^d(r)$, labeled by their radius r. These maximally symmetric backgrounds satisfy

$$R_{\mu\nu} = \tfrac{1}{d} g_{\mu\nu} R\,, \qquad R_{\mu\nu\rho\sigma} = \tfrac{1}{d(d-1)}(g_{\mu\rho}g_{\nu\sigma} - g_{\mu\sigma}g_{\nu\rho})R\,, \tag{4.7}$$

and, in particular, $D_\alpha R_{\mu\nu\rho\sigma} = 0$, so they give a vanishing value to all invariants constructed from $g = \bar{g}$ containing covariant derivatives acting on curvature tensors. What remains (among the local invariants) are terms of the form $\int\sqrt{g}P(R)$, where P is a polynomial in the Ricci scalar. Up to linear order in R the two invariants relevant for the Einstein-Hilbert truncation are discriminated by the S^d metrics as the latter scale differently with the radius of the sphere: $\int\sqrt{g} \sim r^d$, $\int\sqrt{g}R \sim r^{d-2}$. Thus, in order to compute the beta functions of $\bar{\lambda}_k$ and Z_{Nk} it is sufficient to insert an S^d metric with arbitrary r and to

compare the coefficients of r^d and r^{d-2}. If one wants to do better and include the three quadratic invariants $\int R_{\mu\nu\rho\sigma}R^{\mu\nu\rho\sigma}$, $\int R_{\mu\nu}R^{\mu\nu}$, and $\int R^2$, the family $S^d(r)$ is not general enough to separate them; all scale like r^{d-4} with the radius.

Under the trace we need the operator $\Gamma_k^{(2)}[\bar{h};\bar{g}]$. It is most easily calculated by Taylor expanding the truncation ansatz, $\Gamma_k[\bar{g}+\bar{h},\bar{g}] = \Gamma_k[\bar{g},\bar{g}] + O(\bar{h}) + \Gamma_k^{\rm quad}[\bar{h};\bar{g}] + O(\bar{h}^3)$, and stripping off the two $\bar{h}$'s from the quadratic term, $\Gamma_k^{\rm quad} = \frac{1}{2}\int \bar{h}\Gamma_k^{(2)}\bar{h}$. For $\bar{g}_{\mu\nu}$ the metric on $S^d(r)$ one obtains

$$\begin{aligned}\Gamma_k^{\rm quad}[\bar{h};\bar{g}] \;&=\; \frac{1}{2}Z_{Nk}\kappa^2\int d^dx\,\Big\{\widehat{h}_{\mu\nu}\left[-\bar{D}^2 - 2\bar{\lambda}_k + C_T\bar{R}\right]\widehat{h}^{\mu\nu} \\ &\qquad - \left(\frac{d-2}{2d}\right)\phi\left[-\bar{D}^2 - 2\bar{\lambda}_k + C_S\bar{R}\right]\phi\Big\}\,, \qquad (4.8)\end{aligned}$$

with $C_T \equiv (d(d-3)+4)/(d(d-1))$, $C_S \equiv (d-4)/d$. In order to partially diagonalize this quadratic form $\bar{h}_{\mu\nu}$ has been decomposed into a traceless part $\widehat{h}_{\mu\nu}$ and the trace part proportional to ϕ: $\bar{h}_{\mu\nu} = \widehat{h}_{\mu\nu} + d^{-1}\bar{g}_{\mu\nu}\phi$, $\bar{g}^{\mu\nu}\widehat{h}_{\mu\nu} = 0$. Further, $\bar{D}^2 = \bar{g}^{\mu\nu}\bar{D}_\mu\bar{D}_\nu$ is the covariant Laplace operator corresponding to the background geometry, and $\bar{R} = d(d-1)/r^2$ is the numerical value of the curvature scalar on $S^d(r)$.

At this point we can fix the constants $\mathcal{Z}_k$ which appear in the cutoff operators $\mathcal{R}_k^{\rm grav}$ and $\mathcal{R}_k^{\rm gh}$ of (3.13). They should be adjusted in such a way that for every low–momentum mode the cutoff combines with the kinetic term of this mode to $-\bar{D}^2+k^2$ times a constant. Looking at (4.8) we see that the respective kinetic terms for $\widehat{h}_{\mu\nu}$ and ϕ differ by a factor of $-(d-2)/2d$. This suggests the following choice:

$$\left(\mathcal{Z}_k^{\rm grav}\right)^{\mu\nu\rho\sigma} = \left[(\mathbb{1}-P_\phi)^{\mu\nu\rho\sigma} - \frac{d-2}{2}P_\phi^{\mu\nu\rho\sigma}\right]Z_{Nk}\,. \qquad (4.9)$$

Here $(P_\phi)_{\mu\nu}{}^{\rho\sigma} = d^{-1}\bar{g}_{\mu\nu}\bar{g}^{\rho\sigma}$ is the projector on the trace part of the metric. For the traceless tensor (4.9) gives $\mathcal{Z}_k^{\rm grav} = Z_{Nk}\mathbb{1}$, and for ϕ the different relative normalization is taken into account. (See ref. [11] for a detailed discussion of the subtleties related to this

choice.) Thus we obtain in the $\widehat{h}$ and the ϕ-sector, respectively:

$$\begin{aligned}\left(\kappa^{-2}\Gamma_k^{(2)}[g,g]+\mathcal{R}_k^{\rm grav}\right)_{\widehat{h}\widehat{h}} &= Z_{Nk}\left[-D^2+k^2R^{(0)}(-D^2/k^2)-2\bar{\lambda}_k+C_TR\right], \qquad (4.10)\\ \left(\kappa^{-2}\Gamma_k^{(2)}[g,g]+\mathcal{R}_k^{\rm grav}\right)_{\phi\phi} &= -\frac{d-2}{2d}Z_{Nk}\left[-D^2+k^2R^{(0)}(-D^2/k^2)-2\bar{\lambda}_k+C_SR\right]\end{aligned}$$

From now on we may set $\bar{g}=g$ and for simplicity we have omitted the bars from the metric and the curvature. Since we did not take into account any renormalization effects in the ghost action we set $Z_k^{\rm gh}\equiv 1$ in $\mathcal{R}_k^{\rm gh}$ and obtain

$$-\mathcal{M}+\mathcal{R}_k^{\rm gh}=-D^2+k^2R^{(0)}(-D^2/k^2)+C_VR\,, \qquad (4.11)$$

with $C_V\equiv -1/d$. At this point the operator under the first trace on the RHS of (4.3) has become block diagonal, with the $\widehat{h}\widehat{h}$ and $\phi\phi$ blocks given by (4.10). Both block operators are expressible in terms of the Laplacian D^2, in the former case acting on traceless symmetric tensor fields, in the latter on scalars. The second trace in (4.3) stems from the ghosts; it contains (4.11) with D^2 acting on vector fields.

It is now a matter of straightforward algebra to compute the first two terms in the derivative expansion of those traces, proportional to $\int d^dx\sqrt{g}\sim r^d$ and $\int d^dx\sqrt{g}R\sim r^{d-2}$. Considering the trace of an arbitrary function of the Laplacian, $W(-D^2)$, the expansion up to second order derivatives of the metric is given by

$$\begin{aligned}{\rm Tr}[W(-D^2)] &= (4\pi)^{-d/2}{\rm tr}(I)\Bigg\{Q_{d/2}[W]\int d^dx\,\sqrt{g}\\ &\qquad +\frac{1}{6}Q_{d/2-1}[W]\int d^dx\,\sqrt{g}R+O(R^2)\Bigg\}. \qquad (4.12)\end{aligned}$$

The Q_n's are defined as

$$Q_n[W]=\frac{1}{\Gamma(n)}\int_0^\infty dz\,z^{n-1}W(z)\,, \qquad (4.13)$$

for $n>0$, and $Q_0[W]=W(0)$ for $n=0$. The trace ${\rm tr}(I)$ counts the number of independent

field components. It equals 1, d, and $(d-1)(d+2)/2$, for scalars, vectors, and symmetric traceless tensors, respectively. The expansion (4.12) is easily derived using standard heat kernel and Mellin transform techniques [11].

Using (4.12) it is easy to calculate the traces in (4.3) and to obtain the RG equations in the form $\partial_t Z_{Nk} = \cdots$ and $\partial_t(Z_{Nk}\bar{\lambda}_k) = \cdots$. We shall not display them here since it is more convenient to rewrite them in terms of the dimensionless running cosmological constant and Newton constant, respectively:

$$\lambda_k \equiv k^{-2}\bar{\lambda}_k\,, \qquad g_k \equiv k^{d-2}G_k \equiv k^{d-2}Z_{Nk}^{-1}\bar{G}\,. \tag{4.14}$$

In terms of the dimensionless couplings g and λ the RG equations become a system of autonomous differential equations

$$\partial_t g_k = \beta_g(g_k,\lambda_k)\,, \qquad \partial_t \lambda_k = \beta_\lambda(g_k,\lambda_k)\,, \tag{4.15}$$

where

$$\begin{aligned}\beta_\lambda(g,\lambda) &= (\eta_N - 2)\lambda + \tfrac{1}{2}\,(4\pi)^{1-d/2}\,g \\ &\quad\times\left[2d(d+1)\Phi^1_{d/2}(-2\lambda) - 8d\Phi^1_{d/2}(0) - d(d+1)\eta_N\tilde{\Phi}^1_{d/2}(-2\lambda)\right]\,, \\ \beta_g(g,\lambda) &= (d-2+\eta_N)g\,.\end{aligned} \tag{4.16}$$

Here the anomalous dimension of Newton's constant η_N is given by

$$\eta_N(g,\lambda) = \frac{gB_1(\lambda)}{1-gB_2(\lambda)} \tag{4.17}$$

with the following functions of the dimensionless cosmological constant:

$$\begin{aligned}B_1(\lambda) &\equiv \tfrac{1}{3}\,(4\pi)^{1-d/2}\left[d(d+1)\Phi^1_{d/2-1}(-2\lambda) - 6d(d-1)\Phi^2_{d/2}(-2\lambda)\right. \\ &\qquad\left. - 4d\Phi^1_{d/2-1}(0) - 24\Phi^2_{d/2}(0)\right]\,, \\ B_2(\lambda) &\equiv -\tfrac{1}{6}(4\pi)^{1-d/2}\left[d(d+1)\tilde{\Phi}^1_{d/2-1}(-2\lambda) - 6d(d-1)\tilde{\Phi}^2_{d/2}(-2\lambda)\right]\,.\end{aligned} \tag{4.18}$$

The system (4.15) constitutes an approximation to a 2-dimensional projection of the RG flow. Its properties, and in particular the domain of applicability and reliability will be discussed in section 5.

The "threshold functions" Φ and $\widetilde{\Phi}$ appearing in (4.16) and (4.18) are certain integrals involving the normalized cutoff function $R^{(0)}$:

$$\begin{aligned}\Phi_n^p(w) &\equiv \frac{1}{\Gamma(n)}\int_0^\infty dz\, z^{n-1}\frac{R^{(0)}(z)-zR^{(0)\prime}(z)}{[z+R^{(0)}(z)+w]^p}\,,\\ \widetilde{\Phi}_n^p(w) &\equiv \frac{1}{\Gamma(n)}\int_0^\infty dz\, z^{n-1}\frac{R^{(0)}(z)}{[z+R^{(0)}(z)+w]^p}\,.\end{aligned} \tag{4.19}$$

They are defined for positive integers p, and $n > 0$. While there are (few) aspects of the truncated RG flow which are independent of the cutoff scheme, i.e., independent of the function $R^{(0)}$, the explicit solution of the flow equation requires a specific choice of this function. In the literature various forms of $R^{(0)}$'s have been employed. E.g., the non-differentiable "optimized cutoff" [78] with $R^{(0)}(w) = (1-w)\theta(1-w)$ allows for an analytic evaluation of the integrals [23]

$$\Phi_n^{\rm opt;p}(w) = \frac{1}{\Gamma(n+1)}\frac{1}{1+w}\,, \qquad \widetilde{\Phi}_n^{\rm opt;p}(w) = \frac{1}{\Gamma(n+2)}\frac{1}{1+w}\,. \tag{4.20}$$

Easy to handle, but disadvantageous for high precision calculations is the sharp cutoff [14] defined by $\mathcal{R}_k(p^2) = \lim_{\hat{R}\to\infty}\hat{R}\,\theta(1-p^2/k^2)$, where the limit is to be taken after the p^2 integration. This cutoff also allows for an evaluation of the Φ and $\widetilde{\Phi}$ integrals in closed form. Taking $d = 4$ as an example, eqs. (4.15) boil down to the following simple system of equations:[5]

$$\partial_t\lambda_k = -(2-\eta_N)\lambda_k - \frac{g_k}{\pi}\Big[5\ln(1-2\lambda_k) - 2\zeta(3) + \frac{5}{2}\eta_N\Big]\,, \tag{4.21a}$$

$$\partial_t g_k = (2+\eta_N)\,g_k\,, \tag{4.21b}$$

$$\eta_N = -\frac{2\,g_k}{6\pi+5\,g_k}\Big[\frac{18}{1-2\lambda_k} + 5\ln(1-2\lambda_k) - \zeta(2) + 6\Big]\,. \tag{4.21c}$$

[5] To be precise, (4.21) corresponds to the sharp cutoff with $s = 1$, see [14].

In order to check the scheme (in)dependence of the results it is desirable to perform the calculation for a whole class of $R^{(0)}$'s. For this purpose the following one parameter family of exponential cutoffs has been used [13, 15, 18]:

$$R^{(0)}(w;s) = \frac{sw}{e^{sw}-1}\,. \tag{4.22}$$

The precise form of the cutoff is controlled by the "shape parameter" s. For $s = 1$, (4.22) coincides with the standard exponential cutoff. The exponential cutoffs are suitable for precision calculations, but the price to be paid is that their Φ and $\widetilde{\Phi}$ integrals can be evaluated only numerically. The same is true for a one-parameter family of shape functions with compact support which was used in [13, 15].

Above we illustrated the general ideas and constructions underlying gravitational RG flows by means of the simplest example, the Einstein-Hilbert truncation. In the literature various extensions have been investigated. The derivation and analysis of these more general flow equations, corresponding to higher dimensional truncation subspaces, is an extremely complex and computationally demanding problem in general. For this reason we cannot go into the technical details here and just mention some further developments.

(1) The natural next step beyond the Einstein-Hilbert truncation consists in generalizing the functional $\bar{\Gamma}_k[g]$, while keeping the gauge fixing and ghost sector classical, as in (4.1). During the RG evolution the flow generates all possible diffeomorphism invariant terms in $\bar{\Gamma}_k[g]$ which one can construct from $g_{\mu\nu}$. Both local and non-local terms are induced. The local invariants contain strings of curvature tensors and covariant derivatives acting upon them, with any number of tensors and derivatives, and of all possible index structures. The first truncation of this class which has been worked out completely [15, 16] is the ***R*²-truncation** defined by (4.1) with the same $\widehat{\Gamma}_k$ as before, and the (curvature)^2 action

$$\bar{\Gamma}_k[g] = \int d^dx\sqrt{g}\Big\{(16\pi G_k)^{-1}[-R+2\bar{\lambda}_k] + \bar{\beta}_k R^2\Big\}\,. \tag{4.23}$$

In this case the truncated theory space is 3-dimensional. Its natural (dimensionless)

coordinates are (g, λ, β), where $\beta_k \equiv k^{4-d}\bar{\beta}_k$, and g and λ defined in (4.14). Even though (4.23) contains only one additional invariant, the derivation of the corresponding RG equations is far more complicated than in the Einstein-Hilbert case. We shall summarize the results obtained with (4.23) [15, 16] in section 5.2.

(2) The natural **extension of the R^2-truncation** consists of including all gravitational four-derivative terms in the truncation subspace

$$\bar{\Gamma}_k[g] = \int d^4x\sqrt{g}\left[(16\pi G_k)^{-1}\left[-R + 2\bar{\lambda}_k\right] - \frac{\omega_k}{3\sigma_k}R^2 + \frac{1}{2\sigma_k}C_{\mu\nu\rho\sigma}C^{\mu\nu\rho\sigma} + \frac{\theta_k}{\sigma_k}E\right], \quad (4.24)$$

and adapting the classical gauge-fixing and ghost sectors to higher-derivative gravity. Here $C_{\mu\nu\rho\sigma}C^{\mu\nu\rho\sigma}$ denotes the square of the Weyl tensor, and $E = C_{\mu\nu\rho\sigma}C^{\mu\nu\rho\sigma} - 2R_{\mu\nu}R^{\mu\nu} + \frac{2}{3}R^2$ is the integrand of the (topological) Gauss-Bonnet term in four dimensions. Using the FRGE (3.21), the one-loop beta functions for higher-derivative gravity have recently been recovered in [22, 79, 80], while first non-perturbative results have been obtained in [32, 33]. The key ingredient in the non-perturbative works was the generalization of the background metric $\bar{g}$ from the spherical symmetric background employed in the R^2-truncation to a generic Einstein background. The former case results in a flow equation for $\beta_k = -\frac{\omega_k}{3\sigma_k} + \frac{\theta_k}{6\sigma_k}$, while working with a generic Einstein background metric allows to find the non-perturbative beta functions for two independent combinations of the coupling constants

$$\beta_k = -\frac{\omega_k}{3\sigma_k} + \frac{\theta_k}{6\sigma_k}, \qquad \gamma_k = \frac{1}{2\sigma_k} + \frac{\theta_k}{\sigma_k}. \quad (4.25)$$

The results obtained from this so-called $R^2 + C^2$-truncation are detailed in section 5.3.

(3) The first steps towards analyzing the RG flow of QEG in the **ghost sector** have recently be undertaken in [81–83]. In the first step, the classical ghost sector of the Einstein-Hilbert truncation (3.10) has been supplemented by a scale-dependent curvature ghost coupling $\bar{\zeta}_k$ in the form $\Gamma_k^{\mathrm{R\,gh}} = \bar{\zeta}_k \int d^dx\sqrt{g}\,\bar{\xi}^\mu\, R\,\xi_\mu$ where it was found that $\bar{\zeta}_k = 0$ constitutes a fixed point of the RG flow, with $\bar{\zeta}_k$ being associated with an UV-attractive eigendirection. The backreaction of a non-trivial ghost-wavefunction renormalization on

the flow of g_k and λ_k was subsequently studied in [82, 83], where it was established that the ghost-propagator is UV-suppressed by a negative anomalous dimension. Moreover, the phase-diagram of the ghost-improved Einstein-Hilbert truncation is almost identical to the one obtained without ghost-improvements shown in fig. 4.

(4) There are also partial results concerning the **gauge fixing term**. Even if one makes the ansatz (4.5) for $\Gamma_k[g, \bar{g}]$ in which the gauge fixing term has the classical (or more appropriately, bare) structure one should treat its prefactor as a running coupling: $\alpha = \alpha_k$. The beta function of α has not been determined yet from the FRGE, but there is a simple argument which allows us to bypass this calculation.

In non-perturbative Yang-Mills theory and in perturbative quantum gravity $\alpha = \alpha_k = 0$ is known to be a fixed point for the α evolution. The following reasoning suggests that the same is true within the non-perturbative FRGE approach to gravity. In the standard functional integral the limit $\alpha \to 0$ corresponds to a sharp implementation of the gauge fixing condition, i.e., $\exp(-S_{\rm gf})$ becomes proportional to $\delta[F_\mu]$. The domain of the $\int \mathcal{D}h_{\mu\nu}$ integration consists of those $h_{\mu\nu}$'s which satisfy the gauge fixing condition exactly, $F_\mu = 0$. Adding the IR cutoff at k amounts to suppressing some of the $h_{\mu\nu}$ modes while retaining the others. But since all of them satisfy $F_\mu = 0$, a variation of k cannot change the domain of the $h_{\mu\nu}$ integration. The delta functional $\delta[F_\mu]$ continues to be present for any value of k if it was there originally. As a consequence, α vanishes for all k, i.e., $\alpha = 0$ is a fixed point of the α evolution [84].

Thus we can mimic the dynamical treatment of a running α by setting the gauge fixing parameter to the constant value $\alpha = 0$. The calculation for $\alpha = 0$ is more complicated than at $\alpha = 1$, but for the Einstein-Hilbert truncation the α-dependence of β_g and β_λ, for arbitrary constant α has been found in [13,85]. The R^2-truncations could be analyzed only in the simple $\alpha = 1$ gauge, but the results from the Einstein-Hilbert truncation suggest the UV quantities of interest do not change much between $\alpha = 0$ and $\alpha = 1$ [13, 15].

(5) In refs. [28–30] gravitational RG flows have been explored in an approximation that goes beyond a truncation of theory space. Here only the subsector of the basic path

integral over the conformal degrees of freedom has been considered while all others were omitted. This leads to a scalar-like theory to which the same apparatus underlying the analysis of the full theory has been applied (average action, background decomposition). Remarkably, this **conformally reduced gravity** (contrary to a standard 4-dimensional scalar theory) possesses a NGFP and a RG flow that is qualitatively similar to that of full QEG. It was possible to establish the existence of the NGFP on an *infinite dimensional* theory space consisting of arbitrary potentials for the conformal factor. These somewhat unexpected results find their explanation [28, 29] by noting that the quantization scheme based upon the (conformal reduction of the) gravitational average action is *"background independent"* in the sense that no special metric (flat space, etc.) plays a distinguished role.

(6) Up to now we considered pure gravity. As for as the general formalism, the **inclusion of matter fields** is straightforward. The structure of the flow equation remains unaltered, except that now $\Gamma_k^{(2)}$ and $\mathcal{R}_k$ are operators on the larger Hilbert space of both gravity and matter fluctuations. In practice the derivation of the projected RG equations can be quite a formidable task, however, the difficult part being the decoupling of the various modes (diagonalization of $\Gamma_k^{(2)}$) which in most calculational schemes is necessary for the computation of the functional traces. Various matter systems, both interacting and non-interacting (apart from their interaction with gravity) have been studied in the literature [12, 86, 87]. A rather detailed analysis has been performed by Percacci et al. In [12, 21] arbitrary multiplets of free (massless) fields with spin $0, 1/2, 1$ and $3/2$ were included. In [21] an interacting scalar theory coupled to gravity in the Einstein-Hilbert approximation was analyzed, and a possible solution to the triviality and the hierarchy problem [88] was a first application in this context.

(7) At the perturbative one-loop level, the flow of possibly **non-local form factors** appearing in the curvature expansion of the effective average action has been studied in [89,90]. For a a minimally coupled scalar field on a 2-dimensional curved space-time, the flow equation for the form factor in $\int d^dx\sqrt{g}Rc_k(\Delta)R$ correctly reproduces the Polyakov effective action, while in $d = 4$ this ansatz allows to recover the low energy effective action

as derived in the effective field theory framework [91].

(8) As yet, almost all truncations studied are of the "single metric" type where Γ_k depends on $\bar{g}_{\mu\nu}$ via the gauge fixing term only. The investigation of genuine **bimetric truncations** with a nontrivial dependence on both $g_{\mu\nu}$ and $\bar{g}_{\mu\nu}$ started only recently in [92,93]. Future work on the verification of the NGFP has to go in this direction clearly.

(9) In ref. [94] a first investigation of **Lorentzian gravity** was performed in a 3+1 split setting. In this case the flow equation (1.1) has been formulated in terms of the ADM-decomposed metric degrees of freedom, which imprints a foliation structure on space-time and provides a preferred "time-direction". The resulting FRGE depends on an additional parameter ϵ, which encodes the signature of the space-time metric. For a fixed truncation the resulting Lorentzian renormalization group flow turned out almost identical to the one obtained in the Euclidean case.

(10) A first step towards **new gravitational field variables**, different from the metric, was taken in [95]. Employing the vielbein and spin connection as independent variables, the question of Asymptotic Safety was reconsidered. In principle it is conceivable that an Einstein-Cartan type quantum field theory is inequivalent to QEG. However, the actual calculations support the conjecture that "Quantum Einstein-Cartan Gravity" is asymptotically safe, too.[6]

5 Average action approach to Asymptotic Safety

Based on the exact flow equation (1.1), we now implement the ideas of the Asymptotic Safety construction at the level of explicitly computable approximate RG flows on truncated theory spaces. A summary of the truncations explored to date is provided in fig. 3. For a detailed derivation of the beta functions we refer to [11] (Einstein-Hilbert truncation), [15] (R^2-truncation), [26] ($f(R)$-truncation), and [33] for the $R^2 + C^2$-truncation, respectively.

[6] Also see [96] for a perturbative analysis of the running Immirzi parameter.

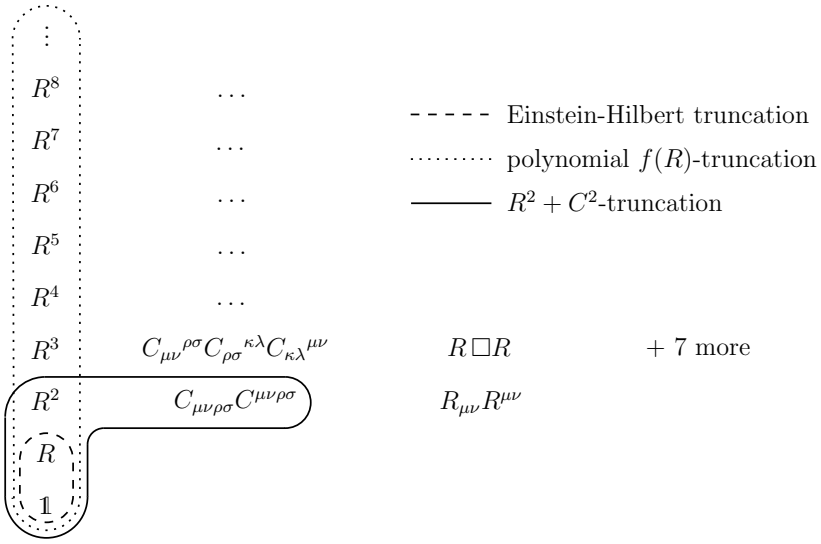

Figure 3: Overview of the various truncations employed in the systematic exploration of the theory space of QEG. The lines indicate the interaction monomials contained in the various truncation ansätze for $\bar{\Gamma}_k[g]$, eq. (4.4). All truncations have confirmed the existence of a non-trivial UV fixed point of the gravitational RG flow.

5.1 The Einstein-Hilbert truncation

The Einstein-Hilbert truncation (4.5) constitutes the most prominent truncation studied to date [11, 13, 14, 18, 23, 27, 36]. In [14] the corresponding RG equations (4.15) have been analyzed in detail, using both analytical and numerical methods. In particular all RG trajectories have been classified, and examples have been computed numerically. The most important classes of trajectories in the phase portrait on the g-$\lambda-$plane are shown in fig. 4. Notably, all cutoffs tested to date confirm this picture at least qualitatively.

The RG flow is found to be dominated by two fixed points (g^*, λ^*): the GFP at $g^* = \lambda^* = 0$, and a NGFP with $g^* > 0$ and $\lambda^* > 0$. There are three classes of trajectories emanating from the NGFP: trajectories of Type Ia and IIIa run towards negative and positive cosmological constants, respectively, and the single trajectory of Type IIa ("separatrix") hits the GFP for $k \to 0$. The high momentum properties of QEG are governed by the NGFP; for $k \to \infty$, in fig. 4 all RG trajectories on the half–plane $g > 0$ run into this point. The fact that at the NGFP the dimensionless coupling constants g_k, λ_k approach

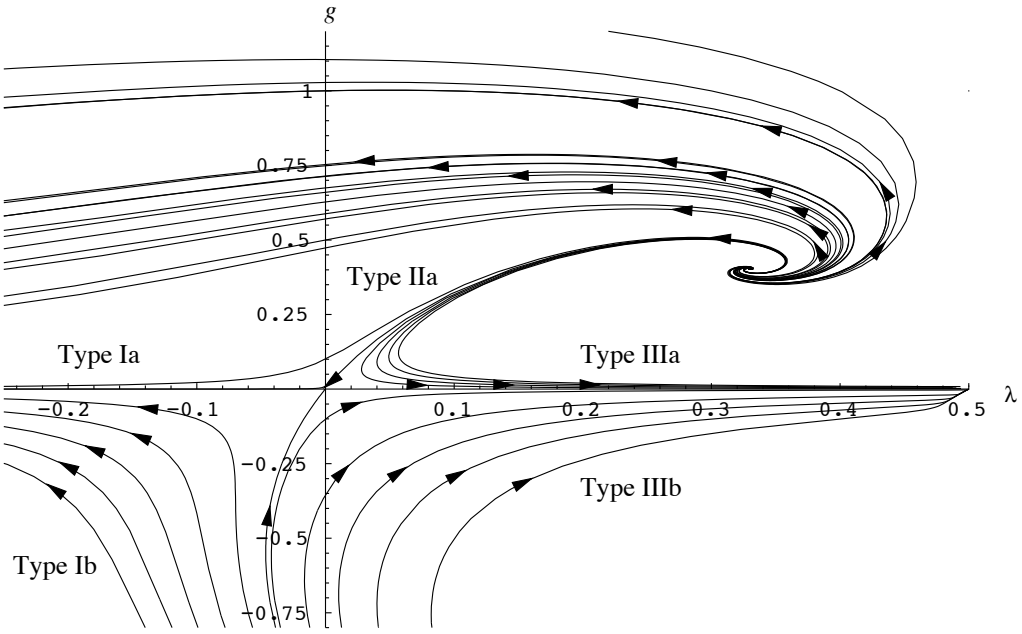

Figure 4: RG flow in the g-$\lambda-$plane. The arrows point in the direction of increasing coarse graining, i.e., of decreasing k. (From [14].)

constant, non-zero values then implies that the dimensionful quantities run according to

$$G_k = g^* k^{2-d}\,, \qquad \bar{\lambda}_k = \lambda^*\, k^2\,. \tag{5.1}$$

Hence for $k \to \infty$ and $d > 2$ the dimensionful Newton constant vanishes while the cosmological constant diverges.

Thus the Einstein-Hilbert truncation does indeed predict the existence of a NGFP with exactly the properties needed for the Asymptotic Safety construction. Clearly the crucial question now is whether this NGFP is the projection of a fixed point in the exact theory or whether it is merely the artifact of an insufficient approximation. We now summarize the properties of the NGFP established within the Einstein-Hilbert truncation. All findings mentioned below are independent pieces of evidence pointing in the direction that QEG is indeed asymptotically safe in four dimensions. Except for point (5) all results refer to $d = 4$.

(1) Universal existence: The non-Gaussian fixed point exists for all cutoff schemes and

shape functions implemented to date. It seems impossible to find an admissible cutoff which destroys the fixed point in $d = 4$. This result is highly non-trivial since in higher dimensions ($d \gtrsim 5$) the existence of the NGFP depends on the cutoff chosen [14].

(2) Positive Newton constant: While the position of the fixed point is scheme dependent, all cutoffs yield *positive* values of g^* and λ^*. A negative g^* might have been problematic for stability reasons, but there is no mechanism in the flow equation which would exclude it on general grounds.

(3) Stability: For any cutoff employed the NGFP is found to be UV attractive in both directions of the λ-$g-$plane. Linearizing the flow equation according to eq. (2.6) we obtain a pair of complex conjugate critical exponents $\theta_1 = \theta_2^*$ with positive real part θ' and imaginary parts $\pm\theta''$. In terms of $t = \ln(k/k_0)$ the general solution to the linearized flow equations reads

$$\begin{aligned}(\lambda_k, g_k)^{\mathbf{T}} &= (\lambda^*, g^*)^{\mathbf{T}} + 2\Big\{ \left[\mathrm{Re}\, C\, \cos\left(\theta'' t\right) + \mathrm{Im}\, C\, \sin\left(\theta'' t\right)\right] \mathrm{Re}\, V \\ &\quad + \left[\mathrm{Re}\, C\, \sin\left(\theta'' t\right) - \mathrm{Im}\, C\, \cos\left(\theta'' t\right)\right] \mathrm{Im}\, V \Big\} e^{-\theta' t}\,. \end{aligned} \tag{5.2}$$

with $C \equiv C_1 = (C_2)^*$ an arbitrary complex number and $V \equiv V^1 = (V^2)^*$ the right-eigenvector of $\mathbf{B}$ with eigenvalue $-\theta_1 = -\theta_2^*$. Eq. (2.6) implies that, due to the positivity of θ', all trajectories hit the fixed point as t is sent to infinity. The non-vanishing imaginary part θ'' has no impact on the stability. However, it influences the shape of the trajectories which spiral into the fixed point for $k \to \infty$. Thus, the fixed point has the stability properties needed in the Asymptotic Safety scenario.

Solving the full, non-linear flow equations [14] shows that the asymptotic scaling region where the linearization (5.2) is valid extends from $k = \infty$ down to about $k \approx m_{\mathrm{Pl}}$ with the Planck mass defined as $m_{\mathrm{Pl}} \equiv G_0^{-1/2}$. Here m_{Pl} plays a role similar to Λ_{QCD} in QCD: it marks the lower boundary of the asymptotic scaling region. We set $k_0 \equiv m_{\mathrm{Pl}}$ so that the asymptotic scaling regime extends from about $t = 0$ to $t = \infty$.

(4) Scheme- and gauge dependence: Analyzing the cutoff scheme dependence of θ', θ'', and $g^*\lambda^*$ as a measure for the reliability of the truncation, the critical exponents were found to be reasonably constant within about a factor of 2. For $\alpha = 1$ and $\alpha = 0$, for instance, they assume values in the ranges $1.4 \lesssim \theta' \lesssim 1.8$, $2.3 \lesssim \theta'' \lesssim 4$ and $1.7 \lesssim \theta' \lesssim 2.1$, $2.5 \lesssim \theta'' \lesssim 5$, respectively. The universality properties of the product $g^*\lambda^*$ are even more impressive. Despite the rather strong scheme dependence of g^* and λ^* separately, their product has almost no visible s-dependence for not too small values of s. Its value is

$$g^*\lambda^* \approx \begin{cases} 0.12 \text{ for } \alpha = 1 \\ 0.14 \text{ for } \alpha = 0\,. \end{cases} \tag{5.3}$$

The difference between the "physical" (fixed point) value of the gauge parameter, $\alpha = 0$, and the technically more convenient $\alpha = 1$ are at the level of about 10 to 20 percent.

(5) Higher and lower dimensions: The beta functions implied by the FRGE are continuous functions of the space-time dimensionality and it is instructive to analyze them for $d \neq 4$. In ref. [11] it has been shown that for $d = 2 + \varepsilon$, $|\varepsilon| \ll 1$, the FRGE reproduces Weinberg's [9] fixed point for Newton's constant, $g^* = \frac{3}{38}\varepsilon$, and also supplies a corresponding fixed point value for the cosmological constant, $\lambda^* = -\frac{3}{38}\Phi^1_1(0)\varepsilon$, with the threshold function given in (4.19). For arbitrary d and a generic cutoff the RG flow is quantitatively similar to the 4-dimensional one for all d smaller than a certain critical dimension $d_{\rm crit}$, above which the existence or non-existence of the NGFP becomes cutoff-dependent. The critical dimension is scheme dependent, but for any admissible cutoff it lies well above $d = 4$. As d approaches $d_{\rm crit}$ from below, the scheme dependence of the universal quantities increases drastically, indicating that the R-truncation becomes insufficient near $d_{\rm crit}$.

In fig. 5 we show the d-dependence of g^*, λ^*, θ', and θ'' for two versions of the sharp cutoff (with $s = 1$ and $s = 30$, respectively) and for the exponential cutoff with $s = 1$. For $2 + \varepsilon \leq d \leq 4$ the scheme dependence of the critical exponents is rather weak; it becomes appreciable only near $d \approx 6$ [14]. Fig. 5 suggests that the Einstein-Hilbert truncation in

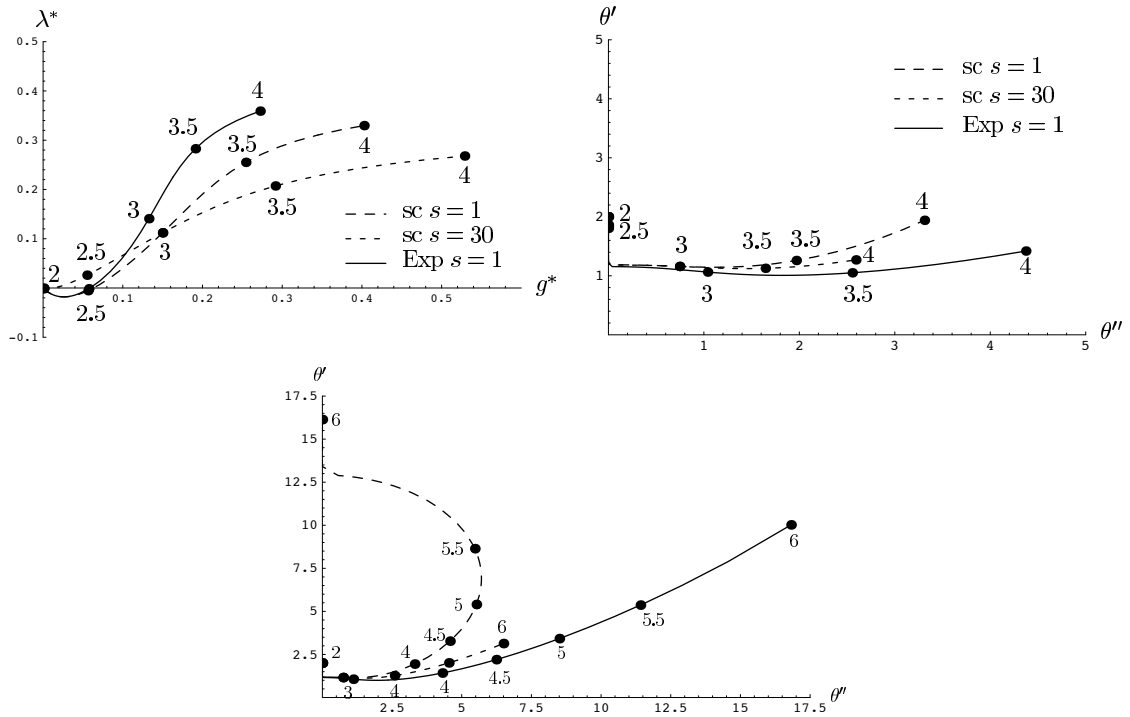

Figure 5: Comparison of λ^*, g^*, θ' and θ'' for different cutoff functions in dependence of the dimension d. Two versions of the sharp cutoff (sc) and the exponential cutoff with $s = 1$ (Exp) have been employed. The upper line shows that for $2 + \varepsilon \leq d \leq 4$ the cutoff scheme dependence of the results is rather small. The lower diagram shows that increasing d beyond about 5 leads to a significant difference in the results for θ', θ'' obtained with the different cutoff schemes. (From [14].)

$d = 4$ performs almost as well as near $d = 2$. Its validity can be extended towards larger dimensionalities by optimizing the shape function [23].

5.2 $f(R)$-type truncations

The ultimate justification of a given truncation consists in checking that if one adds further terms to it, its physical predictions remain robust. The first step towards testing the robustness of the Einstein-Hilbert truncation near the NGFP against the inclusion of other invariants has been taken in refs. [15, 16] where the beta functions for the three generalized couplings g, λ and β entering into the R^2–truncation of eq. (4.23) have been derived and analyzed.

Subsequently, the truncated theory space has been extended to arbitrary functions of the Ricci scalar in [25–27, 35]. In this truncation ansatz $S_{\rm gf}$ and $S_{\rm gh}$ are taken to be classical while, in the language of eq. (4.1),

$$\bar{\Gamma}_k[g] = \int d^4x\sqrt{g}\, f_k(R)\,, \quad \widehat{\Gamma}_k[g,\bar{g}] = 0\,. \tag{5.4}$$

Substituting this ansatz into the flow equation (1.1) results in a rather complicated partial differential equation governing the scale-dependence of $f_k(R)$ [26]. Based on this equation, the search for the NGFP on truncation subspaces involving higher powers of the curvature scalar reduces to an algebraic problem. Substituting the ansatz[7]

$$f_k(R) = \sum_{n=0}^{N} u_n(k)\, k^4\, (R/k^2)^n\,, \quad N \in \mathbb{N}\,, \tag{5.5}$$

and expanding the resulting equation in powers of R allows to extract the non-perturbative beta functions for the dimensionless couplings $u_n(k)$,

$$k\partial_k u_n(k) = \beta_{u_n}(u_0, \cdots, u_N)\,, \quad n = 0, \cdots, N\,. \tag{5.6}$$

The fixed point conditions $\beta_{u_n}(u_0^*, \cdots, u_N^*) = 0, n = 0, \ldots, N$ can then be solved numerically. Notably, the inclusion of higher-derivative terms provided crucial evidence that UV-critical hypersurface of the NGFP known from the Einstein-Hilbert truncation has a finite dimension, indicating that the Asymptotic Safety scenario is predictive. We shall now summarize the central results obtained within this class of truncations.

(1) Position of the fixed point (R^2)**:** Also with the generalized truncation (4.23) the NGFP is found to exist for all admissible cutoffs. Fig. 6 shows its coordinates $(\lambda^*, g^*, \beta^*)$ for the family of shape functions (4.22). For every shape parameter s, the values of λ^* and g^* are almost the same as those obtained with the Einstein-Hilbert truncation.

[7]The Einstein-Hilbert truncation discussed in section 4 corresponds to setting $f_k(R) = (16\pi G_k)^{-1}(-R + 2\Lambda_k)$ and using (4.6) rather than setting $\widehat{\Gamma}[g,\bar{g}] = 0$. Comparing the Einstein-Hilbert ansatz to (5.5) shows $u_1(k) = -(16\pi g_k)^{-1}$, so that a negative $u_1(k)$ actually corresponds to a positive Newton's constant.

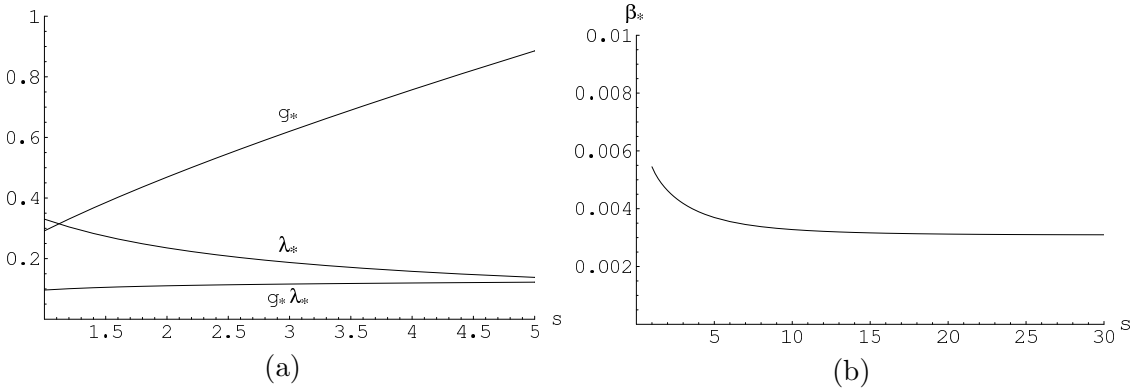

Figure 6: (a) g^*, λ^*, and $g^*\lambda^*$ as functions of s for $1 \leq s \leq 5$, and (b) β^* as a function of s for $1 \leq s \leq 30$, using the family of exponential shape functions (4.22). (From ref. [16].)

In particular, the product $g^*\lambda^*$ is constant with a very high accuracy. For $s = 1$, for instance, one obtains $(\lambda^*, g^*) = (0.348, 0.272)$ from the Einstein-Hilbert truncation and $(\lambda^*, g^*, \beta^*) = (0.330, 0.292, 0.005)$ from the generalized truncation. It is quite remarkable that β^* is always significantly smaller than λ^* and g^*. Within the limited precision of our calculation this means that in the 3-dimensional parameter space the fixed point practically lies on the λ-$g-$plane with $\beta = 0$, i.e., on the parameter space of the pure Einstein-Hilbert truncation.

(2) Eigenvalues and -vectors (R^2)**:** The NGFP of the R^2-truncation proves to be UV attractive in any of the three directions of the $(\lambda, g, \beta)-$space for all cutoffs used. The linearized flow in its vicinity is always governed by a pair of complex conjugate critical exponents $\theta_1 = \theta' + \mathrm{i}\theta'' = \theta_2^*$ with $\theta' > 0$ and a single real, positive critical exponent $\theta_3 > 0$. For the exponential shape function with $s = 1$, for instance, we find $\theta' = 2.15$, $\theta'' = 3.79$, $\theta_3 = 28.8$. The first two are again of the spiral type while the third one is a straight line.

For any cutoff, the numerical results have several quite remarkable properties. They all indicate that, close to the NGFP, the RG flow is rather well approximated by the pure Einstein-Hilbert truncation.

(a) The eigenvectors associated with the spiraling directions span a plane which virtually

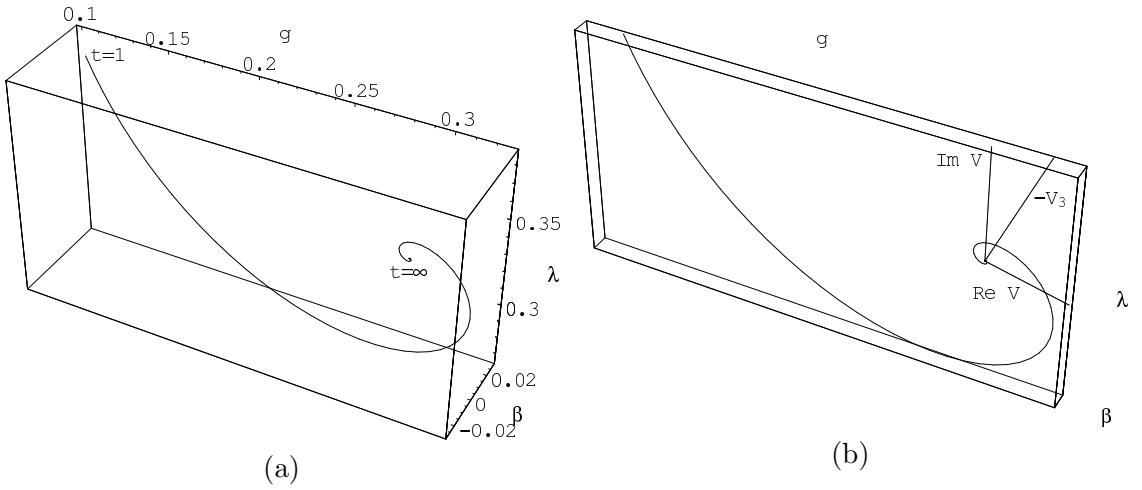

Figure 7: Trajectory of the linearized flow equation obtained from the R^2–truncation for $1 \leq t = \ln(k/k_0) < \infty$. In (b) we depict the eigendirections and the "box" to which the trajectory is confined. (From ref. [16].)

coincides with the g-$\lambda-$subspace at $\beta = 0$, i.e., with the parameter space of the Einstein-Hilbert truncation. As a consequence, the corresponding normal modes are essentially the same trajectories as the "old" normal modes already found without the R^2–term. Also the corresponding θ'– and θ''–values coincide within the scheme dependence.

(b) The new eigenvalue θ_3 introduced by the R^2–term is significantly larger than θ'. When a trajectory approaches the fixed point from below ($t \to \infty$), the "old" normal modes are proportional to $\exp(-\theta' t)$, but the new one is proportional to $\exp(-\theta_3 t)$, so that it decays much quicker. For every trajectory running into the fixed point we find therefore that once t is sufficiently large the trajectory lies entirely in the $\beta = 0$-plane practically. Due to the large value of θ_3, the new scaling field is very "relevant". However, when we start at the fixed point ($t = \infty$) and lower t it is only at the low energy scale $k \approx m_{\rm Pl}$ ($t \approx 0$) that $\exp(-\theta_3 t)$ reaches unity, and only then, i.e., far away from the fixed point, the new scaling field starts growing rapidly.

Thus very close to the fixed point the RG flow seems to be essentially 2-dimensional, and that this 2-dimensional flow is well approximated by the RG equations of the Einstein-Hilbert truncation. In fig. 7 we show a typical trajectory which has all three normal modes

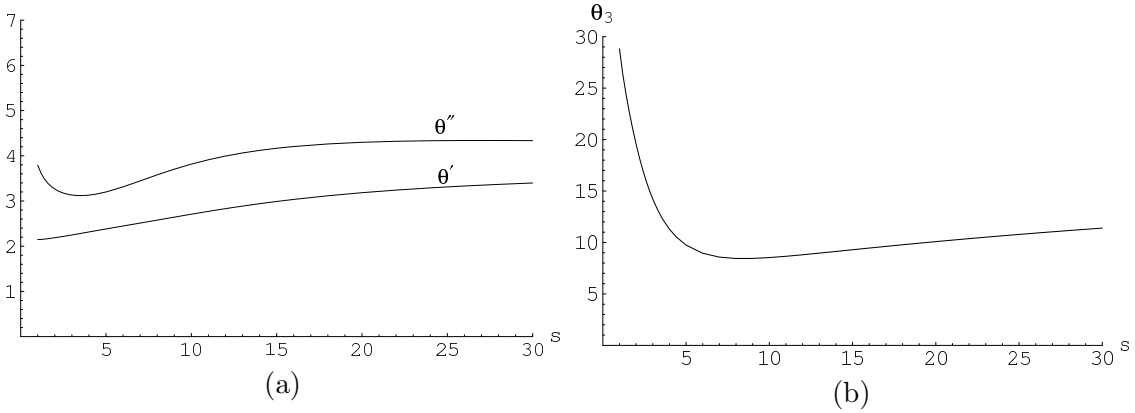

Figure 8: (a) $\theta' = \mathrm{Re}\,\theta_1$ and $\theta'' = \mathrm{Im}\,\theta_1$, and (b) θ_3 as functions of s, using the family of exponential shape functions (4.22). (From [15].)

excited with equal strength. All the way down from $k = \infty$ to about $k = m_{\rm Pl}$ it is confined to a very thin box surrounding the $\beta = 0$–plane.

(3) Scheme dependence (R^2)**:** The scheme dependence of the critical exponents and of the product $g^*\lambda^*$ turns out to be of the same order of magnitude as in the case of the Einstein-Hilbert truncation. Fig. 8 shows the cutoff dependence of the critical exponents, using the family of shape functions (4.22). For the cutoffs employed θ' and θ'' assume values in the ranges $2.1 \lesssim \theta' \lesssim 3.4$ and $3.1 \lesssim \theta'' \lesssim 4.3$, respectively. While the scheme dependence of θ'' is weaker than in the case of the Einstein-Hilbert truncation one finds that it is slightly larger for θ'. The exponent θ_3 suffers from relatively strong variations as the cutoff is changed, $8.4 \lesssim \theta_3 \lesssim 28.8$, but it is always significantly larger than θ'. The product $g^*\lambda^*$ again exhibits an extremely weak scheme dependence. Fig. 6(a) displays $g^*\lambda^*$ as a function of s. It is impressive to see how the cutoff dependences of g^* and λ^* cancel almost perfectly. Fig. 6(a) suggests the universal value $g^*\lambda^* \approx 0.14$. Comparing this value to those obtained from the Einstein-Hilbert truncation we find that it differs slightly from the one based upon the same gauge $\alpha = 1$. The deviation is of the same size as the difference between the $\alpha = 0$– and the $\alpha = 1$–results of the Einstein-Hilbert truncation.

(4) Dimensionality of $\mathcal{S}_{\rm UV}$ (R^2)**:** According to the canonical dimensional analysis, the

s	$\lambda_*\,(+\mathcal{O}(\varepsilon^2))$	$g_*\,(+\mathcal{O}(\varepsilon^2))$	$\beta_*\,(+\mathcal{O}(\varepsilon))$	$\theta_1\,(+\mathcal{O}(\varepsilon))$	$\theta_2\,(+\mathcal{O}(\varepsilon^2))$	$\theta_3\,(+\mathcal{O}(\varepsilon))$
1	-0.131ε	0.087ε	-0.083	2	0.963ε	-1.968
5	-0.055ε	0.092ε	-0.312	2	0.955ε	-1.955
10	-0.035ε	0.095ε	-0.592	2	0.955ε	-1.956

Table 1: Fixed point coordinates and critical exponents of the R^2-truncation in $2+\varepsilon$ dimensions. The negative value $\theta_3 < 0$ implies that $\mathcal{S}_{\rm UV}$ is an (only!) 2-dimensional surface in the 3-dimensional theory space.

(curvature)^n-invariants in 4 dimensions are classically marginal for $n = 2$ and irrelevant for $n > 2$. The results for θ_3 indicate that there are large non-classical contributions so that there might be relevant operators perhaps even beyond $n = 2$. With the R^2-truncation it is clearly not possible to determine their number $\Delta_{\rm UV}$ in $d = 4$. However, as it is hardly conceivable that the quantum effects change the signs of arbitrarily large (negative) classical scaling dimensions, $\Delta_{\rm UV}$ should be finite [9].

The first confirmation of this picture came from the R^2-calculation in $d = 2+\varepsilon$ where the dimensional count is shifted by two units. In this case we find indeed that the third scaling field is *irrelevant* for any cutoff employed, $\theta_3 < 0$. Using the ε-expansion the corresponding numerical results for selected values of the shape parameter s are presented in table 1.

For all cutoffs used we obtain three *real* critical exponents, the first two are positive and the third is negative. This suggests that in $d = 2+\varepsilon$ the dimensionality of $\mathcal{S}_{\rm UV}$ could be as small as $\Delta_{\rm UV} = 2$ and characterized by only two free parameters, the renormalized Newton constant G_0 and the renormalized cosmological constant $\bar{\lambda}_0$, for instance.

(5) Position of the non-Gaussian fixed point ($f(R), d = 4$): The beta functions (5.6) also give rise to a NGFP with $g^* > 0, \lambda^* > 0$, whose N-dependent position is shown in table 2. In particular the product $g^*\lambda^* = u_0/(32\pi(u_1)^2)$ displayed in the last column is remarkably constant. It is in excellent agreement with the Einstein-Hilbert truncation (5.3), and the R^2-truncation, fig. 6(a). Only the value obtained in the case $N = 2$ shows

N	u_0^*	u_1^*	u_2^*	u_3^*	u_4^*	u_5^*	u_6^*	$g^*\lambda^*$
1	0.00523	−0.0202						0.127
2	0.00333	−0.0125	0.00149					0.211
3	0.00518	−0.0196	0.00070	−0.0104				0.134
4	0.00505	−0.0206	0.00026	−0.0120	−0.0101			0.118
5	0.00506	−0.0206	0.00023	−0.0105	−0.0096	−0.00455		0.119
6	0.00504	−0.0208	0.00012	−0.0110	−0.0109	−0.00473	0.00238	0.116

Table 2: Location of the NGFP obtained within the $f(R)$-truncation by expanding the partial differential equation in a power series in R up to order R^N, including k-dependent dimensionless coupling constants $u_n(k)$, $n = 0, \cdots, N$. (From [26].)

N	θ'	θ''	θ_2	θ_3	θ_4	θ_5	θ_6
1	2.38	−2.17					
2	1.26	−2.44	27.0				
3	2.67	−2.26	2.07	−4.42			
4	2.83	−2.42	1.54	−4.28	−5.09		
5	2.57	−2.67	1.73	−4.40	$-3.97 + 4.57\mathrm{i}$	$-3.97 - 4.57\mathrm{i}$	
6	2.39	−2.38	1.51	−4.16	$-4.67 + 6.08\mathrm{i}$	$-4.67 - 6.08\mathrm{i}$	−8.67

Table 3: Stability coefficients of the NGFP for increasing dimension $N + 1$ of the truncation subspace. The first two critical exponents are a complex pair $\theta_\pm = \theta' \pm \mathrm{i}\theta''$. (From [26].)

a mild deviation from the R^2-computations, which can, most probably, be attributed to the use of a different gauge-fixing procedure, cutoff shape function, and ansatz for $\widehat{\Gamma}_k$.

(6) Dimensionality of $\mathcal{S}_{\rm UV}$ $(f(R), d = 4)$: The critical exponents resulting from the stability analysis of the NGFP emerging from the $f(R)$-truncation are summarized in table 3. In particular we find that only three of the eigendirections associated to the NGFP are relevant, i.e., UV attractive. Including higher derivative terms $R^n, n \geq 3$ in the truncation creates irrelevant directions only. Thus, as in the R^2- and $R^2 + C^2$-truncation, $\Delta_{\rm UV} = 3$, i.e., the UV critical surface associated to the fixed point is a 3-dimensional submanifold

in the truncated theory space. Its dimensionality is stable with respect to increasing N. The RG trajectories tracing out this surface are determined by fixing the three relevant couplings. These describe in which direction tangent to $\mathcal{S}_{\rm UV}$ the trajectory flows away from the fixed point. All remaining couplings, the irrelevant ones, are predictions from Asymptotic Safety. In [27] these results have been extended up to $N = 8$, providing even stronger evidence for the robustness of the RG flow under the inclusion of further invariants.

5.3 The $R^2 + C^2$-truncation in $d = 4$

The extension of the R^2-truncation by including non-scalar curvature terms in the truncation subspace has been investigated in [32,33]. This setup is based on the ansatz (4.24), and includes the characteristic features of higher-derivative gravity as, e.g., a fourth-order propagator for the helicity 2 states. Moreover, it provides an important spring-board for understanding the role of the counterterms arising in the perturbative quantization of gravity in the Asymptotic Safety program.

Including tensor structures like $C_{\mu\nu\rho\sigma}C^{\mu\nu\rho\sigma}$ in the truncation subspace requires the generalization of the background metrics $\bar{g}$. As discussed at the end of section 4, choosing the class of maximally symmetric metrics on S^d as a background considerably simplifies the evaluation of the truncated flow equation, but comes with the drawback that the flow is projected on interaction terms built from the Ricci scalar only. Thus the inclusion of the remaining four-derivative operators requires the use of a more general class of backgrounds. Ideally, this new class is generic enough to disentangle the coefficients multiplying R^2 and the tensorial terms, and, most importantly, simple enough to avoid the appearance of non-minimal higher-derivative differential operators inside the trace. While the maximally symmetric backgrounds used up to now are insufficient in the former respect, a generic compact Einstein background (without Killing or conformal Killing vectors and without boundary for simplicity), satisfying $\bar{R}_{\mu\nu} = \frac{\bar{R}}{4}\,\bar{g}_{\mu\nu}$, is sufficient to meet both criteria and allows one to determine the non-perturbative beta functions of the linear combinations

(4.25).

Surprisingly, projecting the flow equation resulting from the ansatz (4.24) onto an generic Einstein background, the differential operators appearing on its RHS organize themselves into second order differential operators of the Lichnerowicz form

$$\Delta_{2L}\phi_{\mu\nu} \equiv -\bar{D}^2\phi_{\mu\nu} - 2\bar{R}_\mu{}^\alpha{}_\nu{}^\beta\phi_{\alpha\beta}\,, \;\; \Delta_{1L}\phi_\mu \equiv -\bar{D}^2\phi_\mu - \bar{R}_{\mu\nu}\phi^\nu\,, \;\; \Delta_{0L}\phi \equiv -\bar{D}^2\phi, \quad (5.7)$$

which commute with all the other curvature terms inside the trace. This feature makes the traces amenable to standard heat kernel techniques for minimal second order differential operators. The resulting beta functions for the dimensionless coupling constants λ_k, g_k, β_k, and γ_k are somewhat involved, so that we only highlight their main properties

(1) Existence of the NGFP: The beta functions of the $R^2 + C^2$-truncation also give rise to a NGFP with positive Newtons and cosmological constant

$$g^* = 1.960\,, \quad \lambda^* = 0.218\,, \quad \beta^* = 0.008\,, \quad \gamma^* = -0.005\,, \qquad g^*\lambda^* = 0.427\,. \qquad (5.8)$$

The finite values for β^* and γ^* also imply a finite value of σ^*, via eq. (4.25). This should be contrasted to the one-loop result $\sigma^* = 0$ obtained from the perturbative quantization of fourth-order gravity. Thus the non-perturbative corrections captured by the FRGE shift the fixed point underlying the asymptotic freedom obtained within perturbation theory to the NGFP featuring in the Asymptotic Safety program.

(2) Stability properties: An important characteristics of the NGFP are its stability properties. Linearizing the RG flow at the fixed point (5.8) along the lines of section 2, the stability coefficients are found as

$$\theta_0 = 2.51\,, \qquad \theta_1 = 1.69\,, \qquad \theta_2 = 8.40\,, \qquad \theta_3 = -2.11\,. \qquad (5.9)$$

We observe that the inclusion of the C^2-coupling leads to real stability coefficients. This is in contrast to the complex stability coefficients and the corresponding spiraling approach of the RG flow characteristic for $f(R)$-type truncations.

Moreover, eq. (5.9) further indicates that the "new" direction added by extending the R^2-truncation is UV-repulsive. Thus, in this 4-dimensional truncation space, $\mathcal{S}_{\rm UV}$ remains 3-dimensional, as in the case of the R^2-truncation. The condition for a trajectory being inside the UV-critical surface then imposes one constraint between the coupling constants. In the linear regime at the NGFP, this constraint can be used to express γ_k, say, in terms of the other coupling constants contained in the ansatz

$$\gamma_k = -0.116 + 0.030\,\lambda_k\,g_k^{-1} + 0.049\,g_k^{-1} + 11.06\beta_k\,. \tag{5.10}$$

Comparing the results (5.8) and (5.9) to their counterparts in the Einstein-Hilbert and R^2-truncation summarized in the previous subsections, we conclude that the C^2-term leads to a moderate shift on fixed point structure. In particular the universal coupling $g^*\lambda^*$ turns out to be enhanced by a factor of three, while the stability coefficients of the fixed point turn out to be real. Thus the C^2-term significantly influences the RG flow of the theory. It effects the fixed point structure more drastically then the inclusion of the R^2-term or working with different cutoff-schemes or gauge-fixing functions within the Einstein-Hilbert action.

(3) The role of perturbative counterterms: An interesting twist arises from supplementing the truncation ansatz (4.24) with a free scalar field. From perturbative viewpoint the two-derivative terms of the resulting action constitute the prototypical example of a gravitational theory which is perturbatively non-renormalizable at one loop, with the four-derivative terms being the corresponding non-renormalizable on-shell counterterms [2]. At the same time, it has been shown in [21] that the RG flow obtained from the two-derivative truncation possesses a NGFP whose properties are very close to the one found in the Einstein-Hilbert truncation of pure gravity. Thus this setup provides a valuable laboratory, where the influence of perturbative counterterms on the NGFP underlying the Asymptotic Safety scenario can be studied explicitly.

The beta function for the "$R^2 + C^2 + \text{scalar}$"-truncation can be computed completely

analogous to the case of pure gravity. Notably, they also give rise to an NGFP [33]

$$g^* = 2.279\,, \quad \lambda^* = 0.251\,, \quad \beta^* = 0.010\,, \quad \gamma^* = -0.0043\,, \qquad g^*\lambda^* = 0.571\,, \tag{5.11}$$

with stability coefficients

$$\theta_0 = 2.67\,, \qquad \theta_1 = 1.39\,, \qquad \theta_2 = 7.86\,, \qquad \theta_3 = -1.50\,. \tag{5.12}$$

Comparing these to the pure gravity results (5.8), (5.9), we observe that the gravity-matter fixed point has strikingly similar properties. The universal couplings and stability coefficients change their values by roughly 25%. Thus the beta functions are dominated by the contribution from the gravitational sector. This result lends strong support to the assertion that *perturbative counterterms do not play a distinguished role in the Asymptotic Safety program*. In particular they are not fatal for the NGFP, so that the gravity-matter theory remains asymptotically safe despite the inclusion of an perturbative conterterms in the truncation subspace.

Summary: The above results strongly suggest that the non-Gaussian fixed point occurring in the Einstein-Hilbert truncation is not a truncation artifact but rather the projection of a fixed point in the exact theory space. The fixed point and all its qualitative properties are stable against variations of the cutoff and the inclusion of further invariants in the truncation. It is particularly remarkable that within the scheme dependence the additional R^2–term has essentially no impact on the fixed point. Moreover, truncations involving higher-order polynomials in R or the tensor structure C^2 fully confirm the general picture suggested by the simple Einstein-Hilbert truncation and provide a strong indication that the corresponding quantum field theories are characterized by a finite number of free parameters. We interpret the above results and their mutual consistency as quite non-trivial indications supporting the conjecture that 4-dimensional QEG indeed possesses a RG fixed point with precisely the properties needed for Asymptotic Safety.

6 The multifractal properties of QEG space-times

An intriguing consequence arising from the scale-dependence of the gravitational effective action is that the QEG space-times at short distances develop fractal properties [13, 15, 49, 60]. These manifest themselves at the level of the graviton propagator at high energies or in the diffusion processes of test particles. One of the striking conclusions reached in refs. [13, 15] was that the effective dimensionality of space-time equals 4 at macroscopic distances ($\ell \gg \ell_{\rm Pl}$) but, near $\ell \approx \ell_{\rm Pl}$, it gets dynamically reduced to the value 2. The remainder of this review is dedicated to the discussion of the arguments that underlying this conclusion.

6.1 The origin of fractality: scale-dependent metrics

As we have seen, the effective average action $\Gamma_k[g_{\mu\nu}]$ defines a continuous family of effective field theories, where all quantum fluctuations with momenta larger than k have been integrated out. Intuitively speaking, the solution $\langle g_{\mu\nu} \rangle_k$ of the scale dependent field equation

$$\frac{\delta \Gamma_k}{\delta g_{\mu\nu}(x)} \Big[\langle g \rangle_k \Big] = 0 \tag{6.1}$$

can be interpreted as the metric averaged over (Euclidean) space-time volumes of a linear extension ℓ which typically is of the order of $1/k$. Knowing the scale dependence of Γ_k, i.e., the renormalization group trajectory $k \mapsto \Gamma_k$, we can in principle follow the solution $\langle g_{\mu\nu} \rangle_k$ from the ultraviolet ($k \to \infty$) to the infrared ($k \to 0$).

It is an important feature of this approach that the infinitely many equations of (6.1), one for each scale k, are valid *simultaneously*. They all refer *to the same* physical system, the "quantum space-time", but describe its effective metric structure on different scales. An observer using a "microscope" with a resolution $\approx k^{-1}$ will perceive the universe to be a Riemannian manifold with metric $\langle g_{\mu\nu} \rangle_k$. At every fixed k, $\langle g_{\mu\nu} \rangle_k$ is a smooth classical metric. But since the quantum space-time is characterized by the infinity of equations

(6.1) with $k = 0, \cdots, \infty$ it can acquire very nonclassical and in particular fractal features.

Let us describe more precisely what it means to "average" over Euclidean space-time volumes. The quantity we can freely tune is the IR cutoff scale k. The "resolving power" of the microscope, henceforth denoted ℓ, is in general a complicated function of k. (In flat space, $\ell \approx 1/k$.) In order to understand the relationship between ℓ and k we must recall some steps from the construction of $\Gamma_k[g_{\mu\nu}]$ in section 3.

The IR cutoff of the average action is implemented by first expressing the functional integral over all metrics in terms of eigenmodes of $\bar{D}^2$, the covariant Laplacian formed with the aid of the background metric $\bar{g}_{\mu\nu}$. Then a suppression term is introduced which damps the contribution of all $-\bar{D}^2$-modes with eigenvalues smaller than k^2. Following the steps of section 3 this leads to the scale dependent functional $\Gamma_k[g_{\mu\nu}; \bar{g}_{\mu\nu}]$, and the action with one argument is again obtained by equating the two metrics: $\Gamma_k[g_{\mu\nu}] \equiv \Gamma_k[g_{\mu\nu}; \bar{g}_{\mu\nu} = g_{\mu\nu}]$. This is this action which appears in (6.1). Because of the identification of the two metrics we see that it is basically the eigenmodes of $\bar{D}^2 = D^2$, constructed from the argument of $\Gamma_k[g]$, which are cut off at k^2. Since $\langle g_{\mu\nu} \rangle_k$ is the corresponding stationary point, we can say that the metric $\langle g_{\mu\nu} \rangle_k$ applies to the situation where only the quantum fluctuations of $-D^2(\langle g_{\mu\nu} \rangle_k)$ with eigenvalues larger than k^2 are integrated out. Therefore there is a complicated interrelation between the metric and the scale at which it provides an effective description: The covariant Laplacian which ultimately decides about which modes are integrated out is constructed from the "on shell" configuration $\langle g_{\mu\nu} \rangle_k$, so it is k-dependent by itself already.

From these remarks it is clear now how to obtain the "resolving power" ℓ for a given k, at least in principle. We start from a fixed RG trajectory $k \mapsto \Gamma_k$, derive its effective field equations at each k, and solve them. The resulting quantum mechanical counterpart of a classical space-time is specified by the infinity of Riemannian metrics $\{\langle g_{\mu\nu} \rangle_k | k = 0, \cdots, \infty\}$. While the totality of these metrics contains all physical information, the parameter k is only a book keeping device a priori. In a second step, it can be given a physical interpretation by relating it to the (proper) length scale of the

averaging procedure: One constructs the Laplacian $-D^2(\langle g_{\mu\nu}\rangle_k)$, diagonalizes it, looks how rapidly its k^2-eigenfunction varies, and "measures" the length ℓ of typical variations with the metric $\langle g_{\mu\nu}\rangle_k$ itself. By solving the resulting $\ell = \ell(k)$ for $k = k(\ell)$ we can in principle reinterpret the metric $\langle g_{\mu\nu}\rangle_k$ as referring to a microscope with a known position and direction dependent resolving power. The price we have to pay for the background independence is that we cannot freely choose ℓ directly but rather k only.

We now illustrate this procedure at the level of the Einstein-Hilbert truncation discussed in section 5.1. Without matter, the corresponding field equations happen to coincide with the ordinary Einstein equation, but with G_k and $\bar{\lambda}_k$ replacing the classical constants

$$R_{\mu\nu}(\langle g\rangle_k) = \frac{2}{2-d}\,\bar{\lambda}_k\,\langle g_{\mu\nu}\rangle_k\,. \tag{6.2}$$

It is easy to make the k-dependence of $\langle g_{\mu\nu}\rangle_k$ explicit. Picking an arbitrary reference scale k_0 we may rewrite (6.2) as $[\bar{\lambda}_{k_0}/\bar{\lambda}_k]\,R^\mu{}_\nu(\langle g\rangle_k) = \frac{2}{2-d}\bar{\lambda}_{k_0}\,\delta^\mu_\nu$. Since $R^\mu{}_\nu(c\,g) = c^{-1}\,R^\mu{}_\nu(g)$ for any constant $c > 0$, this relation implies that the average metric and its inverse scale as

$$\langle g_{\mu\nu}(x)\rangle_k = [\bar{\lambda}_{k_0}/\bar{\lambda}_k]\langle g_{\mu\nu}(x)\rangle_{k_0}\,, \qquad \langle g^{\mu\nu}(x)\rangle_k = [\bar{\lambda}_k/\bar{\lambda}_{k_0}]\langle g^{\mu\nu}(x)\rangle_{k_0}\,. \tag{6.3}$$

These relations are valid provided the family of solutions considered exists for all scales between k_0 and k, and $\bar{\lambda}_k$ has the same sign always.

Denoting the Laplace operators corresponding to the metrics $\langle g_{\mu\nu}\rangle_k$ and $\langle g_{\mu\nu}\rangle_{k_0}$ by $\Delta(k)$ and $\Delta(k_0)$, respectively, these relations imply

$$\Delta(k) = \left[\bar{\lambda}_k/\bar{\lambda}_{k_0}\right]\Delta(k_0)\,. \tag{6.4}$$

At this stage, the following remark is in order. In the asymptotic scaling regime associated with the NGFP the scale-dependence of the couplings is determined by the

fixed point, see eq. (5.1). Choosing $\bar{\lambda}_{k_0}$ in the classical regime, this implies in particular

$$\langle g_{\mu\nu}(x)\rangle_k \propto k^{-2} \qquad (k \to \infty)\,. \tag{6.5}$$

This asymptotic relation is actually an *exact* consequence of Asymptotic Safety, which solely relies on the scale-independence of the theory at the fixed point. This can be seen as follows. The complete effective average action has the structure (2.2). If $\bar{u}_\alpha(k)$ has the canonical dimension d_α the corresponding dimensionless couplings are $u_\alpha(k) \equiv k^{-d_\alpha}\,\bar{u}_\alpha(k)$ and we have

$$\Gamma_k[g_{\mu\nu}] \;=\; \sum_\alpha u_\alpha(k)\,k^{d_\alpha}\,P_\alpha[g_{\mu\nu}] \;=\; \sum_\alpha u_\alpha(k)\,P_\alpha[k^2\,g_{\mu\nu}]\,. \tag{6.6}$$

In the second equality we used that $P_\alpha[c^2\,g_{\mu\nu}] = c^{d_\alpha}\,P_\alpha[g_{\mu\nu}]$ for any $c > 0$ since P_α has dimension $-d_\alpha$. If the theory is asymptotically safe at the exact level, all $u_\alpha(k)$ approach constant values u^*_α for $k \to \infty$:

$$\Gamma_{k\to\infty}[g_{\mu\nu}] \;=\; \sum_\alpha u^*_\alpha\,P_\alpha[k^2\,g_{\mu\nu}]\,. \tag{6.7}$$

Obviously this functional depends on k^2 and $g_{\mu\nu}$ only via the combination $k^2\,g_{\mu\nu}$. Therefore the solutions of the corresponding field equation, $\langle g_{\mu\nu}\rangle_k$, scale proportional to k^{-2}, and this is exactly the scaling behavior (6.5).

The fact that (6.3) implies a fractal structure of space-time at short distances can be argued as follows. Since in absence of dimensionful constants of integration $\bar{\lambda}_k$ is the only quantity in this equation which sets a scale, every solution to (6.2) has a typical radius of curvature $r_c(k) \propto 1/\sqrt{\bar{\lambda}_k}$. (For instance, the maximally symmetric S^4-solution has the radius $r_c = r = \sqrt{3/\bar{\lambda}_k}$.) If we want to explore the space-time structure at a fixed length scale ℓ we should use the action $\Gamma_k[g_{\mu\nu}]$ at $k = 1/\ell$ because with this functional a tree level analysis is sufficient to describe the essential physics at this scale, including the relevant quantum effects. Hence, when we observe the space-time with a microscope of resolution ℓ, we will see an average radius of curvature given by $r_c(\ell) \equiv r_c(k = 1/\ell)$. Once ℓ is

smaller than the Planck length $\ell_{\rm Pl} \equiv m_{\rm Pl}^{-1}$ we are in the fixed point regime where $\bar{\lambda}_k \propto k^2$ so that $r_c(k) \propto 1/k$, or

$$r_c(\ell) \propto \ell\,. \tag{6.8}$$

Thus, when we look at the structure of space-time with a microscope of resolution $\ell \ll \ell_{\rm Pl}$, the average radius of curvature which we measure is proportional to the resolution itself. If we want to probe finer details and decrease ℓ we automatically decrease r_c and hence *in*crease the average curvature. Space-time seems to be more strongly curved at small distances than at larger ones. The scale-free relation (6.8) suggests that at distances below the Planck length the QEG space-time is a special kind of fractal with a self-similar structure. It has no intrinsic scale because in the fractal regime, i.e., when the RG trajectory is still close to the NGFP, the parameters which usually set the scales of the gravitational interaction, G and $\bar{\lambda}$, are not yet "frozen out". This happens only later on, somewhere half way between the non-Gaussian and the Gaussian fixed point, at a scale of the order of $m_{\rm Pl}$. Below this scale, G_k and $\bar{\lambda}_k$ stop running and, as a result, $r_c(k)$ becomes independent of k so that $r_c(\ell) = \text{const}$ for $\ell \gg \ell_{\rm Pl}$. In this regime $\langle g_{\mu\nu} \rangle_k$ is k-independent, indicating that the macroscopic space-time is describable by a single smooth, classical Riemannian manifold.

6.2 Dynamical dimensional reduction of the graviton propagator

As another consequence of the NGFP, ref. [13] observed that the 4-dimensional graviton propagator undergoes a dynamical dimensional reduction at high energies. The corresponding argument is based upon the anomalous dimension $\eta_N \equiv -\partial_t \ln Z_{Nk}$, eq. (4.17), which for the RG trajectories of the Einstein-Hilbert truncation (within its domain of validity) have $\eta_N \approx 0$ for $k \to 0$[8] and $\eta_N \approx -2$ for $k \to \infty$. The smooth change by two units occurs near $k \approx m_{\rm Pl}$.

[8] In the case of Type IIIa trajectories [14, 97] the macroscopic k-value is still far above $k_{\rm term}$, i.e., in the "GR regime" described in [97].

This information can be used to determine the momentum dependence of the dressed graviton propagator for momenta $p^2 \gg m_{\rm Pl}^2$. Expanding

$$\Gamma_k[g] = (16\pi G_k)^{-1} \int d^4x \, \sqrt{g} \left\{ -R + 2\bar{\lambda}_k \right\} + \text{gauge fixing} \tag{6.9}$$

about flat space and omitting the standard tensor structures we find the inverse propagator $\widetilde{\mathcal{G}}_k(p)^{-1} \propto Z_N(k)\, p^2$. The conventional dressed propagator $\widetilde{\mathcal{G}}(p)$ contained in $\Gamma \equiv \Gamma_{k=0}$ obtains from the *exact* $\widetilde{\mathcal{G}}_k$ in the limit $k \to 0$. For $p^2 > k^2 \gg m_{\rm Pl}^2$ the actual cutoff scale is the physical momentum p^2 itself[9] so that the k-evolution of $\widetilde{\mathcal{G}}_k(p)$ stops at the threshold $k = \sqrt{p^2}$. Therefore

$$\widetilde{\mathcal{G}}(p)^{-1} \propto \; Z_N \left(k = \sqrt{p^2} \right) \, p^2 \propto \; (p^2)^{1-\frac{\eta}{2}} \tag{6.10}$$

because $Z_N(k) \propto k^{-\eta}$ when η is (approximately) constant. In d dimensions, and for $\eta \neq 2 - d$, the Fourier transform of $\widetilde{\mathcal{G}}(p) \propto 1/(p^2)^{1-\eta/2}$ yields the following propagator in position space:

$$\mathcal{G}(x;y) \propto \; \frac{1}{|x-y|^{d-2+\eta}} \; . \tag{6.11}$$

This form of the propagator is well known from the theory of critical phenomena, for instance. (In the latter case it applies to large distances.) Eq. (6.11) is not valid directly at the NGFP. For $d = 4$ and $\eta = -2$ the dressed propagator is $\widetilde{\mathcal{G}}(p) = 1/p^4$ which has the following representation in position space:

$$\mathcal{G}(x;y) = -\frac{1}{8\pi^2} \, \ln\left(\mu \, |x-y|\right) \; . \tag{6.12}$$

Here μ is an arbitrary constant with the dimension of a mass. Obviously (6.12) has the same form as a $1/p^2$-propagator in 2 dimensions.

Slightly away from the NGFP, before other physical scales intervene, the propagator is of the familiar type (6.11) which shows that the quantity η_N has the standard interpre-

[9] See section 1 of ref. [98] for a detailed discussion of "decoupling" phenomena of this kind.

tation of an anomalous dimension in the sense that fluctuation effects modify the decay properties of $\mathcal{G}$ so as to correspond to a space-time of effective dimensionality $4 + \eta_N$. Thus the properties of the RG trajectories imply a remarkable dimensional reduction: Space-time, probed by a "graviton" with $p^2 \ll m_{\rm Pl}^2$ is 4-dimensional, but it appears to be 2-dimensional for a graviton with $p^2 \gg m_{\rm Pl}^2$.

It is interesting to note that in d classical dimensions, where the macroscopic space-time is d-dimensional, the anomalous dimension at the fixed point is $\eta = 2 - d$. Therefore, for any d, the dimensionality of the fractal as implied by η_N is $d + \eta = 2$ [13, 15].

7 Fractal dimensions within QEG

Having encountered the first evidence for the fractal nature of the effective QEG space-times, we now quantify their properties by computing their spectral, walk, and Hausdorff dimensions introduced in appendix A in the framework of QEG [49, 60]. These generalized dimensions can readily be obtained by studying diffusion processes of test particles on the effective space-times.

7.1 Diffusion processes on QEG space-times

Since in QEG one integrates over all metrics, the central idea is to replace the classical return probability of a diffusing test particle $P_g(T)$, eq. (A.3), by its expectation value

$$P(T) \equiv \langle P_\gamma(T) \rangle \equiv \int \mathcal{D}\gamma \mathcal{D}C \mathcal{D}\bar{C}\, P_\gamma(T)\, e^{-S_{\rm bare}[\gamma, C, \bar{C}]}\,. \tag{7.1}$$

Here $\gamma_{\mu\nu}$ denotes the microscopic metric and $S_{\rm bare}$ is the bare action related to the UV fixed point, with the gauge-fixing and the pieces containing the ghosts C and $\bar{C}$ included. For the untraced heat kernel (A.2), we define likewise

$$K(x, x'; T) \equiv \langle K_\gamma(x, x'; T) \rangle\,. \tag{7.2}$$

Following the discussion in subsection 6.1, these expectation values are most conveniently calculated from the effective average action. Since Γ_k defines an effective field theory at the scale k we know that $\langle \mathcal{O}(\gamma_{\mu\nu})\rangle \approx \mathcal{O}(\langle g_{\mu\nu}\rangle_k)$ provided the observable $\mathcal{O}$ involves only momentum scales of the order of k. We apply this rule to the RHS of the diffusion equation, $\mathcal{O} = -\Delta_\gamma K_\gamma(x, x'; T)$. The subtle issue here is the correct identification of k. If the diffusion process involves (approximately) only a small interval of scales near k over which $\bar{\lambda}_k$ does not change much, the corresponding heat equation contains the operator $\Delta(k)$ for this specific, fixed value of k: $\partial_T K(x, x'; T) = -\Delta(k)K(x, x'; T)$. Denoting the eigenvalues of $\Delta(k_0)$ by $\mathcal{E}_n$ and the corresponding eigenfunctions by ϕ_n, this equation is solved by

$$K(x, x'; T) = \sum_n \phi_n(x)\phi_n(x') \exp\Big(- F(k^2)\mathcal{E}_n T\Big) . \tag{7.3}$$

Here we introduced the convenient notation $F(k^2) \equiv \bar{\lambda}_k/\bar{\lambda}_{k_0}$. Knowing the propagation kernel, we can time-evolve any initial probability distribution $p(x; 0)$ according to

$$p(x; T) = \int d^d x' \sqrt{g_0(x')}\, K(x, x'; T)\, p(x'; 0) \tag{7.4}$$

with g_0 the determinant of $\langle g_{\mu\nu}\rangle_{k_0}$. If the initial distribution has an eigenfunction expansion of the form $p(x; 0) = \sum_n C_n\phi_n(x)$ we obtain

$$p(x; T) = \sum_n C_n\phi_n(x) \exp\Big(- F(k^2)\mathcal{E}_n T\Big) . \tag{7.5}$$

If the C_n's are significantly different from zero only for a single eigenvalue $\mathcal{E}_N$, we are dealing with a single-scale problem and would identify $k^2 = \mathcal{E}_N$ as the relevant scale at which the running couplings are to be evaluated. In general the C_n's are different from zero over a wide range of eigenvalues. In this case we face a multiscale problem where different modes ϕ_n probe the space-time on different length scales. If $\Delta(k_0)$ corresponds to flat space, say, the eigenfunctions $\phi_n = \phi_p$ are plane waves with momentum p^μ, and they resolve structures on a length scale ℓ of order $1/|p|$. Hence, in terms of the eigenvalue

$\mathcal{E}_n \equiv \mathcal{E}_p = p^2$ the resolution is $\ell \approx 1/\sqrt{\mathcal{E}_n}$. This suggests that when the manifold is probed by a mode with eigenvalue $\mathcal{E}_n$ it "sees" the metric $\langle g_{\mu\nu}\rangle_k$ for the scale $k = \sqrt{\mathcal{E}_n}$. Actually, the identification $k = \sqrt{\mathcal{E}_n}$ is correct also for curved space since, in the construction of Γ_k, the parameter k is introduced precisely as a cutoff in the spectrum of the covariant Laplacian.

As a consequence, under the spectral sum of (7.5), we must use the scale $k^2 = \mathcal{E}_n$ which depends explicitly on the resolving power of the corresponding mode. Likewise, in eq. (7.3), $F(k^2)$ is to be interpreted as $F(\mathcal{E}_n)$:

$$\begin{aligned} K(x,x';T) &= \sum_n \phi_n(x)\phi_n(x') \exp\Big(- F(\mathcal{E}_n)\mathcal{E}_n T\Big) \\ &= \sum_n \phi_n(x) \exp\Big(- F\big(\Delta(k_0)\big)\Delta(k_0) T\Big)\phi_n(x') \,. \end{aligned} \tag{7.6}$$

As in [49], we choose k_0 as a macroscopic scale in the classical regime, and we assume that at k_0 the cosmological constant is small, so that $\langle g_{\mu\nu}\rangle_{k_0}$ can be approximated by the flat metric on $\mathbb{R}^d$. The eigenfunctions of $\Delta(k_0)$ are plane waves then and eq. (7.6) becomes

$$K(x,x';T) = \int \frac{d^d p}{(2\pi)^d}\, e^{ip\cdot(x-x')}\, e^{-p^2 F(p^2)T} \tag{7.7}$$

where the scalar products are performed with respect to the flat metric, $\langle g_{\mu\nu}\rangle_{k_0} = \delta_{\mu\nu}$. The kernel (7.7) satisfies $K(x,x';0) = \delta^d(x-x')$ and, provided that $\lim_{p\to 0} p^2 F(p^2) = 0$, also $\int d^d x K(x,x';T) = 1$.

Taking the normalized trace of (7.7) within this "flat space-approximation" yields [49]

$$P(T) = \int \frac{d^d p}{(2\pi)^d}\, e^{-p^2 F(p^2)T} \,. \tag{7.8}$$

Introducing $z = p^2$, the final result for the average return probability reads

$$P(T) = \frac{1}{(4\pi)^{d/2}} \frac{1}{\Gamma(d/2)} \int_0^\infty dz\, z^{d/2-1} \exp\Big(- zF(z)T\Big) \,, \tag{7.9}$$

where $F(z) \equiv \bar{\lambda}(k^2 = z)/\bar{\lambda}_{k_0}$. In the classical case, $F(z) = 1$, this relation reproduces

the familiar result $P(T) = 1/(4\pi T)^{d/2}$. Thus, in this case, the spectral dimension (A.5) is given by $\mathcal{D}_s(T) = d$ independently of T.

7.2 The spectral dimension in QEG

We shall now discuss the spectral dimension (A.5) for several other illustrative and important examples.

(A) To start with, let us evaluate the average return probability (7.9) for a simplified RG trajectory where the scale dependence of the cosmological constant is given by a power law, with the same exponent δ for all values of k:

$$\bar{\lambda}_k \propto k^\delta \quad \Longrightarrow \quad F(z) \propto z^{\delta/2} \,. \tag{7.10}$$

By rescaling the integration variable in (7.9) we see that in this case

$$P(T) = \frac{\text{const}}{T^{d/(2+\delta)}} \,. \tag{7.11}$$

Hence (A.5) yields the important result

$$\boxed{\mathcal{D}_s(T) = \tfrac{2d}{2+\delta}} \,. \tag{7.12}$$

It happens to be T-independent, so that for $T \to 0$ trivially

$$d_s = \frac{2d}{2+\delta} \,. \tag{7.13}$$

(B) Next, let us be slightly more general and assume that the power law (7.10) is valid only for squared momenta in a certain interval, $p^2 \in [z_1, z_2]$, but $\bar{\lambda}_k$ remains unspecified otherwise. In this case we can obtain only partial information about $P(T)$, namely for T in the interval $[z_2^{-1}, z_1^{-1}]$. The reason is that for $T \in [z_2^{-1}, z_1^{-1}]$ the integral in (7.9) is dominated by momenta for which approximately $1/p^2 \approx T$, i.e., $z \in [z_1, z_2]$. This leads

us again to the formula (7.12), which now, however, is valid only for a restricted range of diffusion times T; in particular the spectral dimension of interest may not be given by extrapolating (7.12) to $T \to 0$.

(C) Let us consider an arbitrary asymptotically safe RG trajectory so that its behavior for $k \to \infty$ is controlled by the NGFP. For $k \geq m_{\rm Pl}$ the scale-dependence of the cosmological constant is governed by the fixed point, i.e., $\bar{\lambda}_k = \lambda_* k^2$, independently of d. This corresponds to a power law with $\delta = 2$, which entails in the **NGFP regime**, i.e., for $T \lesssim 1/m_{\rm Pl}^2$,

$$\mathcal{D}_s(T) = \frac{d}{2} \qquad \Big(\text{NGFP regime}\Big)\,. \tag{7.14}$$

This dimension, again, is locally T-independent. It coincides with the $T \to 0$ limit:

$$d_s = \frac{d}{2}\,. \tag{7.15}$$

This is the result first derived in ref. [49]. As it was explained there, it is actually an exact consequence of Asymptotic Safety which relies solely on the existence of the NGFP and does not depend on the Einstein-Hilbert truncation.

(D) Returning to the Einstein-Hilbert truncation, let us consider the piece of the Type IIIa RG trajectory depicted in Fig. 9 which lies inside the linear regime of the GFP. Newton's constant is approximately k-independent there and the cosmological constant evolves according to

$$\bar{\lambda}_k = \bar{\lambda}_0 + \nu G_0 k^d. \tag{7.16}$$

Here $\nu = (4\pi)^{1-d/2}(d-3)\Phi^1_{d/2}(0)$ is a scheme-dependent constant [11, 14]. When k is not too small, so that $\bar{\lambda}_0$ can be neglected relative to $\nu G_0 k^d$, we are in what we shall call the "k^d regime"; it is characterized by a pure power law $\bar{\lambda}_k \approx k^\delta$ with $\delta = d$. The physics behind this scale dependence is simple and well-known: It represents exactly the vacuum energy density obtained by summing up the zero point energies of all field modes

integrated out. For T in the range of scales pertaining to the k^d regime we find

$$\mathcal{D}_s(T) = \frac{2d}{2+d} \qquad (k^d \text{ regime}) \,. \tag{7.17}$$

Note that for every $d > 2$ the spectral dimension in the k^d regime is even *smaller* than in the NGFP regime.

7.3 The walk dimension in QEG

In order to determine the walk dimension for the diffusion on the effective QEG spacetimes we return to eq. (7.7) for the untraced heat kernel. We restrict ourselves to a regime with a power law running of $\bar{\lambda}_k$, whence $F(p^2) = (Lp)^\delta$ with some constant length-scale L.

Introducing $q_\mu \equiv p_\mu T^{1/(2+\delta)}$ and $\xi_\mu \equiv (x_\mu - x'_\mu)/T^{1/(2+\delta)}$ we can rewrite (7.7) in the form

$$K(x, x'; T) = \frac{1}{T^{d/(2+\delta)}} \, \Phi\left(\frac{|x - x'|}{T^{1/(2+\delta)}}\right) \tag{7.18}$$

with the function

$$\Phi(|\xi|) \equiv \int \frac{d^d q}{(2\pi)^d} \, e^{iq\cdot\xi} \, e^{-L^\delta q^{2+\delta}} \,. \tag{7.19}$$

For $\delta = 0$, this obviously reproduces (A.6). From the argument of Φ in (7.18) we infer that $r = |x - x'|$ scales as $T^{1/(2+\delta)}$ so that the walk dimension can be read off as

$$\boxed{\mathcal{D}_w(T) = 2 + \delta} \,. \tag{7.20}$$

In analogy with the spectral dimension, we use the notation $\mathcal{D}_w(T)$ rather than d_w to indicate that it might refer to an approximate scaling law which is valid for a finite range of scales only.

For $\delta = 0, 2$, and d we find in particular, for any topological dimension d,

$$\mathcal{D}_w = \begin{cases} 2 & \text{classical regime} \\ 4 & \text{NGFP regime} \\ 2+d & k^d \text{ regime} \end{cases} \tag{7.21}$$

Regimes with all three walk dimensions of (7.21) can be realized along a single RG trajectory. Again, the result for the NGFP regime, $\mathcal{D}_w = 4$, is exact in the sense that it does not rely on the Einstein-Hilbert truncation.

7.4 The Hausdorff dimension in QEG

The smooth manifold underlying QEG has per se no fractal properties whatsoever. In particular, the volume of a d-ball $\mathcal{B}^d$ covering a patch of the smooth manifold of QEG space-time scales as

$$V(\mathcal{B}^d) = \int_{\mathcal{B}^d} d^d x \sqrt{g_k} \propto (r_k)^d \,. \tag{7.22}$$

Thus, by comparing to eq. (A.7), we read off that the Hausdorff dimension is strictly equal to the topological one:

$$\boxed{d_H = d} \,. \tag{7.23}$$

We emphasize that the effective QEG space-times should *not* be visualized as a kind of sponge. Their fractal-like properties have no simple geometric interpretation; they are not due to a "removing" of space-time points. Rather they are of an entirely *dynamical* nature, reflecting certain properties of the *quantum states* the system "space-time metric" can be in.

7.5 The Alexander-Orbach relation

For standard fractals the quantities d_s, d_w, and d_H are not independent but are related by [99]

$$\frac{d_s}{2} = \frac{d_H}{d_w}\,. \tag{7.24}$$

By combining eqs. (7.12), (7.20), and (7.23) we see that the same relation holds true for the effective QEG space-times, at least within the Einstein-Hilbert approximation and when the underlying RG trajectory is in a regime with power-law scaling of $\bar{\lambda}_k$. For every value of the exponent δ we have

$$\frac{\mathcal{D}_s(T)}{2} = \frac{d_H}{\mathcal{D}_w(T)}\,. \tag{7.25}$$

The results $d_H = d$, $\mathcal{D}_w = 2+\delta$ imply that, as soon as $\delta > d-2$, we have $\mathcal{D}_w > d_H$ and the random walk is *recurrent* then [100]. Classically ($\delta = 0$) this condition is met only in low dimensions $d < 2$, but in the case of the QEG space-times it is always satisfied in the k^d regime ($\delta = d$), for example. So also from this perspective the QEG space-times, due to the specific quantum gravitational dynamics to which they owe their existence, appear to have a dimensionality smaller than their topological one.

It is particularly intriguing that, in the NGFP regime, $\mathcal{D}_w = 4$ independently of d. Hence the walk is recurrent ($\mathcal{D}_w > d_H$) for $d < 4$, non-recurrent for $d > 4$, and the marginal case $\mathcal{D}_w = d_H$ is realized if and only if $d = 4$, making $d = 4$ a distinguished value. Notably, there is another feature of the QEG space-times which singles out $d = 4$: it is the only dimensionality for which $\mathcal{D}_s$(NGFP regime)$= d/2$ coincides with the effective dimension $d_{\text{eff}} = d + \eta_* = 2$ derived from the graviton propagator in section 6.2.

8 The scale-dependence of $\mathcal{D}_s$ and $\mathcal{D}_w$

We now proceed by discussing the scale-dependence of the spectral and walk dimension, arising within the Einstein-Hilbert truncation. For this purpose, we consider an arbitrary

RG trajectory $k \mapsto (g_k, \lambda_k)$. Along such an RG trajectory there might be isolated intervals of k-values where the cosmological constant evolves according to a power law, $\bar{\lambda}_k \propto k^\delta$, for some constant exponents δ which are not necessarily the same on different such intervals. If the intervals are sufficiently long, it is meaningful to ascribe a spectral and walk dimension to them since $\delta = \text{const}$ implies k-independent values $\mathcal{D}_s = 2d/(2+\delta)$ and $\mathcal{D}_w = 2 + \delta$.

In between the intervals of approximately constant $\mathcal{D}_s$ and $\mathcal{D}_w$, where the k-dependence of $\bar{\lambda}_k$ is not a power law, the notion of a spectral or walk dimension might not be meaningful. The concept of a *scale-dependent* dimension $\mathcal{D}_s$ or $\mathcal{D}_w$ is to some extent arbitrary with respect to the way it connects the "plateaus" on which $\delta = \text{const}$ for some extended period of RG time. While RG methods allow the computation of the $\mathcal{D}_s$ and $\mathcal{D}_w$ values on the various plateaus, it is a matter of convention how to combine them into continuous functions $k \mapsto \mathcal{D}_s(k), \mathcal{D}_w(k)$ which interpolate between the respective values.

8.1 The exponent δ as a function on theory space

In this subsection, we describe a special proposal for a k-dependent $\mathcal{D}_s(k)$ and $\mathcal{D}_w(k)$ which is motivated by technical simplicity and the general insights it allows. We retain eqs. (7.12) and (7.20), but promote $\delta \to \delta(k)$ to a k-dependent quantity

$$\delta(k) \equiv k\partial_k \ln(\bar{\lambda}_k)\,. \tag{8.1}$$

When $\bar{\lambda}_k$ satisfies a power law, $\bar{\lambda}_k \propto k^\delta$ this relation reduces to the case of constant δ. If not, δ has its own scale dependence, but no direct physical interpretation should be attributed to it. The particular definition (8.1) has the special property that it actually can be evaluated without first solving for the RG trajectory. The function $\delta(k)$ can be seen as arising from a certain scalar function on theory space, $\delta = \delta(g, \lambda)$, whose k-dependence results from inserting an RG trajectory: $\delta(k) \equiv \delta(g_k, \lambda_k)$. In fact, (8.1) implies $\delta(k) = k\partial_k \ln(k^2\lambda_k) = 2 + \lambda_k^{-1} k\partial_k \lambda_k$ so that $\delta(k) = 2 + \lambda_k^{-1}\beta_\lambda(g_k, \lambda_k)$ upon using the RG equation $k\partial_k\lambda_k = \beta_\lambda(g_k, \lambda_k)$. Thus when we consider δ as a function on theory

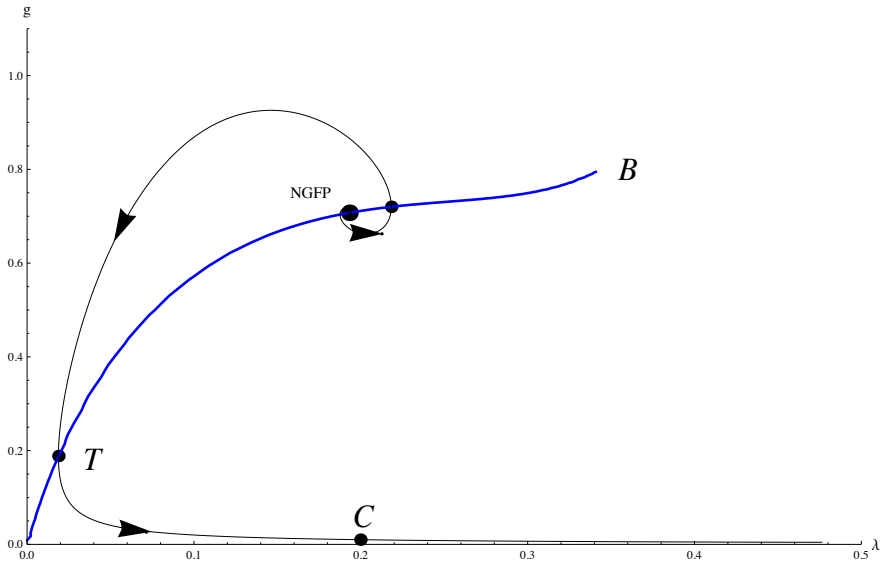

Figure 9: The g-$\lambda-$theory space with the line of turning points, $\mathcal{B}$, and a typical trajectory of Type IIIa. The arrows point in the direction of decreasing k. The big black dot indicates the NGFP while the smaller dots represent points at which the RG trajectory switches from increasing to decreasing λ or vice versa. The point T is the lowest turning point, and C is a typical point within the classical regime. For $\lambda \gtrsim 0.35$, the RG flow leaves the classical regime and is no longer reliably captured by the Einstein-Hilbert truncation. (From [60].)

space, coordinatized by g and λ, it reads

$$\delta(g,\lambda) = 2 + \frac{1}{\lambda}\,\beta_\lambda(g,\lambda)\,. \tag{8.2}$$

Substituting this relation into (7.12) and (7.20), the spectral and the walk dimensions become functions on the g-λ-plane

$$\mathcal{D}_s(g,\lambda) = \frac{2d}{4+\lambda^{-1}\beta_\lambda(g,\lambda)}\,, \qquad \mathcal{D}_w(g,\lambda) = 4+\lambda^{-1}\beta_\lambda(g,\lambda)\,. \tag{8.3}$$

To evaluate these expressions further, we use the beta functions (4.16). As we already discussed, the scaling regime of a NGFP has the exponent $\delta = 2$. From eq. (8.2) we learn that this value is realized at all points (g,λ) where $\beta_\lambda = 0$. The second condition for the NGFP, $\beta_g = 0$, is not required here, so that we have $\delta = 2$ along the entire line in theory

space:

$$\mathcal{B} = \left\{ (g,\lambda) \,\middle|\, \beta_\lambda(g,\lambda) = 0 \right\}. \tag{8.4}$$

For $d = 4$ the curve $\mathcal{B}$ is shown as the bold blue line in fig. 9. Both the GFP $(g,\lambda) = (0,0)$ and the NGFP, $(g,\lambda) = (g_*,\lambda_*)$, are located on this curve. Furthermore, the turning points T of all Type IIIa trajectories are also situated on $\mathcal{B}$, and the same holds for all the higher order turning points which occur when the trajectory spirals around the NGFP. This observation leads us to an important conclusion: The values $\delta = 2 \Longleftrightarrow \mathcal{D}_s = d/2, \mathcal{D}_w = 4$ which (without involving any truncation) are found in the NGFP regime, actually also apply to all points $(g,\lambda) \in \mathcal{B}$, provided the Einstein-Hilbert truncation is reliable and no matter is included.

8.2 The spectral and walk dimensions along a RG trajectory

We proceed by investigating how the spectral and walk dimension of the effective QEG space-times change along a given RG trajectory. Our interest is in scaling regimes where $\mathcal{D}_s$ and $\mathcal{D}_w$ remain (approximately) constant for a long interval of k-values. For the remainder of this subsection, we will restrict ourselves to the case $d = 4$ for concreteness.

We start by numerically solving the coupled differential equations (4.15) with the beta functions (4.16) evaluated with the optimized cutoff for a series of initial conditions keeping $\lambda_{\text{init}} = \lambda(k_0) = 0.2$ fixed and successively lowering $g_{\text{init}} = g(k_0)$. The result is a family of RG trajectories where the classical regime becomes more and more pronounced. These solutions are substituted into (8.3), which give $\mathcal{D}_s(t; g_{\text{init}}, \lambda_{\text{init}})$ and $\mathcal{D}_w(t; g_{\text{init}}, \lambda_{\text{init}})$ in dependence of the RG-time $t \equiv \ln(k)$ and the RG trajectory. One can verify explicitly, that substituting the RG trajectory into the return probability (7.9) and computing the spectral dimension from (A.4) by carrying out the resulting integrals numerically gives rise to the same picture.

Fig. 10 then shows the resulting spectral dimension, the walk dimension, and the localization of the plateau-regimes on the RG trajectory in the top-left, top-right and lower diagram, respectively. In the top diagrams, g_{init} decreases by one order of magnitude for

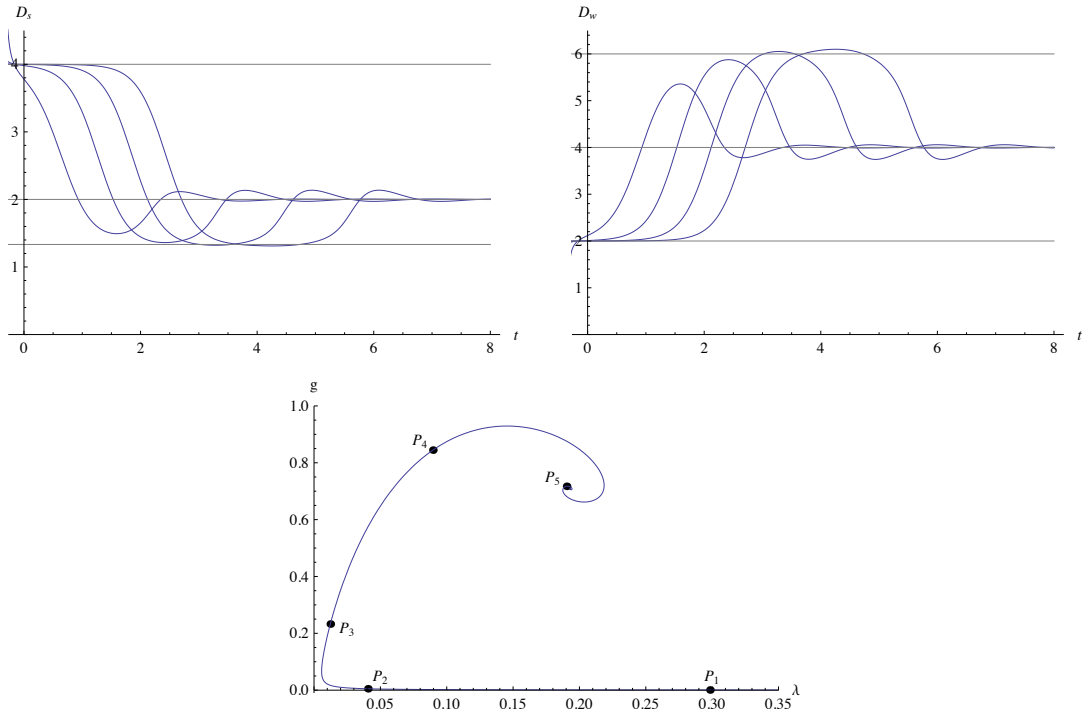

Figure 10: The $t \equiv \ln(k)$-dependent spectral dimension (upper left) and walk dimension (upper right) along illustrative solutions of the RG equations (4.15) in $d = 4$. The trajectories develop three plateaus: the classical plateau with $\mathcal{D}_s = 4, \mathcal{D}_w = 2$, the semi-classical plateau where $\mathcal{D}_s = 4/3, \mathcal{D}_w = 6$ and the NGFP plateau with $\mathcal{D}_s = 2, \mathcal{D}_w = 4$. These plateau values are indicated by the gray horizontal lines and connected by crossover parts. The lower figure shows the location of these plateaus on the RG trajectory: the classical, k^4, and NGFP regime appear between the points P_1 and P_2, P_3 and P_4, and above P_5, respectively. (From [60].)

each shown trajectory, starting with the highest value to the very left. As a central result, fig. 10 establishes that the RG flow gives rise to *three* plateaus where $\mathcal{D}_s(t)$ and $\mathcal{D}_w(t)$ are approximately constant:

(i) For small values k, below $t \simeq 1.8$, say, one finds a *classical plateau* where $\mathcal{D}_s = 4, \mathcal{D}_w = 2$ for a long range of k-values. Here $\delta = 0$, indicating that the cosmological constant is indeed constant.

(ii) Following the RG flow towards the UV (larger values of t) one next encounters the *semi-classical plateau* where $\mathcal{D}_s = 4/3, \mathcal{D}_w = 6$. In this case $\delta(k) = 4$ so that $\bar{\lambda}_k \propto k^4$ on the corresponding part of the RG trajectory.

(iii) Finally, the *NGFP plateau* is characterized by $\mathcal{D}_s = 2, \mathcal{D}_w = 4$, which results from

the scale-dependence of the cosmological constant at the NGFP $\bar{\lambda}_k \propto k^2 \Longleftrightarrow \delta = 2$.

At this stage, it is worthwhile to see which parts of a typical RG trajectory realize the scaling relations underlying the plateau-values of $\mathcal{D}_s$ and $\mathcal{D}_w$. This is depicted in the lower diagram of fig. 10 where we singled out the third solution with $g_{\rm init} = 10^{-3}$ for illustrative purposes. In this case the classical plateau is bounded by the points P_1 and P_2 and appears well below the turning point T, while the semi-classical plateau is situated between the points P_3 and P_4 well above the turning point. The NGFP plateau is realized by the piece of the RG trajectory between P_5 and the NGFP. The turning point T is not situated in any scaling region but appears along the crossover from the classical to the semi-classical regime of the QEG space-times. For $t < 0$, the spectral dimension (walk dimension) increases (decreases) rapidly. In this region, the underlying RG trajectory is evaluated outside the classical regime at points $\lambda \gtrsim 0.35$. In this region of the theory space, the Einstein-Hilbert truncation is no longer trustworthy, so that this rapid increase of $\mathcal{D}_s$ is most likely an artifact, arising from the use of an insufficient truncation.

The plateaus observed above become more and more extended the closer the trajectories turning point T gets to the GFP, i.e., the smaller the IR value of the cosmological constant. The first RG trajectory with the largest value $g_{\rm init} = 0.1$ does not even develop a classical and semi-classical plateau, so that a certain level of fine-tuning of the initial conditions is required in order to make these structures visible. Interestingly enough, when one matches the observed data against the RG trajectories of the Einstein-Hilbert truncation [51, 97] one finds that the "RG trajectory realized by Nature" displays a very extreme fine-tuning of this sort. The coordinates of the turning point are approximately $g_T \approx \lambda_T \approx 10^{-60}$ and it is passed at the scale $k_T \approx 10^{-30} m_{\rm Pl} \approx 10^{-2}{\rm eV} \approx (10^{-2}{\rm mm})^{-1}$, so that there will be very pronounced plateau structures in this case.

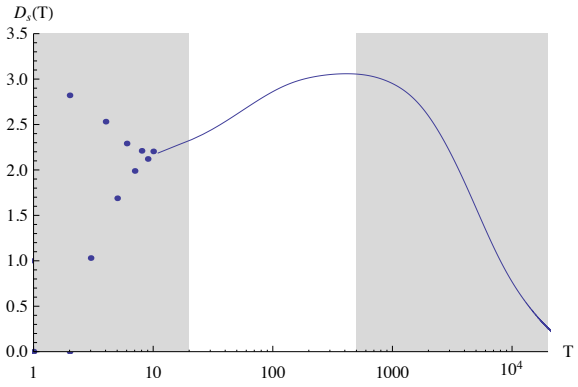

Figure 11: Spectral dimension $\mathcal{D}_s^{\rm CDT}(T)$ determined from random walks on a CDT space-time built from $N = 200$k simplices [56].

8.3 Matching the spectral dimensions of QEG and CDT

The key advantage of the spectral dimension $\mathcal{D}_s(T)$ is that it may be defined and computed within various a priori unrelated approaches to quantum gravity. In particular, it is easily accessible in Monte Carlo simulations of the Causal Dynamical Triangulations (CDT) approach in $d = 4$ [54] and $d = 3$ [56] as well as in Euclidean Dynamical Triangulations (EDT) [59]. This feature allows a direct comparison between $\mathcal{D}_s^{\rm CDT}(T)$ and $\mathcal{D}_s^{\rm EDT}(T)$ obtained within the discrete approaches and $\mathcal{D}_s^{\rm QEG}(T)$ capturing the fractal properties of the QEG effective space-times. We conclude this section by reviewing this comparison for $d = 3$, following ref. [60].[10] In particular we shall determine the specific RG trajectory of QEG which, we believe, underlies the numerical data obtained in [56].

Let us start by looking into the typical features of the spectral dimension $\mathcal{D}_s^{\rm CDT}(T)$ obtained from the simulations. A prototypical data set showing $\mathcal{D}_s^{\rm CDT}(T)$ as function of the length of the random walk T is given in fig. 11. The resulting curve is conveniently split into three regimes:

(i) For $T \leq 20$, corresponding to the left gray region in fig. 11, $\mathcal{D}_s^{\rm CDT}(T)$ undergoes rapid oscillations. These originate from the discrete structure of the triangulation to which the short random walks are particular sensitive.

(ii) For long random walks with $T \geq 500$, the data shows an exponential fall-off. This

[10] For a similar fit in Hořava gravity see ref. [101].

feature is due to the compact nature of the triangulation, which implies that for long random walks $\mathcal{D}_s^{\rm CDT}(T)$ is governed by the lowest eigenvalue of the Laplacian on the compact space. This regime is marked by the right gray region in fig. 11.
(iii) Between these two regimes, $\mathcal{D}_s^{\rm CDT}(T)$ is affected neither by the discreteness nor the compactness of the triangulation. Since for $\mathcal{D}_s^{\rm QEG}(T)$, determined by the flat-space approximation (7.8), we do not expect any of these effects to appear, we use this middle region to compare the T-dependent spectral dimensions arising from the two, a priori different, approaches.

The comparison between the CDT-data and the QEG effective space-times is carried out as follows:
(i) First, we numerically construct a RG trajectory $g_k(g_0,\lambda_0), \lambda_k(g_0,\lambda_0)$ depending on the initial conditions g_0, λ_0, by solving the flow equations (4.15).
(ii) Subsequently, we evaluate the resulting spectral dimension $\mathcal{D}_s^{\rm QEG}(T; g_0, \lambda_0)$ of the corresponding effective QEG space-time. This is done by first finding the return probability $P(T; g_0, \lambda_0)$, eq. (7.9), for the RG trajectory under consideration and then substituting the resulting expression into (A.5). Besides on the length of the random walk, the spectral dimension constructed in this way also depends on the initial conditions of the RG trajectory.
(iii) Finally, we determine the RG trajectory underlying the CDT-simulations by fitting the parameters g_0, λ_0 to the Monte Carlo data. The corresponding best-fit values are obtained via an ordinary least-square fit, minimizing the squared Euclidean distance

$$(\Delta\mathcal{D}_s)^2 \equiv \sum_{T=20}^{500} \left(\mathcal{D}_s^{\rm QEG}(T; g_0^{\rm fit}, \lambda_0^{\rm fit}) - \mathcal{D}_s^{\rm CDT}(T)\right)^2 , \tag{8.5}$$

between the (continuous) function $\mathcal{D}_s^{\rm QEG}(T; g_0, \lambda_0)$ and the points $\mathcal{D}_s^{\rm CDT}(T)$. We thereby restrict ourselves to the random walks with discrete, integer length $20 \leq T \leq 500$, which constitute the white part of fig. 11 and correspond to the regime **(iii)** discussed above.

The resulting best-fit values $g_0^{\rm fit}, \lambda_0^{\rm fit}$ for the triangulations with $N = 70.000$, $N = 100.000$, and $N = 200.000$ simplices are collected in table 4. Notably, the sum over

	$g_0^{\rm fit}$	$\lambda_0^{\rm fit}$	$(\Delta\mathcal{D}_s)^2$
70k	0.7×10^{-5}	7.5×10^{-5}	0.680
100k	8.8×10^{-5}	39.5×10^{-5}	0.318
200k	13×10^{-5}	61×10^{-5}	0.257

Table 4: Initial conditions $g_0^{\rm fit}, \lambda_0^{\rm fit}$ for the RG trajectory providing the best fit to the Monte Carlo data [56]. The fit-quality $(\Delta\mathcal{D}_s)^2$, given by the sum of the squared residues, improves systematically when increasing the number of simplices in the triangulation.

the squared residuals in the third column of the table improves systematically with an increasing number of simplices. By integrating the flow equation for $g(k), \lambda(k)$ for the best-fit initial conditions one furthermore observes that the points $g_0^{\rm fit}, \lambda_0^{\rm fit}$ are actually located on *different* RG trajectories. Increasing the size of the simulation N leads to a mild, but systematic increase of the distance between the turning point T and the GFP of the corresponding best-fit trajectories.

Fig. 12 then shows the direct comparison between the spectral dimensions obtained by the simulations (blue curves) and the best-fit QEG trajectories (green curves) for 70k, 100k and 200k simplices in the upper left, upper right and lower left panel, respectively. This data is complemented by the relative error

$$\epsilon \equiv -\frac{\mathcal{D}_s^{\rm QEG}(T; g_0^{\rm fit}, \lambda_0^{\rm fit}) - \mathcal{D}_s^{\rm CDT}(T)}{\mathcal{D}_s^{\rm QEG}(T; g_0^{\rm fit}, \lambda_0^{\rm fit})} \tag{8.6}$$

for the three fits in the lower right panel. The 70k data still shows a systematic deviation from the classical value $\mathcal{D}_s(T) = 3$ for long random walks, which is not present in the QEG results. This mismatch decreases systematically for larger triangulations where the classical regime becomes more and more pronounced. Nevertheless and most remarkably we find that for the 200k-triangulation that $\epsilon \lesssim 1\%$, throughout. All three sets of residues thereby show a systematic oscillatory structure. These originate from tiny oscillations in the CDT data which are not reproduced by $\mathcal{D}_s^{\rm QEG}(T)$. Such oscillations commonly appear in systems with discrete symmetries [70] and are thus likely to be absent in the

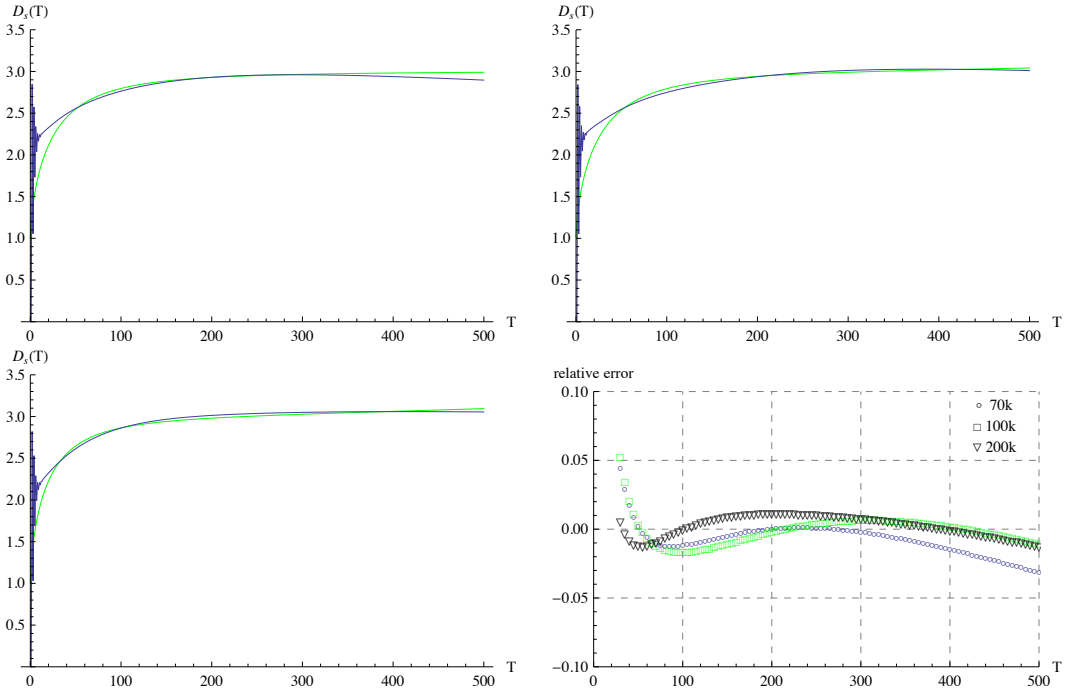

Figure 12: Comparison between the 3-dimensional CDT data-sets 70k (upper left), 100k (upper right), and 200k (lower left) obtained in [56] (blue curves) and the best fit values for $\mathcal{D}_s^{\rm QEG}(T; g_0^{\rm fit}, \lambda_0^{\rm fit})$ (green curves). The relative errors for the fits to the CDT-datasets with $N = 70.000$ (circles), $N = 100.000$ (squares) and $N = 200.000$ (triangles) simplices are shown in the lower right. The residuals grow for very small and very large durations T of the random walk, consistent with discreteness effects at small distances and the compactness of the simulation for large values of T, respectively. The quality of the fit improves systematically for triangulations containing more simplices. For the $N = 200$k data the relative error is $\approx 1\%$. (From [60].)

continuum computation. As a curiosity, we observe that the QEG result matching the most extensive simulation with $N = 200$k "overshoots" the classical value $\mathcal{D}_s(T) = 3$, yielding $\mathcal{D}_s^{\rm QEG}(T) > 3$ for $T \gtrsim 450$. At this stage, the RG trajectory is evaluated outside the classical regime in a region of theory space where the Einstein-Hilbert approximation starts to become unreliable. It is tempting to speculate that larger triangulations may also be sensitive to quantum gravity effects at distances beyond the classical regime.

We conclude this section by extending $\mathcal{D}_s^{\rm QEG}(T; g_0^{\rm fit}, \lambda_0^{\rm fit})$ obtained from the 200k data to the region of very short random walks $T < 20$. The result is depicted in fig. 13 which displays the CDT-data $\mathcal{D}_s^{\rm CDT}(T)$ (blue curve), the best-fit QEG result $\mathcal{D}_s^{\rm QEG}(T; g_0^{\rm fit}, \lambda_0^{\rm fit})$

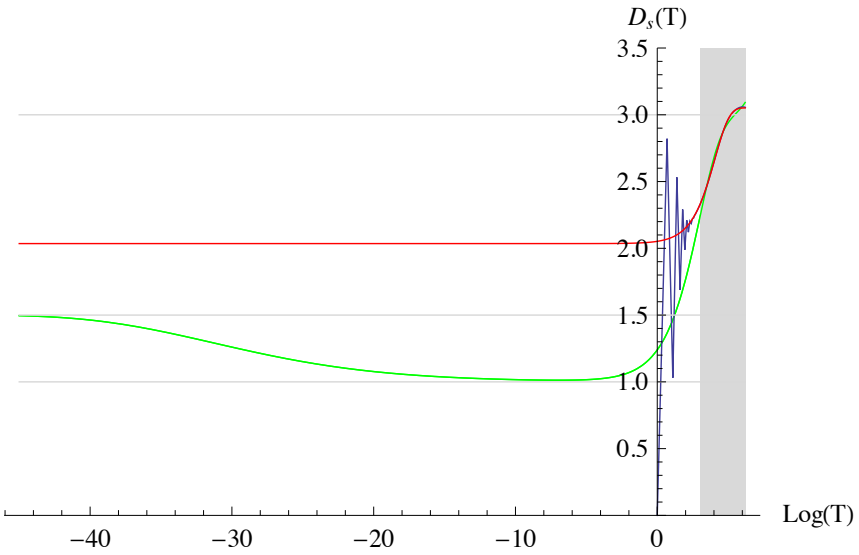

Figure 13: Extrapolation of the CDT-data for the spectral dimension measured from Monte Carlo simulations with 200.000 simplices [56] (blue curve) to infinitesimal random walks. The green and the red curve show the QEG-prediction $\mathcal{D}_s^{\rm QEG}(T; g_0^{\rm fit}, \lambda_0^{\rm fit})$ and the best-fit function (8.7) employed in [56], respectively. Notably, the scaling regime corresponding to the NGFP is reached for $\log(T) < -40$, which is well below the distance scales probed by the Monte Carlo simulation.

(green curve) and the best-fit function

$$\mathcal{D}_s^{\rm CDT-fit}(T) = a + b{\rm e}^{-cT}\,, \qquad a = 3.05\,,\quad b = -1.02\,,\quad c = 0.017\,, \tag{8.7}$$

employed in [56] (red curve) as a function of $\log(T)$. Similarly to the 4-dimensional case discussed in fig. 10, the function $\mathcal{D}_s^{\rm QEG}(T; g_0^{\rm fit}, \lambda_0^{\rm fit})$ obtained for $d = 3$ develops three plateaus where the spectral dimension is approximately constant over a long T-interval. For successively decreasing duration of the random walks, these plateaus correspond to the classical regime $\mathcal{D}_s^{\rm QEG}(T) = 3$, the semi-classical regime where $\mathcal{D}_s^{\rm QEG}(T) \approx 1$ and the NGFP regime where $\mathcal{D}_s^{\rm QEG}(T) = 3/2$. The figure illustrates that $\mathcal{D}_s^{\rm CDT}(T)$ probes the classical regime and part of the first crossover towards the semi-classical regime only. This is in perfect agreement with the assertion [56] that *the present simulations do not yet probe structures below the Planck scale.* The different predictions for the spectral dimensions obtained for infinitesimal random walks solely arise from different extrapolation schemes.

9 Concluding remarks

In this article we reviewed the basic concepts underlying the gravitational Asymptotic Safety program and summarized evidence supporting the existence of the non-Gaussian renormalization group fixed point (NGFP) at the heart of this scenario. The NGFP constitutes a highly non-trivial feature of the gravitational renormalization group flow and defines a consistent and predictive quantum theory of gravity, Quantum Einstein Gravity or QEG for short. Based on the continuum average action approach [11], we then outlined our present understanding of the multifractal features characteristic for the effective QEG space-times. These structures are at least to some extend captured by the spectral, walk, and Hausdorff dimension seen by a fictitious diffusion process set up on the effective space-times. Their explicit computation allows a direct comparison between the results obtained from the continuum functional renormalization group and other approaches to quantum gravity like the discrete Causal Dynamical Triangulations [52–54, 57, 58] and Euclidean Dynamical Triangulation [59] programs. We close our review with the following comments:

(1) We stress that the construction of an effective average action for gravity reviewed in section 3 represents a *"background independent"* approach to quantum gravity. Somewhat paradoxically, this background independence is achieved by means of the background field formalism: One fixes an arbitrary background, quantizes the fluctuation field in this background, and afterwards adjusts $\bar{g}_{\mu\nu}$ in such a way that the expectation value of the fluctuation vanishes: $\bar{h}_{\mu\nu} = 0$. In this way the background gets fixed dynamically. The results of refs. [28,29] suggest that a proper implementation of "background independence" might be crucial for Asymptotic Safety.

(2) The combination of the effective average action with the background field method has been successfully tested within conventional field theory. In QED and Yang-Mills type gauge theories it reproduces the known results and extends them into the non-perturbative domain [39, 41].

(3) The coexistence of Asymptotic Safety and perturbative non-renormalizability is well

understood. In particular upon fixing $\bar{g}_{\mu\nu} = \eta_{\mu\nu}$ and expanding the trace on its RHS in powers of G the FRGE reproduces the divergences of perturbation theory; see ref. [5] for a detailed discussion of this point.

(4) It is to be emphasized that in the average action framework the RG flow, i.e., the vector field $\vec{\beta}$, is completely determined once a theory space is fixed. As a consequence, the choice of theory space determines the set of fixed points Γ^* at which asymptotically safe theories can be defined. Therefore, in the Asymptotic Safety scenario the bare action S related to Γ^* is a *prediction* of the theory rather than an ad hoc postulate as usually in quantum field theory. Ambiguities could arise only if there is more than one suitable NGFP.

(5) According to the results available to date, the Einstein-Hilbert action of classical General Relativity seems not to play any distinguished role in the Asymptotic Safety context, at least not at the conceptual level. The only known NGFP on the theory space of QEG has the structure Γ^* = Einstein-Hilbert action + "more" where "more" stands for both local and non-local corrections. So it seems that the Einstein-Hilbert action is only an approximation to the true fixed point action, albeit an approximation which was found to be rather reliable for many purposes.

(6) A solution to the FRGE, as such, does not define a regularized functional integral; a priori it is not even clear whether or not a path integral representation exists for a given RG trajectory. In [77] it was shown how, upon specification of a UV regularized measure, the information contained in $\Gamma_{k\to\infty}$ may be used to obtain the cutoff dependence of the bare action. A thorough understanding of this relationship is essential in comparing the average action to other approaches, such as Monte Carlo simulations of discrete models of gravity, for instance.

(7) Any quantum theory of gravity must reproduce the successes of classical General Relativity. As for QEG, it cannot be expected that this will happen for all RG trajectories in $\mathcal{S}_{\rm UV}$, but it should happen for some or at least one of them. Within the Einstein-Hilbert truncation it has been shown [97] that there actually do exist trajectories (of Type IIIa)

which have an extended classical regime and are consistent with all observations.

(8) In the classical regime mentioned above the dynamics of space-time geometry is unaffected by quantum effects to a very good approximation. In this regime the familiar methods of quantum field theory in curved classical space-times apply, and it is clear therefore that effects such as Hawking radiation or cosmological particle production are reproduced by the general framework of QEG with matter.

(9) Coupling free massless matter fields to gravity, it turned out [21] that the fixed point continues to exist under very weak conditions concerning the number of various types of matter fields (scalars, fermions, etc.). No fine tuning with respect to the matter multiplets is necessary. In particular Asymptotic Safety does not seem to require any special constraints or symmetries among the matter fields such as supersymmetry, for instance.

(10) Since the NGFP seems to exist already in pure gravity it is likely that a widespread prejudice about gravity may be incorrect: its quantization seems not to require any kind of unification with the other fundamental interactions.

(11) To the best of our knowledge, the effective space-times arising within QEG carry a multifractal structure [60]. Some of these features are captured by the spectral, walk, and Hausdorff dimension seen by a fictitious diffusion process set up on the effective space-time. The resulting Hausdorff dimension is constant and equal to the topological dimension of the (background) space-time. Thus the fractal properties do not originate from the QEG space-times "loosing points" at short distances but rather represent a genuine dynamical effect of quantum field theory. In contrast to the Hausdorff dimension the spectral dimension and the walk dimension seen by the diffusion process depend on the diffusion time. Fig. 10 identifies *three* regimes in which these generalized dimensions are constant for a wide range of scales, the classical, semi-classical and NGFP regime, which are connected by short crossovers.

(12) In section 8.3 we performed a direct comparison between the spectral dimension of the 3-dimensional effective QEG space-times with the one measured in Causal Dynamical Triangulations (CDT) [56]. Notably, the best-fit RG trajectory reproduces the CDT data

with approximately 1% accuracy for the range of diffusion times where the simulation data is reliable. Notably current Monte Carlo data neither probes the semi-classical plateau nor the scaling regime of the NGFP. Determining the spectral dimension for infinitesimal random walks by extrapolating the leading quantum corrections to the classical regime may therefore miss the imprints of the NGFP on the structure of space-time.

Acknowledgements

We thank D. Benedetti and J. Henson for sharing the Monte Carlo data underlying their work [56] with us. We are also grateful to A. Nink for a careful reading of the manuscript. The research of F.S. is supported by the Deutsche Forschungsgemeinschaft (DFG) within the Emmy-Noether program (Grant SA/1975 1-1).

A Generalized dimensions on classical manifolds

Investigating random walks and diffusion processes on fractals, one is led to introduce various notions of fractal dimensions, such as the spectral or walk dimension [100]. These notions also prove useful when characterizing properties of space-time in quantum gravity, and we will review these concepts in the remainder of this section.

A.1 The spectral dimension

To start with, consider the diffusion process where a spin-less test particle performs a Brownian random walk on an ordinary Riemannian manifold with a fixed classical metric $g_{\mu\nu}(x)$. It is described by the heat kernel $K_g(x, x'; T)$ which gives the probability density for a transition of the particle from x to x' during the fictitious time T. It satisfies the heat equation

$$\partial_T K_g(x, x'; T) = -\Delta_g K_g(x, x'; T)\,, \tag{A.1}$$

where $\Delta_g = -D^2$ denotes the Laplace operator. In flat space, this equation is easily solved by

$$K_g(x, x'; T) = \int \frac{d^d p}{(2\pi)^d} \, \mathrm{e}^{ip\cdot(x-x')} \, \mathrm{e}^{-p^2 T} \tag{A.2}$$

In general, the heat kernel is a matrix element of the operator $\exp(-T\Delta_g)$. In the random walk picture its trace per unit volume,

$$P_g(T) = V^{-1} \int d^d x \sqrt{g(x)} \, K_g(x, x; T) \equiv V^{-1} \, \mathrm{Tr} \, \exp(-T\Delta_g) \,, \tag{A.3}$$

has the interpretation of an average return probability. Here $V \equiv \int d^d x \sqrt{g(x)}$ denotes the total volume. It is well known that P_g possesses an asymptotic early time expansion (for $T \to 0$) of the form $P_g(T) = (4\pi T)^{-d/2} \sum_{n=0}^{\infty} A_n T^n$, with A_n denoting the Seeley-DeWitt coefficients. From this expansion one can motivate the definition of the spectral dimension d_s as the T-independent logarithmic derivative

$$d_s \equiv -2 \frac{d \ln P_g(T)}{d \ln T} \bigg|_{T=0} \,. \tag{A.4}$$

On smooth manifolds, where the early time expansion of $P_g(T)$ is valid, the spectral dimension agrees with the topological dimension d of the manifold.

Given $P_g(T)$, it is natural to define a, in general T-dependent, generalization of the spectral dimension by

$$\mathcal{D}_s(T) \equiv -2 \frac{d \ln P_g(T)}{d \ln T} \,. \tag{A.5}$$

According to (A.4), we recover the true spectral dimension of the space-time by considering the shortest possible random walks, i.e., by taking the limit $d_s = \lim_{T\to 0} \mathcal{D}_s(T)$. Note that in view of a possible comparison with other (discrete) approaches to quantum gravity the generalized, scale-dependent version (A.5) plays a central role.

A.2 The walk dimension

Regular Brownian motion in flat space has the celebrated property that the random walker's average square displacement increases linearly with time: $\langle r^2 \rangle \propto T$. Indeed, performing the integral (A.2) we obtain the familiar probability density

$$K(x, x'; T) = (4\pi T)^{-d/2} \exp\left(-\frac{\sigma(x, x')}{2T}\right) \tag{A.6}$$

with $\sigma(x, x') = \frac{1}{2}|x - x'|^2$ half the squared geodesic distance between the points x, x'. Using (A.6) yields the expectation value $\langle r^2 \rangle \equiv \langle x^2 \rangle = \int d^d x \, x^2 \, K(x, 0; T) \propto T$.

Many diffusion processes of physical interest (such as diffusion on fractals) are anomalous in the sense that this linear relationship is generalized to a power law $\langle r^2 \rangle \propto T^{2/d_w}$ with $d_w \neq 2$. The interpretation of the so-called walk dimension d_w is as follows. The trail left by the random walker is a random object, which is interesting in its own right. It has the properties of a fractal, even in the "classical" case when the walk takes place on a regular manifold. The quantity d_w is precisely the fractal dimension of this trail. Diffusion processes are called regular if $d_w = 2$, and anomalous when $d_w \neq 2$.

A.3 The Hausdorff dimension

Finally, we introduce the Hausdorff dimension d_H. Instead of working with its mathematically rigorous definition in terms of the Hausdorff measure and all possible covers of the metric space under consideration, the present, simplified definition may suffice for our present purposes. On a smooth set, the scaling law for the volume $V(r)$ of a d-dimensional ball of radius r takes the form

$$V(r) \propto r^{d_H} \, . \tag{A.7}$$

The Hausdorff dimension is then obtained in the limit of infinitely small radius,

$$d_H \equiv \lim_{r \to 0} \frac{\ln V(r)}{\ln r} \, . \tag{A.8}$$

Contrary to the spectral or walk dimension whose definitions are linked to dynamical diffusion processes on space-time, there is no such dynamics associated with d_H.

References

[1] C. Kiefer, *Quantum Gravity*, Second Edition, Oxford Science Publications, Oxford, 2007;
C. Rovelli, *Quantum Gravity*, Cambridge University Press, Cambridge, 2004;
A. Ashtekar, *Lectures on non-perturbative canonical gravity*, World Scientific, Singapore, 1991;
A. Ashtekar and J. Lewandowski, Class. Quant. Grav. 21 (2004) R53;
H. Hamber, *Quantum Gravitation*, Springer, Berlin, 2008.

[2] G. 't Hooft and M. J. G. Veltman, Annales Poincaré Phys. Theor. A 20 (1974) 69 .

[3] M. H. Goroff and A. Sagnotti, Phys. Lett. B 160 (1985) 81.

[4] A. E. M. van de Ven, Nucl. Phys. B 378 (1992) 309.

[5] M. Niedermaier and M. Reuter, Living Reviews in Relativity 9 (2006) 5;
M. Reuter and F. Saueressig, in *Geometric and Topological Methods for Quantum Field Theory*, H. Ocampo, S. Paycha and A. Vargas (Eds.), Cambridge Univ. Press, Cambridge, 2010, arXiv:0708.1317;
R. Percacci, in *Approaches to Quantum Gravity: Towards a New Understanding of Space, Time and Matter*, D. Oriti (Ed.), Cambridge University Press, Cambridge, 2009, arXiv:0709.3851.

[6] O. Lauscher and M. Reuter in *Quantum Gravity*, B. Fauser, J. Tolksdorf and E. Zeidler (Eds.), Birkhäuser, Basel, 2007, hep-th/0511260.

[7] S. M. Christensen and M. J. Duff, Phys. Lett. B **79** (1978) 213.

[8] R. Gastmans, R. Kallosh and C. Truffin, Nucl. Phys. B **133** (1978) 417.

[9] S. Weinberg in *General Relativity, an Einstein Centenary Survey*, S.W. Hawking and W. Israel (Eds.), Cambridge University Press, 1979;
S. Weinberg, hep-th/9702027.

[10] S. Weinberg, arXiv:0903.0568; PoS C D09 (2009) 001, arXiv:0908.1964.

[11] M. Reuter, Phys. Rev. D 57 (1998) 971, hep-th/9605030.

[12] D. Dou and R. Percacci, Class. Quant. Grav. 15 (1998) 3449, hep-th/9707239.

[13] O. Lauscher and M. Reuter, Phys. Rev. D 65 (2002) 025013, hep-th/0108040.

[14] M. Reuter and F. Saueressig, Phys. Rev. D 65 (2002) 065016, hep-th/0110054.

[15] O. Lauscher and M. Reuter, Phys. Rev. D 66 (2002) 025026, hep-th/0205062.

[16] O. Lauscher and M. Reuter, Class. Quant. Grav. 19 (2002) 483, hep-th/0110021.

[17] O. Lauscher and M. Reuter, Int. J. Mod. Phys. A17 (2002) 993, hep-th/0112089.

[18] W. Souma, Prog. Theor. Phys. 102 (1999) 181, hep-th/9907027.

[19] M. Reuter and F. Saueressig, Phys. Rev. D 66 (2002) 125001, hep-th/0206145; Fortschr. Phys. 52 (2004) 650, hep-th/0311056.

[20] A. Bonanno and M. Reuter, JHEP 02 (2005) 035, hep-th/0410191.

[21] R. Percacci and D. Perini, Phys. Rev. D 67 (2003) 081503, hep-th/0207033; Phys. Rev. D 68 (2003) 044018, hep-th/0304222; Class. Quant. Grav. 21 (2004) 5035, hep-th/0401071.

[22] A. Codello and R. Percacci, Phys. Rev. Lett. 97 (2006) 221301, hep-th/0607128.

[23] D. Litim, Phys. Rev. Lett. 92 (2004) 201301, hep-th/0312114.
P. Fischer and D. Litim, Phys. Lett. B 638 (2006) 497, hep-th/0602203.

[24] R. Percacci and D. Perini, Class. Quant. Grav. 21 (2004) 5035, hep-th/0401071.

[25] A. Codello, R. Percacci and C. Rahmede, Int. J. Mod. Phys. A 23 (2008) 143, arXiv:0705.1769.

[26] P. F. Machado and F. Saueressig, Phys. Rev. D 77 (2008) 124045, arXiv:0712.0445.

[27] A. Codello, R. Percacci and C. Rahmede, Annals Phys. 324 (2009) 414, arXiv:0805.2909.

[28] M. Reuter and H. Weyer, Phys. Rev. D 79 (2009) 105005, arXiv:0801.3287; Gen. Rel. Grav 41 (2009) 983, arXiv:0903.2971.

[29] M. Reuter and H. Weyer, Phys. Rev. D 80 (2009) 025001, arXiv:0804.1475.

[30] P. F. Machado and R. Percacci, Phys. Rev. D 80 (2009) 024020, arXiv:0904.2510.

[31] J. E. Daum and M. Reuter, Adv. Sci. Lett. 2 (2009) 255, arXiv:0806.3907.

[32] D. Benedetti, P. F. Machado and F. Saueressig, Mod. Phys. Lett. A24 (2009) 2233, arXiv:0901.2984.

[33] D. Benedetti, P. F. Machado and F. Saueressig, Nucl. Phys. B **824** (2010) 168, arXiv:0902.4630; arXiv:0909.3265

[34] J.-E. Daum, U. Harst and M. Reuter, JHEP 01 (2010) 084, arXiv:0910.4938.
U. Harst and M. Reuter, JHEP 05 (2011) 119, arXiv:1101.6007.

[35] C. Rahmede, PoS CLAQG 08 (2011) 011.

[36] D. Benedetti, K. Groh, P. F. Machado and F. Saueressig, JHEP 06 (2011) 079, arXiv:1012.3081.

[37] P. Forgács and M. Niedermaier, hep-th/0207028;
M. Niedermaier, JHEP 12 (2002) 066; Nucl. Phys. B 673 (2003) 131; Class. Quant. Grav. 24 (2007) R171.

[38] C. Wetterich, Phys. Lett. B 301 (1993) 90.

[39] M. Reuter and C. Wetterich, Nucl. Phys. B 417 (1994) 181, Nucl. Phys. B 427 (1994) 291, Nucl. Phys. B 391 (1993) 147, Nucl. Phys. B 408 (1993) 91; M. Reuter, Phys. Rev. D 53 (1996) 4430, Mod. Phys. Lett. A 12 (1997) 2777.

[40] J. Berges, N. Tetradis and C. Wetterich, Phys. Rep. 363 (2002) 223, hep-ph/0005122
C. Wetterich, Int. J. Mod. Phys. A 16 (2001) 1951, hep-ph/0101178.

[41] M. Reuter, hep-th/9602012.
J. Pawlowski, Annals Phys. 322 (2007) 2831, hep-th/0512261.
H. Gies, hep-ph/0611146.

[42] C. Bagnuls and C. Bervillier, Phys. Rep. 348 (2001) 91, hep-th/0002034.
T.R. Morris, Prog. Theor. Phys. Suppl. 131 (1998) 395, hep-th/9802039.
J. Polonyi, Central Eur. J. Phys. 1 (2004) 1.
O. J. Rosten, arXiv:1003.1366.

[43] M. Reuter and J. Schwindt, JHEP 01 (2006) 070, hep-th/0511021.

[44] M. Reuter and J. Schwindt, JHEP 01 (2007) 049, hep-th/0611294.

[45] B. Mandelbrot, *The Fractal Geometry of Nature*, Freeman, New York (1977).

[46] H. Kawai, M. Ninomiya, Nucl. Phys. B 336 (1990) 115.

[47] R. Floreanini and R. Percacci, Nucl. Phys. B 436 (1995) 141, hep-th/9305172.

[48] H. Kawai and M. Ninomiya, Nucl. Phys. B 336 (1990) 115;
I. Antoniadis, P.O. Mazur and E. Mottola, Phys. Lett. B 444 (1998) 284, hep-th/9808070.

[49] O. Lauscher and M. Reuter, JHEP 10 (2005) 050, hep-th/0508202.

[50] A. Bonanno and M. Reuter, Phys. Rev. D 65 (2002) 043508, hep-th/0106133;
M. Reuter and F. Saueressig, JCAP 09 (2005) 012, hep-th/0507167.

[51] A. Bonanno and M. Reuter, JCAP 08 (2007) 024, arXiv:0706.0174.

[52] J. Ambjørn, J. Jurkiewicz and R. Loll, Phys. Rev. Lett. 93 (2004) 131301, hep-th/0404156.

[53] J. Ambjørn, J. Jurkiewicz and R. Loll, Phys. Lett. B 607 (2005) 205, hep-th/0411152.

[54] J. Ambjørn, J. Jurkiewicz and R. Loll, Phys. Rev. Lett. 95 (2005) 171301, hep-th/0505113; Phys. Rev. D 72 (2005) 064014, hep-th/0505154; Contemp. Phys. 47 (2006) 103, hep-th/0509010.

[55] J. Ambjørn, S. Jordan, J. Jurkiewicz and R. Loll, Phys. Rev. Lett. 107 (2011) 211303, arXiv:1108.3932.

[56] D. Benedetti, J. Henson, Phys. Rev. D 80 (2009) 124036, arXiv:0911.0401.

[57] R. Kommu, arXiv:1110.6875.

[58] J. Ambjørn, J. Jurkiewicz and R. Loll, Lect. Notes Phys. 807 (2010) 59, arXiv:0906.3947.

[59] J. Laiho and D. Coumbe, Phys. Rev. Lett. 107 (2011) 161301, arXiv:1104.5505.

[60] M. Reuter and F. Saueressig, JHEP 12 (2011) 012, arXiv:1110.5224.

[61] L. Modesto, Class. Quant. Grav. 26 (2009) 242002.

[62] L. Modesto, arXiv:0905.1665.

[63] F. Caravelli and L. Modesto, arXiv:0905.2170.
E. Magliaro, C. Perini and L. Modesto, arXiv:0911.0437.

[64] S. Carlip, arXiv:0909.3329; arXiv:1009.1136.
S. Carlip and D. Grumiller, Phys. Rev. D 84 (2011) 084029, arXiv:1108.4686.

[65] A. Connes, JHEP 11 (2006) 081, hep-th/0608226;
A.H. Chamseddine, A. Connes and M. Marcolli, Adv. Theor. Math. Phys. 11 (2007) 991, hep-th/0610241.

[66] D. Guido and T. Isola, arXiv:math.OA/0202108, arXiv:math.OA/0404295; C. Antonescu and E. Christensen, arXiv:math.OA/0309044.

[67] D. Benedetti, Phys. Rev. Lett. 102 (2009) 111303, arXiv:0811.1396.

[68] G. Calcagni, Phys. Rev. Lett. 104 (2010) 251301; JHEP 03 (2010) 120; Phys. Lett. B 697 (2011) 251.

[69] M. Arzano, G. Calcagni, D. Oriti and M. Scalisi, Phys. Rev. D 84 (2011) 125002, arXiv:1107.5308.

[70] G. Calcagni, arXiv:1106.5787; arXiv:1107.5041.

[71] E. Akkermans, G. V. Dunne and A. Teplyaev, Phys. Rev. Lett. 105 (2010) 230407, arXiv:1010.1148.

[72] E. Akkermans, G. V. Dunne and A. Teplyaev, Europhys. Lett. 88 (2009) 40007, arXiv:0903.3681.

[73] C. T. Hill, Phys. Rev. D 67 (2003) 085004, hep-th/0210076.

[74] B. S. DeWitt, *The Global Approach to Quantum Field Theory*, Oxford University Press, Oxford, 2003.

[75] L.F. Abbott, Nucl. Phys. B 185 (1981) 189; B.S. DeWitt, Phys. Rev. 162 (1967) 1195; M.T. Grisaru, P. van Nieuwenhuizen and C.C. Wu, Phys. Rev. D 12 (1975) 3203; D.M. Capper, J.J. Dulwich and M. Ramon Medrano, Nucl. Phys. B 254 (1985) 737; S.L. Adler, Rev. Mod. Phys. 54 (1982) 729.

[76] M. Böhm, A. Denner, H. Joos, *Gauge Theories of the Strong and Electroweak Interactions*, Teubner, Stuttgart, 2001.

[77] E. Manrique and M. Reuter, Phys. Rev. D 79 (2009) 025008, arXiv:0811.3888.

[78] D. Litim, Phys. Lett. B 486 (2000) 92, hep-th/0005245.

[79] M. Niedermaier, Phys. Rev. Lett. 103 (2009) 101303.

[80] F. Saueressig, K. Groh, S. Rechenberger and O. Zanusso, arXiv:1111.1743 [hep-th].

[81] A. Eichhorn, H. Gies and M. M. Scherer, Phys. Rev. D **80** (2009) 104003, arXiv:0907.1828.

[82] K. Groh and F. Saueressig, J. Phys. A **43** (2010) 365403, arXiv:1001.5032.

[83] A. Eichhorn and H. Gies, Phys. Rev. D **81** (2010) 104010, arXiv:1001.5033.

[84] D. Litim and J. Pawlowski, Phys. Lett. B 435 (1998) 181, hep-th/9802064.

[85] S. Falkenberg and S.D. Odintsov, Int. J. Mod. Phys. A 13 (1998) 607, hep-th/9612019.

[86] L.N. Granda, Europhys. Lett. 42 (1998) 487, hep-th/0501225.

[87] G.O. Pires, Int. J. Mod. Phys. A 13 (1998) 5425, hep-th/9708111.

[88] R. Percacci, J. Phys. A 40 (2007) 4895, hep-th/0409199.

[89] A. Codello, Annals Phys. 325 (2010) 1727, arXiv:1004.2171.

[90] A. Satz, A. Codello and F. D. Mazzitelli, Phys. Rev. D 82 (2010) 084011, arXiv:1006.3808.

[91] J. F. Donoghue, Phys. Rev. D 50 (1994) 3874, gr-qc/9405057.

[92] E. Manrique and M. Reuter, Annals Phys. 325 (2010) 785, arXiv:0907.2617.

[93] E. Manrique, M. Reuter and F. Saueressig, Annals Phys. 326 (2011) 440, arXiv:1003.5129; Annals Phys. 326 (2011) 463, arXiv:1006.0099.

[94] E. Manrique, S. Rechenberger and F. Saueressig, Phys. Rev. Lett. 106 (2011) 251302, arXiv:1102.5012.

[95] J.-E. Daum and M. Reuter, arXiv:1012.4280; PoS (CNCFG 2010) 003; arXiv:1111.1000.

[96] D. Benedetti and S. Speziale, JHEP 06 (2011) 107, arXiv:1104.4028.

[97] M. Reuter and H. Weyer, JCAP 12 (2004) 001, hep-th/0410119.

[98] M. Reuter and H. Weyer, Phys. Rev. D 69 (2004) 104022, hep-th/0311196.

[99] S. Alexander and R. Orbach, J. Phys. Lett. (Paris) 43 (1982) L625.

[100] D. ben-Avraham and S. Havlin, *Diffusion and reactions in fractals and disordered systems*, Cambridge University Press, Cambridge, 2004.

[101] T. P. Sotiriou, M. Visser and S. Weinfurtner, Phys. Rev .Lett. 107 (2011) 131303, arXiv:1105.5646.